

BIOMECHANICAL ASSESSMENT OF ALL-POLYMER TOTAL KNEE REPLACEMENT



Lennert de Ruiter

Biomechanical assessment of all-polymer total knee replacement

Lennert de Ruitter

Colofon

Biomechanical assessment of all-polymer total knee replacement.
Thesis Radboud University, Nijmegen, with summary in Dutch.

The work presented in this thesis was carried out within the Radboud Institute for Health Sciences at the Orthopaedic Research Laboratory (Radboud university medical center Nijmegen)

ISBN: 978-94-6416-006-2
Cover design: Studio 0404
Lay-out: Studio 0404
Printed by: Ridderprint

© 2020, Lennert de Ruiter

All rights reserved. No part of this publication may be reproduced, distributed, or transmitted in any form or by any means, including photocopying, recording, or other electronic or mechanical methods, without the prior written permission of the author.

Biomechanical assessment of all-polymer total knee replacement

PROEFSCHRIFT

ter verkrijging van de graad van doctor
aan de Radboud Universiteit Nijmegen
op gezag van de rector magnificus prof. dr. J.H.J.M. van Krieken,
volgens besluit van het college van decanen
in het openbaar te verdedigen
op vrijdag 11 september 2020
om 14.30 uur precies

door

Leendert de Ruiter
geboren op 27 december 1987
te Geldrop

Promotor

Prof. dr. ir. Nico Verdonshot

Copromotor

Dr. ir. Dennis Janssen

Manuscriptcommissie

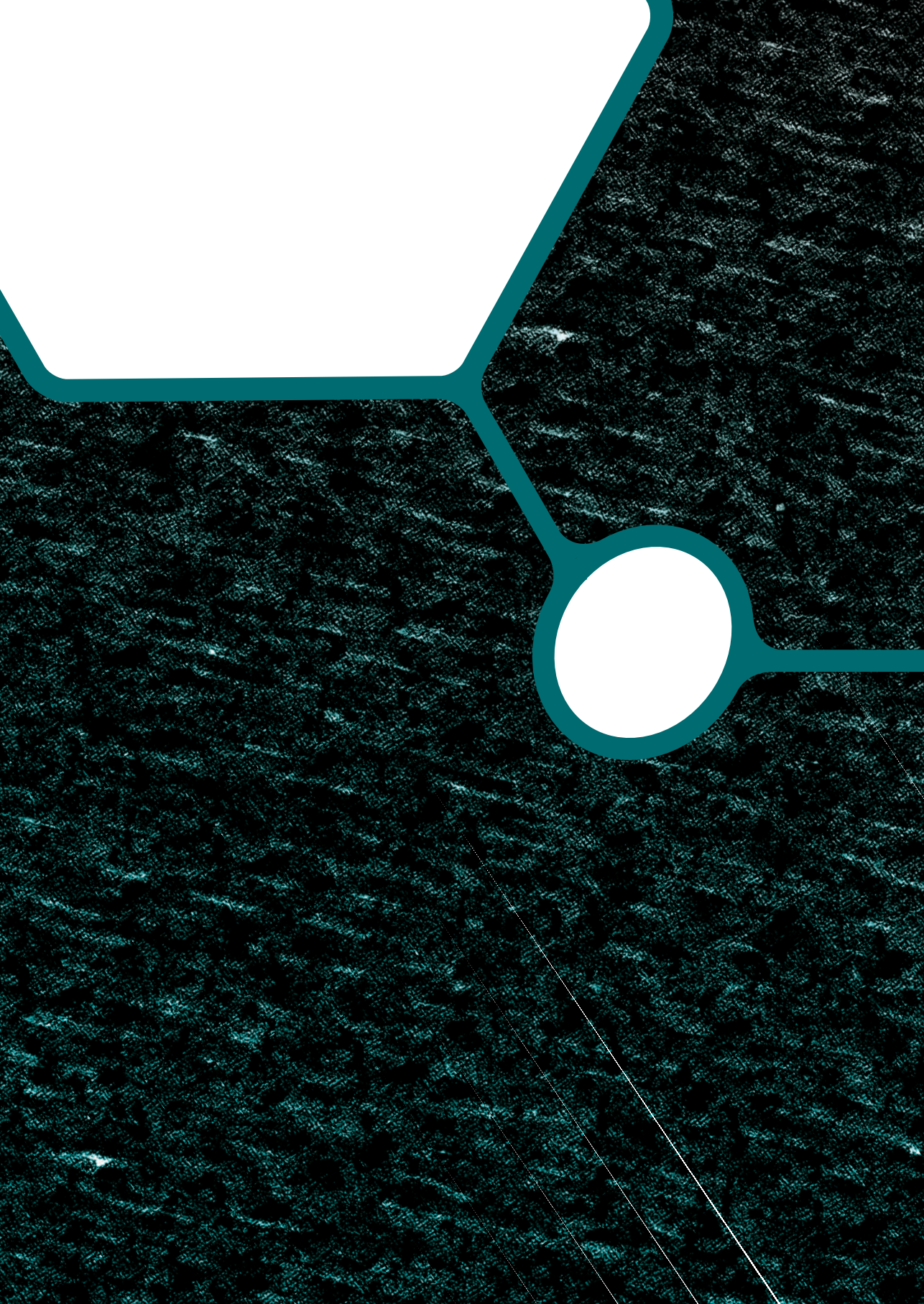
Prof. dr. Thomas Maal

Prof. dr. ir. Bart Koopman (Universiteit Twente)

Dr. Stan Buckens

Table of contents

Chapter 1	General introduction and outline	9
Chapter 2	A preclinical numerical assessment of a polyetheretherketone femoral component in total knee arthroplasty during gait	21
Chapter 3	The mechanical response of a polyetheretherketone femoral knee implant under a deep squatting loading condition	39
Chapter 4	Decreased stress shielding with a PEEK femoral total knee prosthesis measured in validated computational models	57
Chapter 5	Fixation strength of a polyetheretherketone femoral component in total knee arthroplasty	75
Chapter 6	The effects of cyclic loading and motion on the implant-cement interface and cement mantle of PEEK and cobalt-chromium femoral total knee arthroplasty implants: a preliminary study	91
Chapter 7	Clinical imaging protocols for in-vivo assessment of an all-polymer PEEK-on-UHMWPE total knee replacement with magnetic resonance imaging, computed tomography and X-ray radiography	113
Chapter 8	Summary and general discussion	141
Chapter 9	Nederlandse samenvatting en discussie	159
Appendix	List of publications	181
	Data management	185
	PhD portfolio	187
	Curriculum Vitae	189
	Dankwoord	191



Chapter 1

General introduction and outline

Societal context

Total Knee Arthroplasty, or TKA, is a surgical procedure to replace damaged cartilage surfaces in the knee joint. The leading indication for TKA worldwide is osteoarthritis (OA), which accounts for over 95% of the reasons for primary knee replacement surgery. Other indications include rheumatoid arthritis, trauma, osteonecrosis and malignities¹⁻³. Patients receiving TKA have often received extensive therapeutic treatment for years, before invasive TKA is advised and performed^{4,5}. The annual incidence rate of TKA in the Western world is about 150 procedures per 100,000 citizens, which makes it one of the most common surgical interventions to date⁶. Many studies have provided projections for the future disease burden and, although the extent varies, all agree that the incidence rate of TKA will continue to increase. Reasons for the increase include an ageing population and improved life expectancy, an increase in obesity, improved healthcare access and acceptance of the technology.

For instance, the incidence rate in Australia has more than doubled in the period 1994 to 2014 and is projected to increase with an additional 26% by 2046⁷. Models for the US population, published in 2007, have predicted a staggering 673% increase between 2005 and 2030, based on procedural data from 1990-2003⁸. In 2014, the authors updated their predictions with a dataset from 1993-2010⁹. This update corroborated the predictions from their previous paper for the number of procedures in 2005 and 2010 and predicted similar but slightly lower numbers for 2015 and 2020. A more conservative predictive study by Inacio *et al.* (2017) concluded that the rate of growth for TKA procedures will decrease substantially after 2028, following saturation of TKA prevalence in the population. Still, they predict an annual 1.2 million TKA procedures by 2030 and 1.5 million by 2050, in contrast to ~650,000 in 2010^{9,10}. In The Netherlands, the Dutch Arthroplasty Register (LROI) reemphasized that growth rates of TKA procedures are high and heterogeneous among countries. They reported a 45% increase in TKA procedures between 2010 and 2017¹¹. Such increases in the incidence rate demonstrate that the decrease described by Inacio *et al.* (2017) for the US is not (yet) prevalent in other societies. Better yet, rates in the US may be exemplary for the potential procedure growth in the rest of the world.

TKA design history

The first application of the technology for knee replacement was accredited to Theophilus Gluck in the late 19th century, who devised a hinged knee implant out of ivory. Although these were not very successful for a number of reasons, the hinged design was picked up by Dr. Walldius in 1951, who created a knee replacement from acrylic and later Cobalt-Chromium (CoCr). It was not until the 1970's that the development of modern TKA prostheses intensified. Surgeons and engineers around the globe independently set out to reduce the mechanical

constraints of hinged prostheses as these constraints led to high mechanical failure rates¹². As a result, numerous designs and techniques were developed that revolutionized knee arthroplasty, and many of the contemporary prosthesis designs are still related to the shapes that were introduced in the 1970's and 1980's. Ever since Dr. Walldius introduced Cobalt-Chromium in TKA back in the 1950's, this material has remained the most commonly used material for femoral knee implants. Reports show that over 95% of the implants used to date is of a Cobalt-Chromium alloy for the femoral implant, sliding against a polyethylene (UHMWPE) tibial component^{2,3,11}. The CoCr-UHMWPE combination has proven to be a highly successful bearing couple, but since the leading cause for revision surgery was implant wear of the polyethylene tibial component, engineers continued exploring other materials, like improved polyethylene and ceramics.

Ceramic TKA

The ability to manufacture very hard and smooth ceramic materials made them an suitable candidate for improving the wear resistance of the tibiofemoral bearing couple. Borrowed from total hip replacements, alumina ceramic (Al_2O_3) was already considered in the 1970's and used as an alternative to CoCr to reduce wear of the tibial polyethylene implant¹³⁻¹⁵. Later on in the 1990's, Zirconia-based ceramics (ZrO_2 , (Y)-TZP) were being used to address mechanical difficulties encountered with alumina ceramic. Although several research projects were initiated, most devices have never reached large-scale manufacturing or were abandoned. More recent developments in ceramic composites are seemingly successful. The matrix composite ceramic of mainly ZrO_2 and Al_2O_3 combines the benefits of both materials that have been used in TKA separately. Since their arrival, these implants have established a good reputation and are now starting to show good clinical survival rates¹⁵. The paradigm of ceramics in TKA is that the 'new' materials should replicate the strength and rigidity of conventional metal components, but further improve the wear resistance of the bearing couples. Stiff implants, however, introduce a substantial mechanical mismatch between the implant and the bone it is seated on, which causes stress-shielding of the bone and can eventually lead to failure of the reconstruction. Besides improved wear resistance, ceramic implants are generally marketed as a solution to metal-(hyper)sensitivity, which is a contraindication for metal TKA in a small percentage of patients. Metal ions that are released from the implant during service may provoke an immunological or allergic reaction that may cause joint inflammation, disturbed wound healing, osteolysis and in rare cases leads to revision surgery with a non-metal prosthesis. Modern ceramics are designed such that they do not release these metal ions, even though they do contain metallic elements.

Polymer TKA

All-polymer TKA implants have not been studied as extensively as metal and ceramic prostheses. This can in part be explained by the direction in which TKA engineering was moving, which was to increase wear resistance of the bearing couple by varying the material compositions. Polymer-on-polymer bearing surfaces were generally less wear resistant due to high friction, damage accumulation and creep deformations. However, all-polymer TKA was considered a solution to other problems that were encountered with metal or ceramic implants. Similar to, or better than, ceramic implants, polymer devices provide a solution to metal ion release. Polymers are also more readily available and can thus be made cheaper. This is particularly desirable since Cobalt and Chromium are relatively scarce and are, just like ceramic implants, expensive resources. Additionally, Bradley *et al.* (1993) postulated that the mechanical compatibility of plastics and bone may provide advantages for reconstructed knees on long-term use. Also, radiolucent polymer would allow better visualization of the bone-implant interface on clinical imaging¹⁶. These arguments led Dr. Tuke and Dr. Freeman to investigate all bearing couples from polymers that were used in implants at the time. Since all polymers would remove metal ions from the equation and provide more iso-elastic joint replacement, they set out to find the bearing couple that would be most wear resistant. To their surprise, polyacetal (Delrin[®])-on-UHMWPE wore less than when UHMWPE was oscillating against polished metal¹⁷. The investigators set up a clinical trial and published the results for a polyacetal-on-UHMWPE TKA implant with a minimum follow-up of 10 years. No failures were attributed to implant wear. Moreover, retrievals showed less wear compared to the CoCr-on-UHMWPE bearing couple; substantial, but not significantly different. Unfortunately, the uncemented fixation technique and sterilization method resulted in high rates of aseptic tibial loosening and infection. This resulted in substantially lower survival and the project, and, like many TKA design projects in that time, this all polymeric solution was abandoned^{16,17}.

Stricter medical device regulations

The abundant experimental use of new orthopedic joint replacement designs was halted by a paradigm shift in the 1990's. Poor outcomes and product recalls, a result from the trial-and-error design culture, led orthopedic societies around the world to install tools for more systematic design evaluation and data driven decision-making. In this period, many orthopedic registries were founded to enable a population-based approach to implant evaluation and selection¹⁸⁻²¹. Moreover, regulation and legislation was further intensified to better monitor and control the development of medical devices^{22,23}.

The cycle of product development and quality control has since considerably increased in duration. More thorough pre-market evaluations and post-market surveillance demands have slowed down the time-to-market for new devices, and product introductions are now often preceded by rigorous research. In that light, the work in this thesis contributes to the

development of a knee prosthesis made of polyetheretherketone (PEEK), articulating against UHMWPE, which is another attempt to introduce all-polymer TKA for its potential advantages to patients and healthcare systems.

PEEK in orthopedics

Prior to the conception of this thesis, PEEK had already been in use in orthopedic implants. Identified as a potential material for medical applications in 1987, PEEK has become a common material in dentistry, spine surgery, traumatology and small joint arthroplasties^{24,25}. The loads and torques involved in these applications are usually small enough to accommodate unfilled PEEK, while for more demanding applications the PEEK can be reinforced with carbon fiber. Carbon fiber reinforced (CFR-)PEEK combines the desired mechanical properties of the polymer with the added strength and rigidity of the carbon fiber, resulting in a strong and relatively flexible composite. These properties have made CFR-PEEK a candidate for large joint implants. Laminated CFR-PEEK in THA was proposed by Yildiz *et al.* (1996) and studied with computational finite element (FE) simulations^{26,27}. They found that the composite laminate provided more favorable stresses and deformations, compared to Cobalt-Chrome and Titanium. Different designs of injection molded CFR-PEEK hip stems, studied numerically and in an animal model, yielded similar conclusions. However, unpublished studies have shown that when CFR-PEEK is located at the bearing surface, any exposed carbon fibers heavily scratch the mating material and was deemed unfit as a TKA bearing material. These observations and the fact that large joint replacement development has mainly focused on longevity of implants and devices for younger and active patients, caused conservative adoption of PEEK technologies. A strong determinant for long-lasting implants is the wear resistance. At the start of this thesis, in 2012, several studies already had been published investigating this parameter in a variety of settings for joint replacement²⁸⁻³³. Yet, articulation of unfilled PEEK on common UHMWPE has remained uninvestigated, or at least unpublished.

Outline of this thesis

Since 2012, a consortium of investigators has initiated the investigation into unfilled PEEK-on-UHMWPE total knee arthroplasty. The above mentioned potential drawbacks, advantages and historic and regulatory considerations were identified and incorporated in the different research disciplines. This thesis contains mechanical considerations, mechanobiological parameters and a clinical/radiological review of the complete implanted TKA system, and is divided into 6 chapters.

The research questions that were addressed in these chapters are:

- 1) How safe is PEEK-on-UHMWPE TKA compared to CoCr-on-UHMWPE? (Ch 2-6)
 - Sub 1. *How does PEEK cope mechanically with activities of daily living?*
 - Sub 2. *What is the impact of altered mechanics on the underlying cement mantle?*
 - Sub 3. *Does the PEEK implant provide adequate short- and long-term fixation?*
- 2) Can PEEK improve the mechanobiology of the periprosthetic bone tissue? (Ch 2-4)
- 3) What are the consequences of PEEK TKA on clinical imaging? (Ch 7)

Chapter 2: Mechanics during normal activity

This first research chapter describes the mechanics of the TKA reconstruction during 'normal' activity. The effects of the material change from CoCr to PEEK on the load transfer through the implant, cement, and bone were assessed in a side-by-side comparison of computer models. The loading regime consisted of a standardized level gait, as prescribed in the corresponding ISO standard, to provide a first estimate of how the PEEK implant would behave.

Chapter 3: Mechanics during high-demand loading

Following the results of the standardized level gait analysis, computer models were further improved to study the reconstructed knee joint in a more demanding loading configuration. A quasi-static finite element simulation provided data on a deep flexion activity, allowing a comparison of the current and new TKA design under more strenuous circumstances. A more physiological bone model also increased the level of confidence for bone remodeling findings.

Chapter 4: Biological adaptation

Inspired by the findings of the previous two chapters, a combined experimental and numerical study was performed to investigate the effects of PEEK on the stimulus for mechanical bone stock adaptation. Paired cadaveric knees were tested and implanted with bilateral CoCr and PEEK implants. Detailed imaging of the periprosthetic bone surface yielded valuable corroboration for the computational study-component, which was employed to quantify the internal bone strains.

Chapter 5: Short-term fixation

At the start of this thesis, PEEK implant prototypes were subjected to pull-off experiments. Cemented onto bone-analogue foam they were extracted while the applied force was measured. This led to a design change of the PEEK implant cement pockets, which were tested side-by-side with CoCr implants and the first prototypes to quantify the evolution of implant fixation with implant design and to determine if the redesigned PEEK implant provide adequate fixation.

Chapter 6: Long-term fixation

To investigate the long-term stability of knee implants, experiments were performed with specimens that were previously dynamically loaded in wear tests, to investigate the effect of long-term loading on the integrity of the cement-implant interface. For this purpose, UV-sensitive dye was inserted into the experiment basins, which could migrate into cracks and gaps. UV-microscopy was then used to investigate the mechanical integrity of the cement and the implant-cement interface .

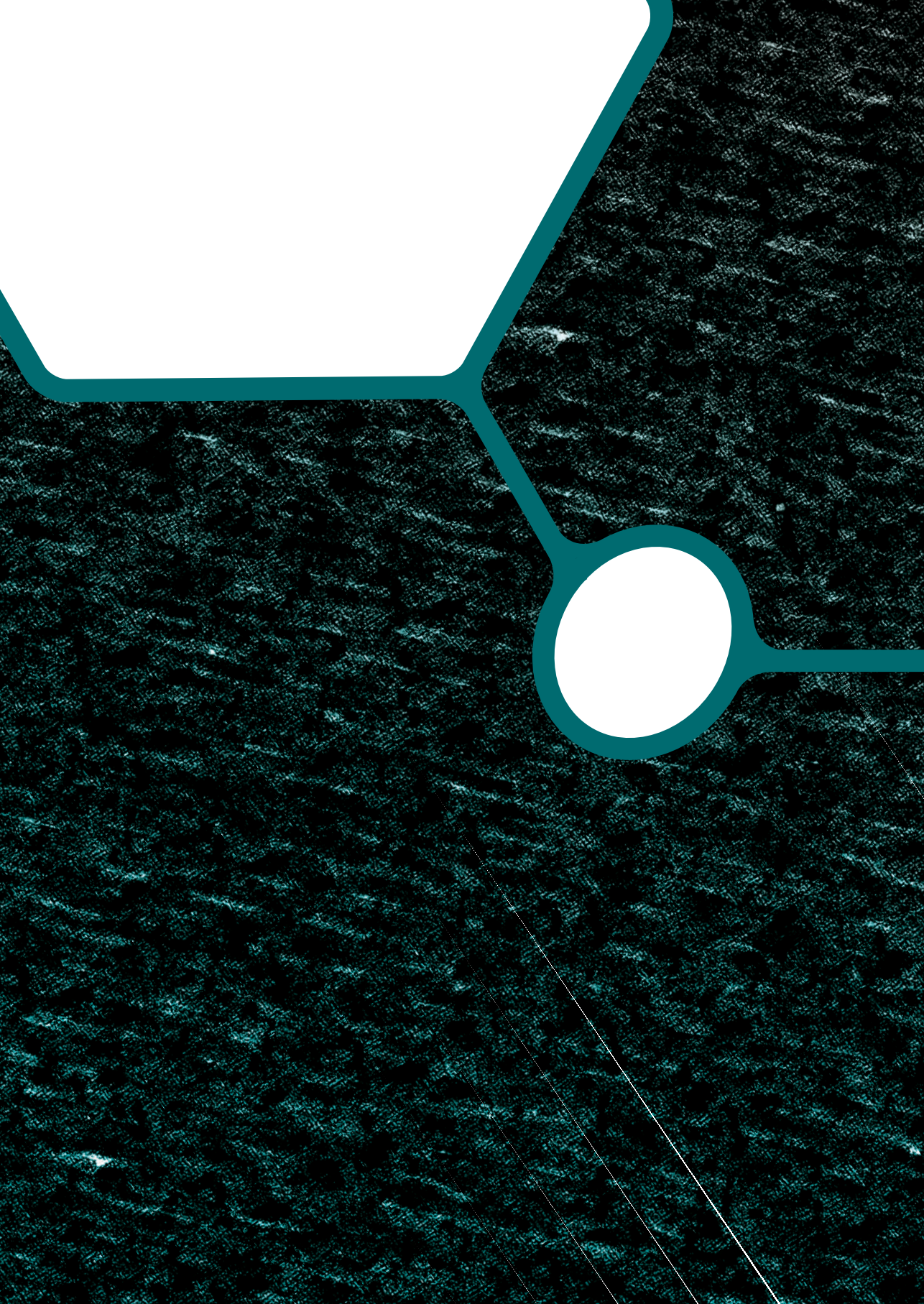
Chapter 7: Radiological assessment

The fact that PEEK is radiolucent, while standard CoCr implants are radiopaque opens up new challenges, but also possibilities for post-surgery assessment of the TKA. With a polymer implant there are more opportunities to visualize the seating of the implant and the surrounding structures. But, it does require re-training and rebuilding experience to evaluate this new implant, as the visibility of it is reduced on standard X-ray. On other imaging modalities, such as CT and MRI, it enables the visualization. This chapter studied the clinical imaging parameters with which the PEEK implant can optimally be visualized, and how imaging modalities may be applied in clinical practice.

References

1. Australian Orthopaedic Association National Joint Replacement Registry (AOANJRR). *Hip, Knee & Shoulder Arthroplasty: 2017 Annual Report*.
2. National Joint Registry for England, Wales, Northern Ireland and the Isle of Man. *2017 Annual Report*.
3. The Swedish Knee Arthroplasty Register. *2018 Annual Report*.
4. Koninklijk Nederlands Genootschap voor Fysiotherapie. *KNGF-richtlijn Artrose heup-knie 2018*.
5. Nederlandse Orthopaedische Vereniging. *Richtlijn Totale Knieprothese 2014*.
6. Kurtz SM, Ong KL, Lau E, et al. *International survey of primary and revision total knee replacement*. *Int Orthop* 2011; 35: 1783–1789.
7. Inacio MCS, Mbbs SEG, Pratt NL, et al. *Increase in Total Joint Arthroplasty Projected from 2014 to 2046 in Australia : A Conservative Local Model With International Implications*. *Clin Orthop Relat Res* 2017; 475: 2130–2137.
8. Kurtz SM, Ong KL, Lau E, et al. *Projections of Primary and Revision Hip and Knee Arthroplasty in the United States from 2005 to 2030*. *J Bone Joint Surg Am* 2007; 89: 780–785.
9. Kurtz SM, Ong KL, Lau E, et al. *Impact of the Economic Downturn on Total Joint Replacement Demand in the United States Updated Projections to 2021*. *J Bone Joint Surg Am* 2014; 96: 624–630.
10. Inacio MCS, Paxton EW, Graves SE, et al. *Projected increase in total knee arthroplasty in the United States - an alternative projection model*. *Osteoarthritis Cartilage* 2017; 25: 1797–1803.
11. Dutch Arthroplasty Register (LROI). *2018 Annual Report*.
12. Ranawat AS, Ranawat AS, Ranawat CS. *The history of total knee arthroplasty*. In: Bonnin M (ed) *The Knee Joint*. Springer-Verlag France, Paris, 2012.
13. Oonishi H, Ueno M, Kim C. *Ceramic Versus Cobalt-Chrome Femoral Components ; Wear of Polyethylene Insert in Total Knee Prosthesis*. *J Arthroplasty* 2009; 24: 374–382.
14. Oonishi H, Aono M, Murata N, et al. *Alumina versus polyethylene in total knee arthroplasty*. *Clin Orthop Relat Res* 1992; 95–104.
15. Solarino G, Piconi C, De Santis V, et al. *Ceramic Total Knee Arthroplasty: Ready to Go?*. *Joints* 2017; 5: 224–228.
16. Bradley G, Freeman M, Tuke M, et al. *Evaluation of wear in an all-polymer total knee replacement. Part 2: clinical evaluation of wear in a polyethylene on polyacetal total knee*. *Clin Mater* 1993; 14: 127–32.
17. Moore D, Freeman M, Revell P, et al. *Can a total knee replacement prosthesis be made entirely of polymers?*. *J Arthroplasty* 1998; 13: 388–395.
18. Huiskes RR. *Failed innovation in total hip replacement. Diagnosis and proposals for a cure*. *Acta Orthop Scand* 1993; 64: 699–716.
19. Torre M, Romanini E, Zanoli G, et al. *Monitoring Outcome of Joint Arthroplasty in Italy: Implementation of the National Registry*. *Joints* 2017; 5: 70–78.
20. Sérgio L, Gomes M, Roos MV, et al. *Advantages and limitations of national*

- arthroplasty registries. *The need for multicenter registries: the Rempro-SBQ*. Rev Bras Ortop 2017; 52: 3–13.
21. Serra-sutton V, Allepuz A, Espallargues M, et al. *Arthroplasty registers: A review of international experiences*. Int J Technol Assess Health Care 2009; 25: 63–72.
 22. *Regulation (EU) 2017/745 of the European Parliament and of the Council on medical devices, amending Directive 2001/83/EC, Regulation (EC) No 178/2002 and Regulation (EC) No 1223/2009 and repealing Council Directives 90/385/EEC and 93/42/EE*. Brussel, 2017.
 23. MedTech Europe. *Code of Ethical Business Practice*. 2017.
 24. Kurtz S, Devine J. *PEEK biomaterials in trauma, orthopedic, and spinal implants*. Biomaterials 2007; 28: 4845–69.
 25. Lee W, Koak J, Lim Y, et al. *Stress shielding and fatigue limits of poly-ether-ether-ketone dental implants*. J Biomed Mater Res Part B 2012; 100B: 1044–52.
 26. Yildiz H, Ha SK, Chang FK. *Composite hip prosthesis design. I. Analysis*. J Biomed Mater Res 1997; 39: 92–101.
 27. Yildiz H, Chang FK, Goodman S. *Composite hip prosthesis design. II. Simulation*. J Biomed Mater Res 1997; 39: 102–119.
 28. Scholes SC, Unsworth A. *The wear performance of PEEK-OPTIMA based self-mating couples*. Wear 2010; 268: 380–387.
 29. Scholes SC, Unsworth A. *Pitch-based carbon-fibre-reinforced poly (ether-ether-ketone) OPTIMA assessed as a bearing material in a mobile bearing unicondylar knee joint*. Proc Inst Mech Eng H 2009; 223: 13–25.
 30. Wang A, Lin R, Stark C, et al. *Suitability and limitations of carbon fiber reinforced PEEK composites as bearing surfaces for total joint replacements*. Wear 1999; 225–229: 724–727.
 31. Polineni VK, Wang A, Essner A, et al. *Characterization of carbon fiber-reinforced PEEK composite for use as a bearing material in total hip replacements*. In: Jacobs J, Craig T (eds) *Alternative Bearing Surfaces in Total Joint Replacement*. West Conshohocken, PA: ASTM International, 1998, pp. 266–273.
 32. Howling GI, Sakoda H, Antonarulajah A, et al. *Biological response to wear debris generated in carbon based composites as potential bearing surfaces for artificial hip joints*. J Biomed Mater Res Part B 2003; 67: 758–764.
 33. Davim JP, Marques N, Baptista AM. *Effect of carbon fibre reinforcement in the frictional behaviour of Peek in a water lubricated environment*. Wear 2001; 251: 1100–1104.



Chapter 2

A preclinical numerical assessment of a polyetheretherketone femoral component in total knee arthroplasty during gait

de Ruiter L, Janssen D, Briscoe A, Verdonschot N. A preclinical numerical assessment of a polyetheretherketone femoral component in total knee arthroplasty during gait. *Journal of Experimental Orthopaedics* 2017; 4(1): 3

Introduction

Total knee arthroplasty (TKA) is a highly effective procedure for patients who suffer from severe chronic knee pain and injury. In the USA and Europe combined, over one million implantations are performed every year, which have high survival rates of up to 97% after 10 years¹⁻⁵. Despite its success, failure of the reconstruction is still a matter of concern. Most causes for revision can be summarized in five failure modes: aseptic loosening, infection, polyethylene wear/osteolysis, instability and periprosthetic bone fractures⁶⁻⁸. Literature is not always in agreement about the underlying mechanisms for these types of failure. At least three of these failure modes can be induced (not exclusively) by stress shielding. As bone turnover is regulated by mechanical loading, stress shielding will eventually lead to a loss of bone stock (osteolysis/resorption), which in turn can lead to aseptic loosening of the implant or, to a lesser extent, can weaken the bone such that it will fracture^{9,10}. Additionally, revision surgery is complicated by poor bone stock, even if this is not the reason for revision.

One possible solution to these problems is the use of more compliant materials that allow loads to be distributed more physiologically over the periprosthetic bone. Although the effects of a more compliant implant material have hardly been studied, a small number of studies can be found in which the conventional metal-on-polymer was replaced with a polymer-on-polymer design^{11,12}. Both studies describe the use of a polyacetal (Delrin[®]) femoral implant against polyethylene. During those studies the implants did not show signs of failure through fracture or wear after a minimum follow-up period of 5 years. Nonetheless, the implant was discontinued due to a decreased survival of the proposed implant, as a consequence of infection caused by poor packaging^{11,12}. Although hypothesized in the polyacetal implant study, none have investigated the effect of a low-stiffness implant on the bone stock.

In this study we introduce a novel polyetheretherketone (PEEK) femoral component combined with an ultra-high molecular weight polyethylene (UHMWPE) tibial component. PEEK is generally known for its rigidity, durability and biocompatibility, and has previously been used in spinal and cranio-maxillofacial surgery, upper extremity arthroplasty and fracture fixation devices¹³. Since the late 1990's, applications are also considered for total hip replacement¹⁴⁻¹⁸.

Changing the implant material will also have an effect on the stress distribution in the reconstruction and could result in local stress intensities in the implant itself and in the underlying cement mantle, potentially causing implant fracture or cement failure. Furthermore, PEEK will bond differently with bone cement, even when the surface features are similar. To that end, fixation at the cement-implant interface needs to be investigated.

Ultimately, new implants and new designs need to be assessed in controlled clinical studies. However, to minimize patient risks extensive pre-clinical evaluations need to be performed. The aim of this study is to explore the feasibility of using a PEEK femoral component in TKA by assessing a number of aspects related to the implant mechanical integrity and its fixation. Furthermore, we assessed the potential benefit of reduced stress shielding of PEEK relative to metal.

Materials and methods

We evaluated a Cobalt-Chromium (CoCr) and PEEK implant using quasi-static finite element simulations (Marc/Mentat 2012, MSC Software Co, Newport Beach, CA, USA) for level walking and adopted the required kinematic and kinetic input for gait from the ISO 14243-1 standard¹⁹. The geometry requirements included a load applicator to which the tibial component was attached (Figure 1). All solid elements were meshed with four-noded tetrahedral elements and an average edge length of 2.5mm, consistent with convergence testing of a similar model²⁰. Interface elements were meshed using six-noded cohesive elements.

Boundary conditions

The applicator was loaded via two hinge joints located on the anterior and posterior side, biased slightly medially to allow for a medial-lateral load distribution. Between these points the varus/valgus axis was situated, around which the applicator was free to rotate. This axis could also move and rotate within the transverse plane, but was restricted in flexion/extension. Together with bone cement and the tibial implant, this part is further on referred to as the tibial construct. Knee flexion was controlled by the femoral construct, consisting of the femoral implant, a layer of bone cement and a distal femur. The knee flexion axis was determined anatomically and fixed during the gait cycle. Medial-lateral translation of the femoral construct along this axis was restricted. These constraints allowed the knee flexion angle to be determined arithmetically and controlled by a node in the hip joint center, which could move in the sagittal plane. The hip joint center control node was attached to the proximal end of the distal femur with stiff springs. Degrees of freedom that were restricted in one construct were allowed in the other, enabling any relative tibiofemoral motion to occur.

Loading conditions

Following the ISO 14243-1 standard, the tibial construct was loaded with three components of load. The first, and most pronounced, was the axial force. This force ran parallel to the tibial axis and represented the ground reaction force. Secondly, an anterior-posterior (AP) force was applied, representing the femoral roll-back/forward mechanism. Finally, a rotational torque was included around the longitudinal axis of the tibia, representing internal/external rotation of the lower leg during gait. Excessive motion resulting from the tibial load application

and degrees of freedom was damped by two components. One component limited AP translation, the other limited internal/external rotation, representing ligaments and soft tissues, respectively. Both constraints were formulated as bilinear springs with a stiffness and slack length provided by the ISO 14243-1 standard. The tibiofemoral friction coefficient was set at 0.2 for both CoCr-UHMWPE and PEEK-UHMWPE bearing couples. No frictional data specific for the PEEK-UHMWPE bearing couple is available, hence the parameter was kept the same for both and set slightly high to not underestimate its contribution to the predicted stresses.

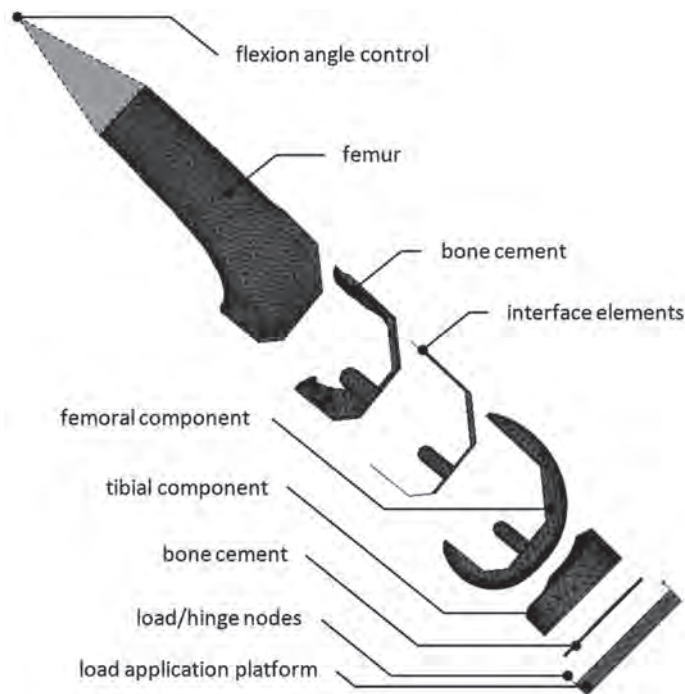


Figure 1. The finite element model and its components.

The gait cycle, as prescribed by the ISO standard was discretized into 100 increments. Due to low contact forces and a relatively high tibial rotational moment, the congruency of the femoral and tibial components could not prevent numerical instabilities during the swing phase. This was resolved by advancing the peak torque in the swing phase of the gait cycle by 3%, restoring the balance between contact forces and torque. Low contact forces in the swing phase meant this adjustment had no significant effect on the stresses in the model.

Geometry and material properties

The implant that was used in this study was a right-sided posterior cruciate ligament retaining cemented femoral implant with a cemented all-poly UHMWPE tibial component. The edges of cement pockets in the femoral component were not modelled, nor were the mechanical interlock features on the bottom of the tibial component, to avoid numerical artefacts. The cement layer was modelled with full coverage and a thickness of 1 millimeter, corresponding to manufacturer specifications.

Material properties for the UHMWPE, CoCr, PEEK and bone cement (polymethyl-methacrylate, PMMA) were provided by the manufacturers of the respective components. Both the geometry and the material properties of the distal femur were obtained from a CT scan of an 81-year old male. The image grey values were linearly scaled between physiological Young's Moduli for distal femora (0-20 GPa) and assigned to the bone elements²¹⁻²³. For evaluating stress shielding, a reference model was used in which the entire femoral construct received material properties from CT data, hence, having the same geometry, yet different material properties (Table 1). To evaluate fixation of the femoral component, the model was expanded with a zero-thickness interface layer between the implant and bone cement. These cement-implant interface elements were given properties that reflected the cohesive behavior of bone cement and CoCr/PEEK (Table 1). Failure, or debonding/loosening, was determined by providing failure criteria for the interface elements. Both interface properties and failure criteria were obtained experimentally or were taken from literature²⁴⁻²⁶. As PEEK-PMMA interface properties are not available, the same values were used as for the CoCr-PMMA interface, with the exception of shear strength, which was experimentally determined at approximately half the strength of CoCr-PMMA.

Table 1. Material properties.

Material	Young's modulus (MPa)	Poisson's ratio	Yield strength (MPa) *
CoCr	210,000	0.3	600/600
PEEK-Optima®	3,700	0.362	117/90
UHMWPE	1,100	0.42	n/a
PMMA	2,866	0.3	97/40
Femur	1-20,000	0.3	n/a
CoCr-PMMA Interface	5,732/57.32/151.36*	n/a	70/2.1/8
PEEK-PMMA Interface	5,732/57.32/151.36*	n/a	70/2.1/4

* Compressive/Tensile/(Shear)

Outcome measures

The model was used to investigate the relative safety of PEEK as compared to CoCr on the femoral implant, bone cement and fixation, and to study the changes in bone remodeling

stimuli of the periprosthetic region. The principal stresses were analyzed for 1) the femoral component and 2) the cement mantle. Both implant and cement mantle of the CoCr and PEEK constructs were compared to one another to determine relative mechanical safety. Fixation of the implant was analyzed at the 3) cement-implant interface using an adopted Hoffman failure index (FI), which is an arithmetic combination (Equation 1) of the normal (σ_n) and shear (σ_s) stress, with respect to the tensile (S_t), compressive (S_c) and shear (S_s) strength^{24,27}.

$$\begin{aligned} \sigma_n \geq 0 &\rightarrow FI = \frac{1}{S_s} \sigma_s + \frac{1}{S_t} \sigma_n \\ \sigma_n < 0 &\rightarrow FI = \frac{1}{S_t S_c} \sigma_n^2 + \left(\frac{1}{S_t} - \frac{1}{S_c} \right) \sigma_n + \frac{1}{S_s^2} \sigma_s^2 \end{aligned} \quad \text{Equation 1.}$$

An FI above 100% would indicate instant failure. Finally, 4) the strain energy density (SED) distribution in the bone was analyzed to assess the stress shielding effects. As demonstrated in many bone remodeling studies a relative increase in SED would indicate stimulation of bone growth, a reduction would induce bone resorption^{9,15,28}. Excessively high SED values would be associated with bone failure²⁹.

Results

The results presented were chosen at the moments at which peak stresses occurred in the femoral implant, which coincided with heel strike (HS), mid-stance (MS) or toe-off (TO). At these moments, the contact forces were the highest, representing the most detrimental instances in the simulated gait cycle.

Stresses within the femoral component

Changing CoCr to PEEK altered the stress patterns found in the femoral component notably. The CoCr device showed compressive stress intensities at the tibiofemoral contact site and the intercondylar notch, which were of similar magnitude. In the PEEK component the stress intensities at the contact site were also present, but no intensity was present at the notch site (Figure 2). At the internal surfaces the location of the most prominent CoCr tensile stresses was closely related to the compressive patterns exteriorly, with the exception of an additional intensity at the tip of the anterior flange. The higher PEEK tensile stresses all accumulated in the anterior flange (Figure 3).

The peak compressive stresses within the components were 75 MPa and 34 MPa for CoCr (TO) and PEEK (MS), respectively, which was well below the compressive yield stress of 600 and 117 MPa. Peak tensile stresses reached up to 53 and 12 MPa for CoCr (HS) and PEEK (TO), respectively. Considering the yield stress of both materials, PEEK was more at risk in

compression than CoCr (13% vs. 29% of yield stress), and similarly loaded in tension (13% vs. 9% of yield stress). As a result, the factor of safety for PEEK was lower under compression, but similar in tension.

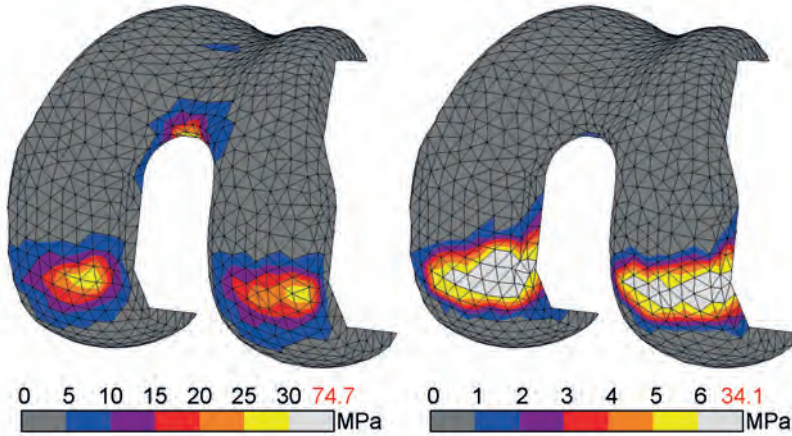


Figure 2. Compressive stress for CoCr (l) and PEEK (r) femoral component. Stresses exceeding 5% of respective yield stress (600 MPa vs. 117 MPa) are colored white, with the peak stress depicted in red.

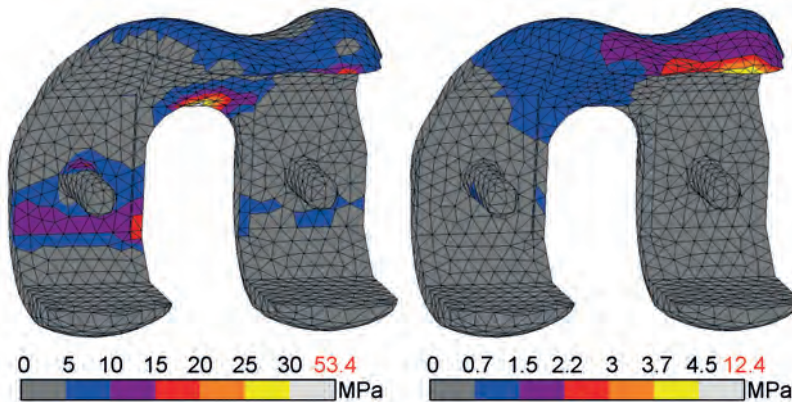


Figure 3. Tensile stress for CoCr (l) and PEEK (r) femoral component. Stresses exceeding 5% of respective yield stress (600 MPa vs. 90 MPa) are colored white, with the peak stress depicted in red.

Stresses within the bone cement

Distinct differences were present in the bone cement below the femoral component. The stiff CoCr component transferred compressive loads mainly in the pegs and cement pocket faces perpendicular to the applied force, away from the tibiofemoral contact site. The highest compressive cement stress occurred during toe-off with 21 MPa (Figure 4). Tensile stresses at that moment reached up to 42 MPa at the tip of the anterior flange (Figure 5). During the

entire gait cycle the cement mantle supporting the PEEK implant was loaded predominantly in the posterodistal area, with no other distinct regions of stress intensities. The peak compressive stresses occurred during mid-stance (14 MPa). The peak tensile stresses were found at heel strike (13 MPa). Cement stresses were well below PEEK/CoCr compressive yield stress (14% vs. 21%). The cement mantles experienced up to 33% and 105% of tensile yield stress for PEEK and CoCr respectively. This resulted in a higher factor of safety for PEEK in both compression and tension.

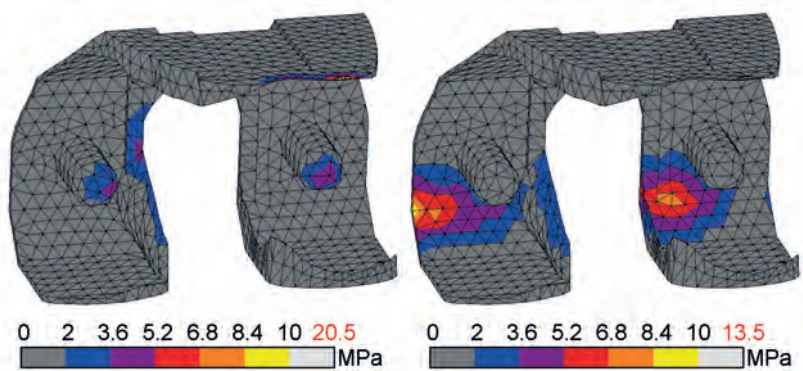


Figure 4. Compressive stress for CoCr (l) and PEEK (r) bone cement. Stresses exceeding 10% of yield stress (97 MPa) are colored white, with the peak stress depicted in red.

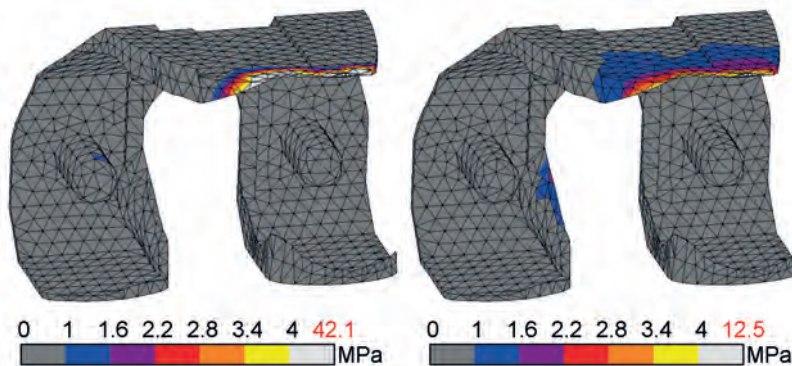


Figure 5. Tensile stress for CoCr (l) and PEEK (r) bone cement. Stresses exceeding 10% of yield stress (40 MPa) are colored white, with the peak stress depicted in red.

Assessment of cement-implant interface failure

The distribution of compressive stresses acting on the interface was similar to that occurring in the bone cement. For the CoCr implant, the highest compressive stress was 23.8 MPa, at toe-off, whilst PEEK generated the highest compressive stress of 15.6 MPa at mid-stance. The total surface area that underwent compression during the gait cycle was largest in CoCr, but generally at a low stress level, in contrast to PEEK, where the surface area was smaller, but with higher stress levels.

The tension patterns suggest that the implant 'opened up' during gait. When the component was loaded distally under compression (during stance phase), the flanges parallel to the loading direction (i.e. the posterior condyles and anterior flange) were moving outward, away from the bone. In both implants this phenomenon occurred, albeit to a different extent. The total surface area in the PEEK construct undergoing tension was higher than for CoCr. However, the loads were distributed over a larger area, resulting in lower stress levels. The CoCr interface was loaded in tension in the most proximal region of the posterior condyles and, distinctly, in the proximal region of the anterior flange. The maximum tensile stress for the PEEK implant was 0.48 MPa, at heel strike, and 0.85 MPa for the CoCr implant, at toe-off.

There was also a pronounced difference between the shear interface stress pattern around the PEEK and CoCr implants. In the CoCr construct all areas parallel to the loading direction underwent relatively high shear stresses. The most affected was the anterior flange, which peaked at 2.2 MPa at toe-off. In the model with the PEEK implant, shear stresses were mainly found in the distal interface and posterior chamfers areas. The highest shear stress around the PEEK implant of 1.4 MPa occurred during mid-stance.

Failure patterns did not change throughout gait for each implant, but did differ between implants. For CoCr the maximum FI was found during toe-off (FI=67%). PEEK showed a peak FI of 45% at heel strike. With both CoCr and PEEK the affected area was concentrated at the proximal anterior flange, where also tensile and shear stresses mainly occurred (Figure 6). These data suggest a higher factor of safety for the PEEK construct interface compared to CoCr.

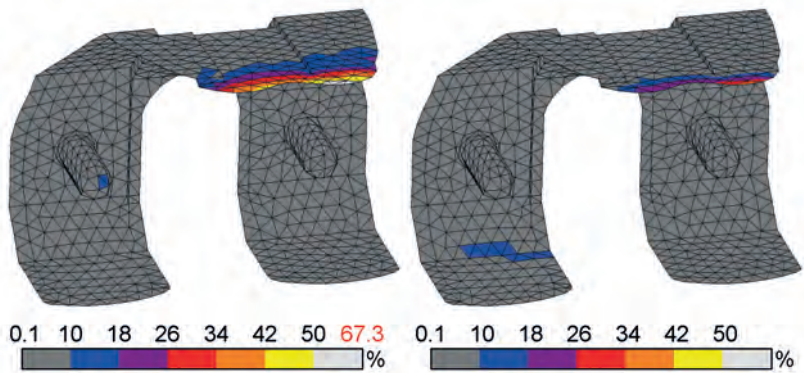


Figure 6. Hoffman failure criterion for CoCr (l) and PEEK (r) cement-implant interface. Peak FI is depicted in red.

Strain energy density levels in the periprosthetic bone

Relative to the 'intact' case, SED levels around the CoCr implant were lower and expanded over a smaller amount of the bone volume during the gait cycle. Higher levels of SED were located in the medial intercondylar notch and extended above the condyles to the entire width of the posterior periprosthetic femur. This pattern recurred in the PEEK configuration. Importantly, additional regions of higher SED were found in the posterior chamfers of the condyles and extended throughout the bone to the proximal section of the periprosthetic femur (Figure 7). Both CoCr and PEEK peaked similarly with 0.014 and 0.016 Nmm/mm³, respectively. The total amount of strain energy was different, with the PEEK strain energy accumulating more distally. Hence, the SED pattern was more similar to the simulated intact case than the one generated around the CoCr implant (Figure 7).

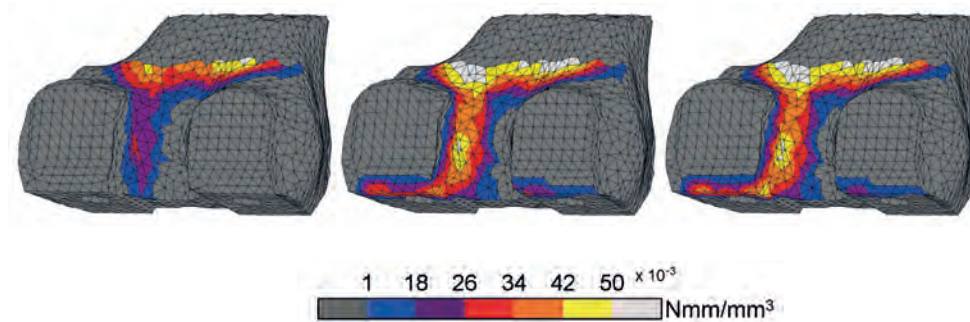


Figure 7. CoCr (l), PEEK (m) and 'intact' (r) strain energy density in the periprosthetic femur.

Element-by-element comparisons between the three cases at toe-off emphasized the strong correlation between 'intact' and PEEK throughout the entire periprosthetic region; in three 10mm sections the slope of the least-squares curve (0.98, 0.99 and 0.98) is near-ideal (Figure 8). Stress shielding in the CoCr reconstruction is most obvious in the distal 10 mm section with a slope of 0.15. This improved towards the metaphysis (0.57) but remained lower than PEEK after 30 mm (0.71). The slopes showed statistically significant differences ($p < 0.05$) in all sections.

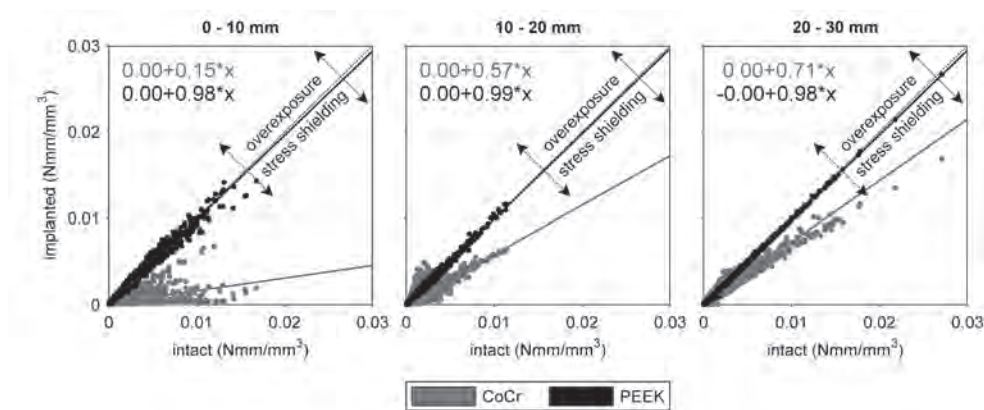


Figure 8. Correlation of strain energy densities between an 'intact' reference and de CoCr and PEEK reconstructions in 10 millimeters thick slices from distal to proximal periprosthetic femur at toe off.

Discussion

Overall, we observed that the PEEK construct generated different stress/strain patterns in all areas of interest for this study. The loads were passed on throughout the reconstructed knee in a manner that appeared to be closer to a physiological situation than a CoCr device³⁰.

The potential failure mechanisms for the implant and cement mantle were different between the devices. PEEK reduced the factor of safety in compression, while in tension the factor of safety for implant, cement mantle and cement-implant interface was increased. Previous studies earlier highlighted the dominant role of tensile loads in failure of reconstructions with metal knee implants³¹⁻³⁵. This implies PEEK may be beneficial with regard to tensile loads under gait loading conditions. However, the PEEK and implant-cement interface stress levels may increase with body-mass index (BMI), more demanding activity levels, or sub-optimal fixation, which have not been investigated here. The mechanical survival of polymer femoral components has previously been demonstrated in a clinical follow-up study by Moore *et al.* (1998), who published on a polyacetal femoral component in combination with a UHMWPE tibial component. After 10 years of postoperative follow-up none of the cemented implant failures were attributed to implant fracture, aseptic loosening or wear of the femoral component¹². Polyacetal has mechanical properties similar to PEEK, implying that the reduced factor of safety for the implant as found in the present study, should be sufficient to accommodate the risks of implant fractures³⁶.

Comparison of the bone strains between both components and the surrogate intact case suggests that the more compliant PEEK indeed reduces stress shielding. Bone strains were more similar between intact and PEEK than between intact and CoCr. The most distinct differences were found at the distal chamfers, where strains were very low in the CoCr construct compared to PEEK and the intact bone, as suggested in several previous studies^{17,37-39}. Although bone adaptation was not simulated in the current study, the current remodeling stimulus patterns coincide with areas of bone loss as reported in the literature^{9,10,40}.

The model that was utilized for this study was limited to level gait as for time-dependent parameters, such as bone remodeling and fatigue, normal walking is considered most determinative^{41,42}. For construct integrity assessment, however, higher demanding activities may be more appropriate, such as squat or stair ascend. In the current model most properties of the cement-implant interface for CoCr were adopted from literature²⁴. The properties of the PEEK-PMMA interface were assumed to be similar to that of CoCr, although it is expected that the interface stiffness will be lower, and likely also the strength in tension. These parameters should be determined further in an experimental setup, after which they can be incorporated in the current model to investigate their effect on the structural integrity of the PEEK femoral reconstruction. Likely, the difference in interface properties will affect the stress magnitudes, but the relative stress distributions will be very similar to what has been simulated. Thirdly, for the comparison with an intact knee, we did not recreate the intact geometry and kinematics of the knee, but only changed the material properties. Obviously, the femoral geometry does not align exactly with the natural bone. This means that cortical bone is not always mapped to the contacting areas and softer elements will alter the natural stress distribution in those

areas. Towards the periprosthetic region the mismatch will be smaller and compliant elements will have encountered stiffer elements to pass on the stresses, cancelling out part (but not all) of the influence of mismatched Young's moduli. We decided to use the same mesh and map CT properties to the construct to avoid influence of differences in mesh geometries, just to see the effect of the change in Young's modulus, and whether or not the PEEK representation is likely to be closer to the intact situation. It is likely that the comparison that was made for stress shielding will be altered, but we do expect the same trend that was observed in this study. In addition, the SED distributions as determined in the current study only represent the initial condition. To study the changes in bone density, a remodeling simulation is required, preferably incorporating additional loading scenarios besides normal walking.

Conclusions

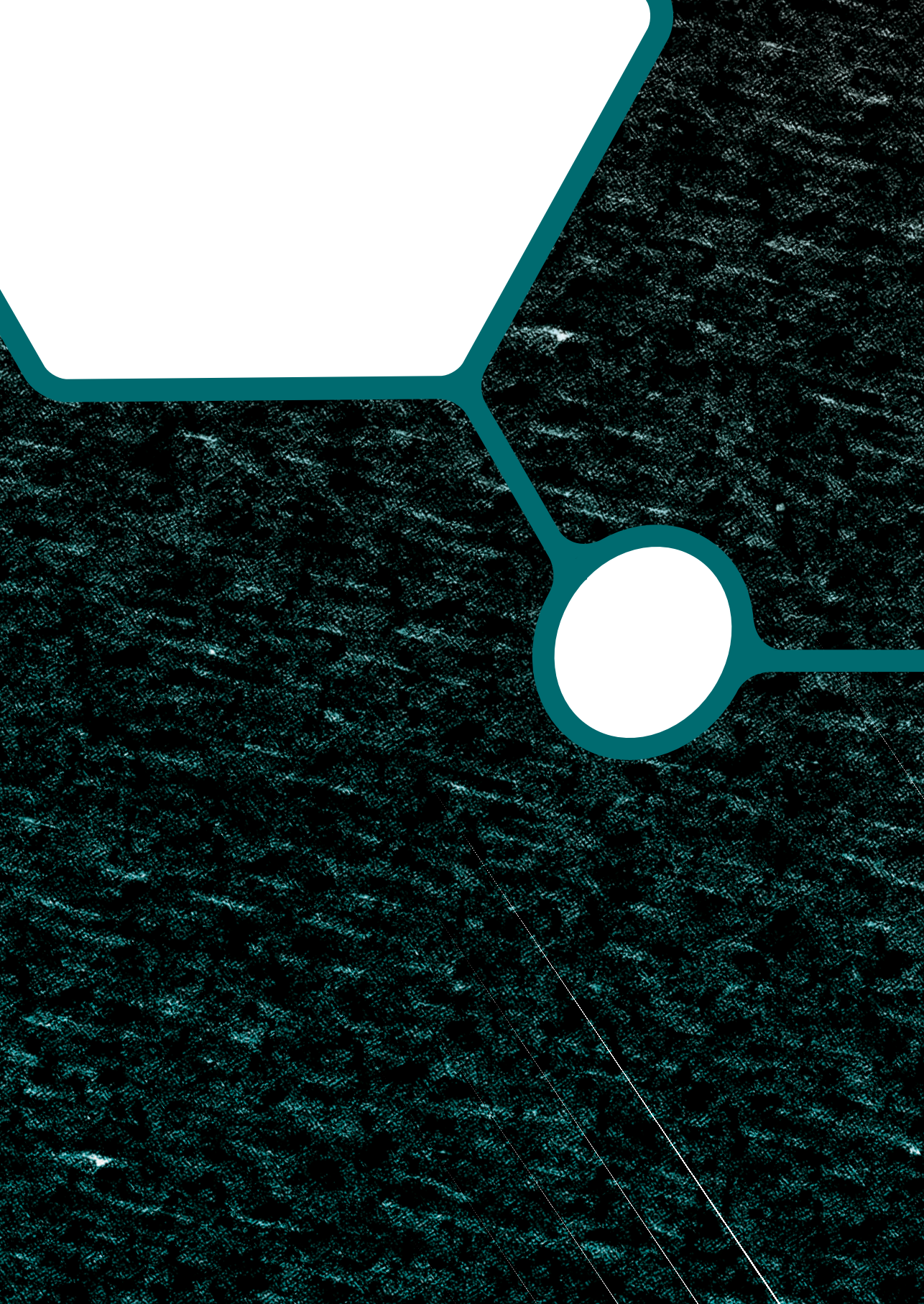
Our aim was to provide insight into the femoral stress distribution when changing the material of the femoral component from CoCr to PEEK. We wanted to investigate whether a PEEK implant would be a feasible solution to relevant issues in current applications. Therefore, as a minimum requirement, we started with the most relevant activity: level walking. This study indicates that during a standard ISO gait cycle the performance of the PEEK femoral component is not inferior to the CoCr implant and that it can reduce the periprosthetic stress shielding. If potential harm of a new implant is excluded during preclinical research, less adverse events can be expected in clinical use. Patients can then benefit from the improved mechanobiological aspects PEEK can deliver over conventional TKA devices.

References

1. National Joint Registry for England, Wales and Northern Ireland. *2013 Annual Report*. 2013.
2. Australian Orthopaedic Association National Joint Replacement Registry (AOA-NJRR). *2013 Annual Report*.
3. Swedish Knee Arthroplasty Register. *2013 Annual Report*.
4. Victor J, Ghijselings S, Tajdar F, et al. *Total knee arthroplasty at 15-17 years: does implant design affect outcome?*. *Int Orthop* 2014; 38: 235–41.
5. Niinimäki T, Eskelinen A, Mäkelä K, et al. *Unicompartmental knee arthroplasty survivorship is lower than TKA survivorship: a 27-year Finnish registry study*. *Clin Orthop Relat Res* 2014; 472: 1496–501.
6. Le D, Goodman S, Maloney W, et al. *Current modes of failure in TKA: Infection, instability, and stiffness predominate*. *Clin Orthop Relat Res* 2014; 472: 2197–200.
7. Kasahara Y, Majima T, Kimura S, et al. *What are the causes of revision total knee arthroplasty in Japan?*. *Clin Orthop Relat Res* 2013; 471: 1533–8.
8. Schroer W, Berend K, Lombardi A, et al. *Why are total knees failing today? Etiology of total knee revision in 2010 and 2011*. *J Arthroplasty* 2013; 28: 116–9.
9. Lenthe G Van, Willems M, Verdonschot N, et al. *Stemmed femoral knee prostheses: effects of prosthetic design and fixation on bone loss*. *Acta Orthop Scand* 2002; 73: 630–637.
10. Lavernia CJ, Rodriguez J a, Iacobelli D a, et al. *Bone mineral density of the femur in autopsy retrieved total knee arthroplasties*. *J Arthroplasty* 2014; 29: 1681–6.
11. Bradley G, Freeman M, Tuke M, et al. *Evaluation of wear in an all-polymer total knee replacement. Part 2: clinical evaluation of wear in a polyethylene on polyacetal total knee*. *Clin Mater* 1993; 14: 127–32.
12. Moore D, Freeman M, Revell P, et al. *Can a total knee replacement prosthesis be made entirely of polymers?*. *J Arthroplasty* 1998; 13: 388–395.
13. Kurtz S, Devine J. *PEEK biomaterials in trauma, orthopedic, and spinal implants*. *Biomaterials* 2007; 28: 4845–69.
14. Nakahara I, Takao M, Bandoh S, et al. *In vivo implant fixation of carbon fiber-reinforced PEEK hip prostheses in an ovine model*. *J Orthop Res* 2012; 31: 485–92.
15. Ghosh R, Gupta S. *Bone remodelling around cementless composite acetabular components: The effects of implant geometry and implant-bone interfacial conditions*. *J Mech Behav Biomed Mater* 2014; 32: 257–269.
16. Pace N, Spurio S, Rizzato G. *Clinical trial of a new CF16-PEEK acetabular insert in hip arthroplasty*. In: *Abstracts from the European Hip Society Domestic Meeting. Baveno, Italy*. 2002.
17. Akay M, Aslan N. *Numerical and experimental stress analysis of a polymeric composite hip joint prosthesis*. *J Biomed Mater Res* 1996; 31: 167–182.
18. Rankin KE, Dickinson AS, Briscoe A, et al. *Does a PEEK Femoral TKA Implant Preserve Intact Femoral Surface Strains Compared With CoCr? A Preliminary Laboratory Study*. *Clin Orthop Relat Res* 2016; 474: 2405–2413.

19. International Organization for Standardization. *ISO 14243-1: Implants for surgery - Wear of total knee-joint prostheses - Part 1: Loading and displacement parameters for wear-testing machines with load control and corresponding environmental conditions for test*. 2009.
20. Zelle J, Van der Zanden AC, De Waal Malefijt M, et al. *Biomechanical analysis of posterior cruciate ligament retaining high-flexion total knee arthroplasty*. *Clin Biomech* 2009; 24: 842–849.
21. Ashman RB, Rho JY. *Elastic modulus of trabecular bone material*. *J Biomech* 1988; 21: 177–181.
22. Cuppone M, Seedhom BB, Berry E, et al. *The Longitudinal Young's Modulus of Cortical Bone in the Midshaft of Human Femur and its Correlation with CT Scanning Data*. *Calcif Tissue Int* 2004; 74: 302–309.
23. Turner CH, Rho J, Takano Y, et al. *The elastic properties of trabecular and cortical bone tissues are similar: results from two microscopic measurement techniques*. *J Biomech* 1999; 32: 437–441.
24. Zelle J, Janssen D, Peeters S, et al. *Mixed-mode failure strength of implant-cement interface specimens with varying surface roughness*. *J Biomech* 2011; 44: 780–3.
25. Murray G, White C, Weise W. *Introduction to engineering materials: behavior, properties, and selection*. Boca Raton: CRC Press, 1993.
26. Lewis G. *Properties of acrylic bone cement: state of the art review*. *J Biomed Mater Res* 1997; 38: 155–82.
27. Hoffman O. *The Brittle Strength of Orthotropic Materials*. *J Compos Mater* 1967; 1: 200–206.
28. Lerch M, Kurtz A, Stukenborg-Colsman C, et al. *Bone remodeling after total hip arthroplasty with a short stemmed metaphyseal loading implant: finite element analysis validated by a prospective DEXA investigation*. *J Orthop Res* 2012; 30: 1822–9.
29. Mirzaei M, Keshavarzian M, Naeini V. *Analysis of strength and failure pattern of human proximal femur using quantitative computed tomography (QCT)-based finite element method*. *Bone* 2014; 64: 108–14.
30. Dickinson A, Taylor A, Browne M. *The influence of acetabular cup material on pelvis cortex surface strains, measured using digital image correlation..* *J Biomech* 2012; 45: 719–23.
31. Gruen T, McNeice G, Amstutz H. *'Modes of failure' of cemented stem-type femoral components: a radiographic analysis of loosening*. *Clin Orthop Relat Res* 1979; 141: 17–27.
32. Harper E, Bonfield W. *Tensile characteristics of ten commercial acrylic bone cements*. *J Biomed Mater Res* 2000; 53: 605–16.
33. Culleton T, Prendergast P, Taylor D. *Fatigue failure in the cement mantle of an artificial hip joint*. *Clin Mater* 1993; 12: 95–102.
34. Stolk J, Verdonschot N, Murphy B, et al. *Finite element simulation of anisotropic damage accumulation and creep in acrylic bone cement*. *Eng Fract Mech* 2004; 71: 513–528.
35. Zelle J, van de Groes S, de Waal Malefijt M, et al. *Femoral loosening of high-flexion total knee arthroplasty: the effect of posterior cruciate ligament retention and bone quality reduction..* *Med Eng Phys* 2014; 36: 318–24.
36. Thompson M, Northmore-Ball M, Tanner K. *Tensile mechanical properties of polyacetal*

- after one and six months' immersion in Ringer's solution. *J Mater Sci Mater Med* 2001; 12: 883–887.
37. Boby J, Mortimer E, Glassman A, et al. *Producing and avoiding stress shielding. Laboratory and clinical observations of noncemented total hip arthroplasty.* *Clin Orthop Relat Res* 1992; 79–96.
 38. Lee W, Koak J, Lim Y, et al. *Stress shielding and fatigue limits of poly-ether-ether-ketone dental implants..* *J Biomed Mater Res Part B* 2012; 100B: 1044–52.
 39. Gillies R, Hogg M, Donohoo S, et al. *A finite element analysis of the reconstructed distal femur and the influence of implant material properties on the trabecular loading patterns.* In: *Proceedings of the 8th congress of the European Federation of National Associations of Orthopaedics and Traumatology.* Florence, Italy, 2009.
 40. Järvenpää J, Soininvaara T, Kettunen J, et al. *Changes in bone mineral density of the distal femur after total knee arthroplasty: a 7-year DEXA follow-up comparing results between obese and nonobese patients..* *Knee* 2014; 21: 232–5.
 41. Morlock M, Schneider E, Bluhm A, et al. *Duration and frequency of every day activities in total hip patients..* *J Biomech* 2001; 34: 873–81.
 42. Lenthe G Van, de Waal Malefijt MC, Huiskes R. *Stress shielding after total knee replacement may cause bone resorption in the distal femur..* *J Bone Joint Surg Br* 1997; 79: 117–122.



Chapter 3

The mechanical response of a polyetheretherketone femoral knee implant under a deep squatting loading condition

de Ruiter L, Janssen D, Briscoe A, Verdonchot N. The mechanical response of a polyetheretherketone femoral knee implant under a deep squatting loading condition. *Proceedings of the Institution of Mechanical Engineers, Part H: Journal of Engineering in Medicine* 2017; 231(12): 1204-1212

Introduction

Over the last few years efforts have been made to study the potential of an all-polymer total joint replacement¹⁻⁷. In the area of total knee arthroplasty (TKA) these efforts started with carbon-fiber reinforced (CFR) polyetheretherketone (PEEK) on ultra-high molecular weight polyethylene (UHMWPE) and were aimed at understanding the wear of this bearing couple. Research revealed that CFR-PEEK was no suitable mating surface for UHMWPE in TKA³. Non-CFR (virgin) PEEK seems to have overcome these problems, paving the way for further mechanical studies^{3,6,7}.

The present study adds to the mechanical understanding of a PEEK femoral TKA implant by focusing on the mechanical integrity of the reconstruction. PEEK is inherently weaker than conventional Cobalt-Chromium (CoCr) alloys, and is also much more compliant (3.7 GPa vs. 210 GPa). The differences in material properties may entail potential risks with regard to the integrity of the implant and underlying cement mantle. On the other hand, the more compliant PEEK could also promote more physiological loading of the periprosthetic bone^{6,8-10}, thereby reducing stress shielding observed in CoCr components in total knee arthroplasty¹¹⁻¹⁶. Rankin at al. demonstrated in an experimental study with digital image correlation techniques that a PEEK femoral component generates more physiological surface strains than a CoCr implant in a synthetic bone under stance phase loading conditions⁶. In the present finite element (FE) study, we are able to get a more holistic perspective of the effects of a PEEK component on the stresses and strains within the bone and implanted materials.

Previously we used finite element analysis to evaluate the biomechanical behavior of a PEEK implant during level gait¹⁷. That study showed that it is unlikely that a PEEK implant would fail under relatively low burden circumstances. In the current study we aim to evaluate the PEEK implant design under high-demand activities. A deep squat represents one of the more demanding loading scenarios for a TKA device, as both the tibiofemoral and patellofemoral loads are substantial, which may have consequences for the mechanical integrity of the reconstruction.

In the present study we addressed the following questions regarding a deep squat: 1) Is a PEEK femoral implant strong enough to endure high-demand loading? 2) Are stresses in the cement mantle elevated with a PEEK implant? 3) Does a PEEK femoral component have potential to reduce periprosthetic bone remodeling after TKA?

Materials and methods

To perform a biomechanical study of the knee reconstruction a finite element model (MARC2012, MSC Software Corporation, Santa Ana, CA, US) of a TKA component (Maxx Freedom Knee) subjected to a deep squatting loading mode, which was earlier reported on¹⁸, was adjusted and used. This was a two-stage model in which the kinetics and kinematics were determined in a 'global' model, while the analyses of structural integrity and local load transfer were performed in a 'local' model. This method improves computational efficiency and reliability, yet retains the ability to capture deformation of the implant and femoral bone in the local model.

The global model

The global model consisted of a femoral implant, tibial implant and cement layer, proximal tibia, fibula, patella, small sections of the epiphyseal femur, the posterior cruciate ligament (PCL), patella tendon and the quadriceps tendon. The model was fixed at the proximal end of the quadriceps tendon and the backside of the femoral component (Figure 1). Distally the model was attached with springs to a node representing the ankle joint. This node transferred a constant ground reaction force from the ankle to the model. Motion in the model was then enabled by gradually releasing (elongating) the quadriceps tendon in each increment, mimicking the eccentric contraction of the quadriceps muscles, in a controlled squat from 40° to 150° of flexion. The model could further move unconstrained (6 DOF) to find a knee joint equilibrium.

The former model¹⁸ included a high-flex implant design with extended condylar curvature. However, in the current study the implant did not have these extended features which is why we introduced the possibility of load sharing between the tibial component and posterior distal femoral bone as this is known to reduce the loads on the implant *in vivo*¹⁹. Also thigh-calf contact was included, which has been shown to affect the intra-knee loading conditions²⁰. Zero friction contact between the femoral and tibial component was modelled, as friction was shown to play a negligible role in a high-demand loading scenario¹⁸. The tibiofemoral, patellofemoral and tendon contact forces that were exerted on the femoral component bearing surface during the squat were incrementally stored and later applied to three versions (intact knee, CoCr-component, PEEK-component) of the 'local' model, under the assumption that femoral contact surface material stiffness does not affect the squatting kinetics and kinematics.

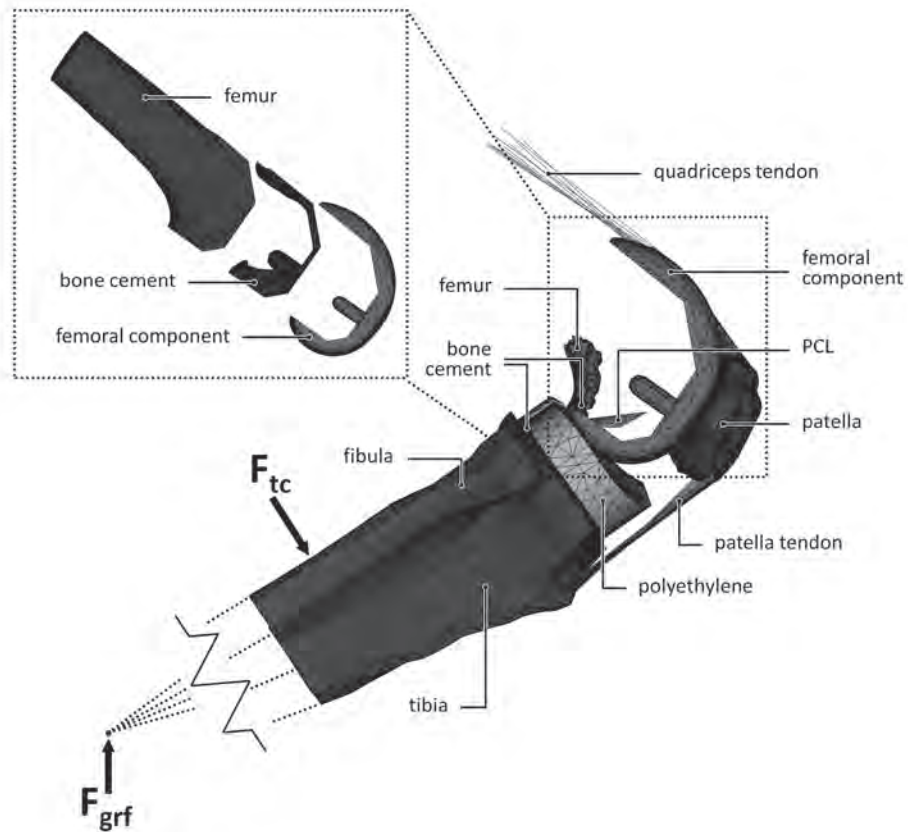


Figure 1. The global and local (top left) finite element model and its components.

The local model

The local model consisted of the distal half of the femur, a cement mantle and femoral implant with the same mesh as present in the global model (Figure 1). Both the geometry and the stiffness of the distal femur were obtained from a CT scan of an 81-year old male with no known history of bone disease. The local bone density was linearly scaled, converted to Young's moduli in a physiological range^{21–23} and assigned to the bone elements. Fully bonded conditions were assumed at the cement-bone and cement-implant interfaces. The proximal 3 centimeters of the femur were constrained for all degrees of freedom and the forces calculated from the global model were applied to corresponding locations on the local model at each increment of the squat cycle.

Material properties

Because of the preclinical nature of this research, clinical data was not available for external validation of the PEEK model. Considering the extensive experience with CoCr TKA devices

and their clinical success, the CoCr reconstruction was used as a benchmark for the PEEK model and comprised the same geometry. The impact of either PEEK or CoCr on the bone stresses and strains was assessed by the comparison to a model of the intact femur. To that end three versions of the model were adopted (intact, CoCr, and PEEK), differing in material properties, obtained from either manufacturer or literature (Table 1)^{18,21–25}. The ‘intact’ model did not differ in geometry from the PEEK and CoCr, but rather used CT bone densities throughout the entire distal femur. Elements overlapping with cartilage tissue or joint space would thus receive an analogue stiffness. Using the same mesh rather than creating a separate model of the intact femur ensured a clean comparison, without artefacts following from differences in the meshes.

Table 1. Material properties.

Material	Young's modulus (MPa)	Poisson's ratio	Yield strength (MPa) *
CoCr	210,000	0.3	600/600
PEEK-Optima®	3,700	0.362	117/90
UHMWPE	974	0.46	n/a
PMMA	2,866	0.3	97/40
Femur	1-20,000	0.3	n/a
Cortical tibia/patella	19,000	0.3	n/a
Trabecular tibia/patella	120	0.2	n/a
Cartilage	250	0.2	n/a
Tendons/ligaments	Zelle <i>et al.</i> (2011) ¹⁸	-	n/a

CoCr: cobalt-chromium; PEEK: polyetheretherketone; UHMWPE: ultra-high molecular weight polyethylene; PMMA: polymethylmethacrylate.

* Compressive/Tensile

Data analysis

For both the femoral component and cement mantle the minimal (compressive) and maximal (tensile) principal stresses were analyzed with respect to the yield stress of either PEEK or CoCr (Table 1). Besides contour plots of stresses on the geometry also the fraction of the mesh volume exposed to certain stress levels are presented. For tensile analyses the mesh volume fraction that exceeded the one million cycle tensile fatigue stress was used to identify areas that may be at risk. For CoCr and PEEK the one million cycle tensile fatigue stress was about 70% of tensile yield stress^{26,27}, for PMMA 40%²⁸. Fatigue failure as a result of compression is not plausible, and was therefore omitted in the current study^{29,30}.

Periprosthetic ‘stress shielding’ was quantified by strain energy density (SED) as this is regarded as the stimulus for bone remodelling^{31,32}. From the SED data obtained in the volume of the periprosthetic bone, a simulated sagittal DEXA reconstruction was made for qualitative

comparison with published clinical and FE studies (Figure 6). The local reduction of the SED in each TKA reconstruction was quantified by a percentage of the original (intact) stimulus. Since the SED was assumed not to be normally distributed, results were described with the median and interquartile range (IQR).

Throughout the deep squat data was recorded to obtain a stress distribution to allow for a quick overview of the effect of flexion angle on the mechanical outcome parameters. The flexion angle was determined as the sagittal angle measured between the node for ground reaction force application (moving), the center of the intercondylar space (fixed) and a node representing the hip joint (fixed). Further analyses were performed at 90° (a common angle in more frequent tasks such as sitting down), 120° of flexion (a relevant maximum post-operative flexion angle clinically observed^{33–35}), and 145° of flexion (where maximum stresses were found in the implant (Figure 2). Although the model was able to achieve a 155° flexion angle, above 145° thigh-calf contact and femoral load sharing substantially reduced the loads on the knee. To avoid inclusion of stress peaks resulting from mesh artefacts the 99th percentile of the stresses is presented.

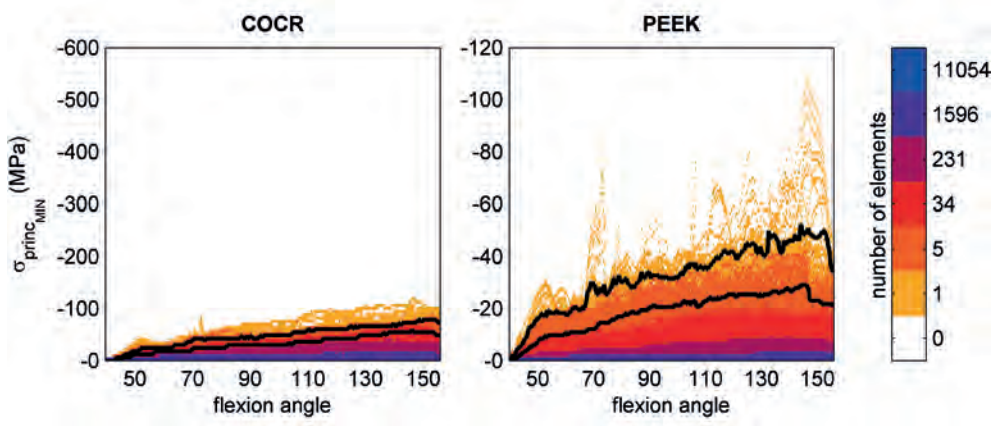


Figure 2. Compressive (minimal principal) stresses in the femoral component throughout the entire squat. Colors represent the number of elements undergoing a certain stress level. The bottom black line marks the stress level below which 99% of the implant elements are loaded, the top black line marks 99.9%.

Results

Stresses in the femoral component

In both implants the stresses increased with knee flexion. While in the PEEK implant compressive (minimal principal) stresses accumulated in the areas where tibiofemoral and patellofemoral contact takes place, for CoCr these were distributed more along the implant

surface (Figure 3). Moreover, the patellofemoral joint did not generate notable compressive stresses at the CoCr internal surfaces. Overall, absolute compressive stresses in the CoCr implant (60 MPa at 145°) were higher than those found in the PEEK femoral component (30 MPa at 145°). Relative to yield stress, the PEEK implant was subjected to higher compressive stresses than the CoCr implant. The PEEK implant was loaded up to 26% of yield stress versus 10% for CoCr in compressive scenarios.

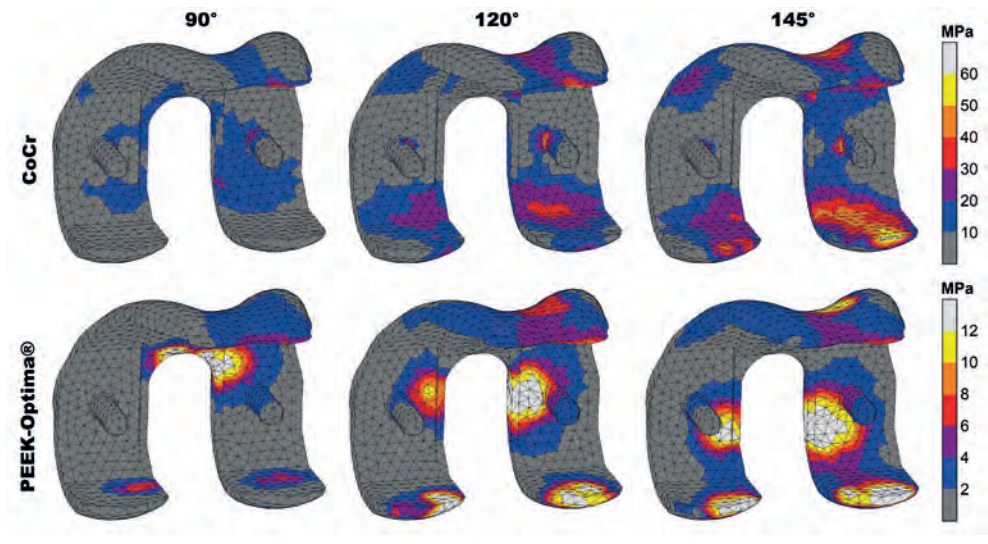


Figure 3. Compressive stress patterns in the femoral component. Stresses are displayed up to 10% of respective yield stress (600 MPa vs. 117 MPa) to visualize the distribution at increasing flexion angles.

For tensile (maximal principal) stresses both absolute and relative stresses were higher in the CoCr implant, which accumulated mostly in the intercondylar notch of both implants. Additionally, the CoCr implant included a stress concentration at the posterior condylar surface, probably caused by bending due to deep flexion tibiofemoral contact. In the PEEK implant these forces were absorbed locally at the contact site instead of initiating a bending moment in the condyles. The maximum tensile stresses in the implants were 55 MPa (145°) and 4 MPa (120°) for CoCr and PEEK, respectively. Relative to the yield stress this amounted to 9% for CoCr and 0.4% for the PEEK implant. In total 83% of the CoCr implant material was subjected to tensile stresses versus 75% of the PEEK device (Figure 4).

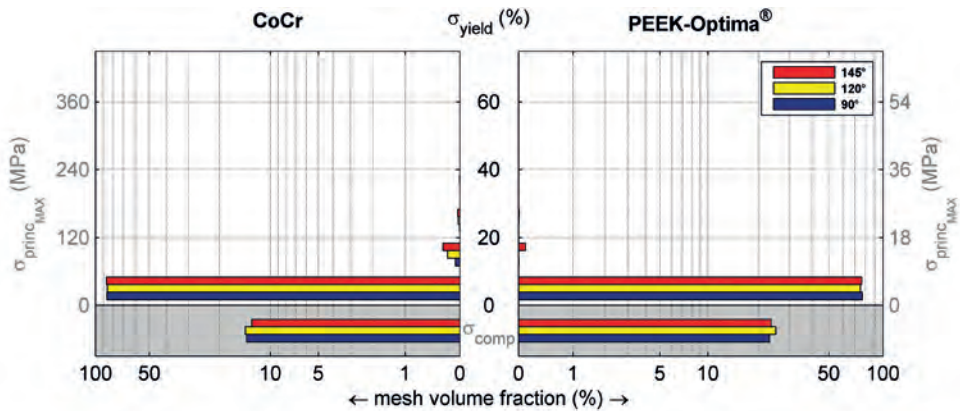


Figure 4. Volumetric distribution of the maximal principal stresses in the femoral component relative to yield stress. The volumes in the gray areas represent parts of the implant that experience no tension. The figure shows that less than 1% of the elements are loaded above 10% of yield stress and that an increased flexion angle increases the volume loaded at higher stress levels. Note that the horizontal axis has a logarithmic scale to visualize small values.

Stresses in the cement mantle

The more rigid behavior of the CoCr component was reflected in the cement mantle stresses. No notable compressive (minimal principal) stresses were found along the cement surface of the CoCr device. High compressive stresses were only seen in the most proximal areas of the anterior and posterior flanges. Compressive stresses in the cement were more abundant in case of a PEEK implant. The maximum compressive stresses in the cement mantle underneath the CoCr and PEEK implant were 12 MPa (120°) and 24 MPa (145°), respectively. Relative to the compressive yield stress this amounted to 12% and 25%, respectively.

Maximal principal (tensile) stresses in the cement were more favorable in the PEEK configuration. Although there were areas of relatively low tensile stresses in the patellofemoral contact region the cement mantle was largely not subjected to any tensile stress. In the CoCr implant, only small sections of higher tensile loads were found in the proximal tip of the anterior flange (Figure 5). For both implants less than 1% of the cement mantle was subjected to a tensile stress level which was higher than 20% of the yield stress. The maximum tensile stress levels were more favorable in the 'PEEK' cement mantle with 4 MPa at 145° of flexion versus 6 MPa for CoCr at 120°. For CoCr this stress intensity occurred at the proximal tip of the anterior flange.

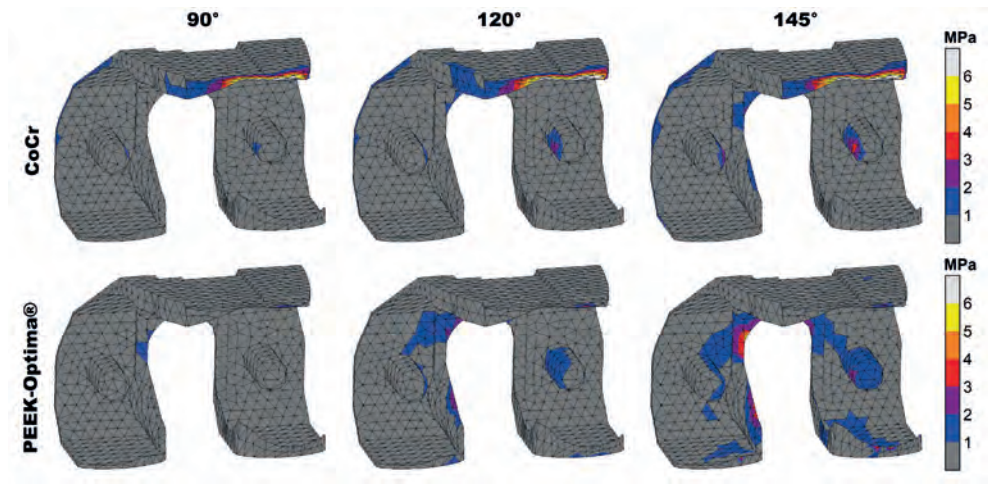


Figure 5. Maximal principal stress patterns in the cement mantle. Stresses are displayed up to 15% of yield stress (40 MPa) to visualize the distribution at increasing flexion angles.

Stress shielding of the periprosthetic femur

Relative to the PEEK implant, the CoCr implant clearly had a larger deviation from the intact-SED distribution (Figure 6). The SED reduction was most prominent in the bone adjacent to tibiofemoral contact sites and extended to the posterodistal and anterior regions of the periprosthetic femur. Relatively small differences between PEEK and intact were present: first, the bone directly adjacent to the implant/cement mantle remained slightly strain-/stress-shielded and secondly, high strain energy foci, mainly in the areas where tibiofemoral contact occurred, were slightly lowered by the PEEK implant. In general, the PEEK implant showed a high similarity to the intact bone remodeling stimulus throughout the full squatting exercise, with a median reduction in SED of 1% (IQR=8%). In contrast, CoCr reduced the stimulus by a median of 56% (IQR=51%).

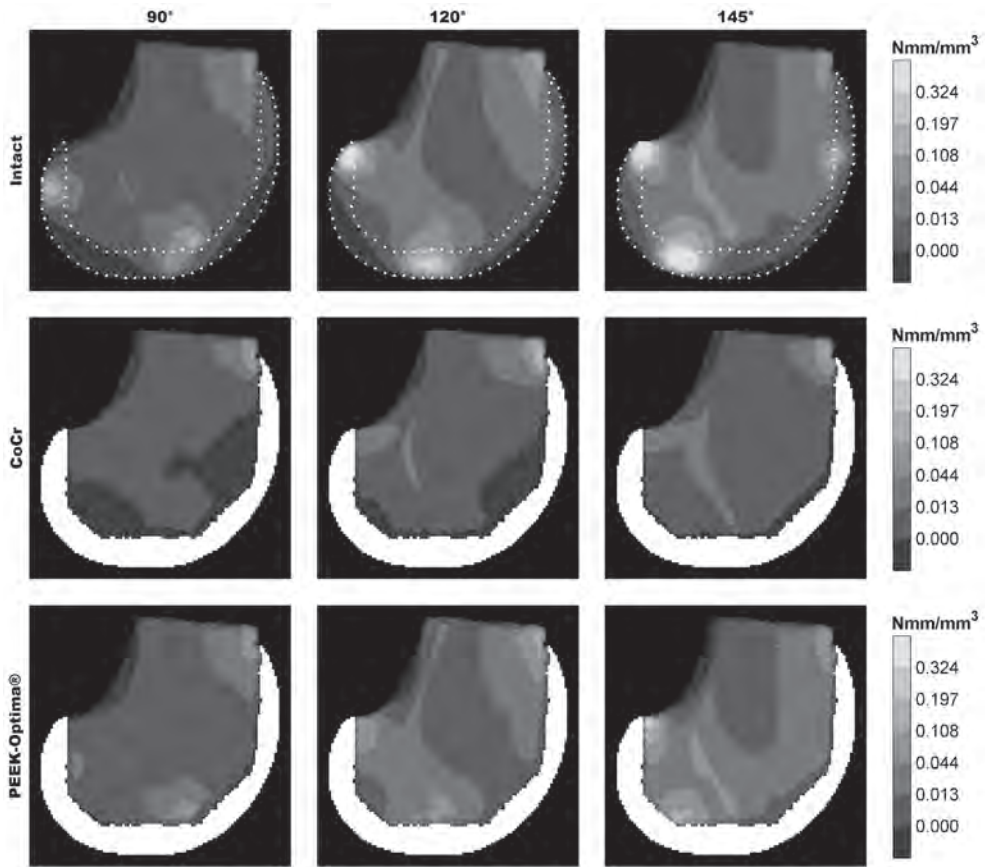


Figure 6. DEXA-like representation of the strain energy density in the periprosthetic volume.

Discussion

The present study aimed to evaluate the mechanical performance of a PEEK femoral component in a high-demand activity such as squatting. Not only should the implant be able to withstand high loads, also the cement mantle must cope with the changed and increased loading situation under demanding conditions. A deep squat including patellofemoral contact was chosen to investigate the structural integrity of the reconstruction, and to evaluate the potential for reduction of the stress shielding phenomenon^{11–16}. The current results indicate that both implant and cement mantle are not more likely to fail when compared to the CoCr reconstruction. The PEEK implant was able to restore the post-operative bone remodeling stimulus to levels similar to an 'intact' femur.

Study limitations

The study was performed by means of the finite element method. For robustness of the model and comparability of the different implant configurations some assumptions were made. First, the kinetics and kinematics, excluding the influence of the knee capsule, for all three models were the same. The PEEK and CoCr reconstructions may be assumed to behave identically in a kinematic sense, but this may be different for the intact reference model. Both the geometry and kinetics/kinematics were simplified to fit the TKA mesh. It is expected that the influence of geometrical differences, the presence of (cruciate) ligaments and their effect on knee joint mechanics may be substantial and that therefore the difference in stress and strain patterns between PEEK and intact may be larger than currently modelled. However, clinical and post-mortem bone loss patterns do agree with the regions identified for stress shielding in this study¹¹⁻¹⁵. The distribution of loads along the bearing surface of the intact knee is further influenced by the articular cartilage and menisci, in contrast to the stiffer and less congruent polyethylene tibial component which generates higher contact stresses

Secondly, a simplified bone material model was used. Bone is an anisotropic viscoelastic material³⁶, but was modelled as linear elastic isotropic. The Young's moduli were calculated from an uncalibrated CT scan and linearly scaled to a physiological range for distal femoral bone that have been reported in other studies²¹⁻²³. Scaling did retain the relative stiffness differences between elements, but local over- or underestimation of the periprosthetic stiffness may have occurred. We believe, however, that due to the comparative nature of this study, the outcome (comparison of PEEK versus CoCr) will hardly be influenced by small deviations in bone stiffness assumptions.

Furthermore, the cement pocket edges and internal surface features (except the pegs) of the femoral component were removed to avoid numerical artefacts at sharp edges³⁷. Also, we assumed a homogeneous 1-millimetre layer of cement, which is the depth of the original cement pockets. In practice the thickness and coverage of the femoral cement layer is highly variable³⁸ and could influence local stress intensities. Another influence on the cement mantle outcomes is the zero-friction assumption in the global model. Although the study on which this study's models were based, determined that friction had a negligible impact on their outcomes, that study did not directly consider cement mantle stresses¹⁸. The absence of friction may thus have underestimated the cement mantle stresses.

Finally, this FE analysis used a single loading scenario, bone geometry and bone quality. It should be considered that either femoral implant could be more sensitive to changes in these parameters than the other. Although the current results provide insights into the differences between a PEEK and CoCr implant, additional analyses including parametric variations related to patient, implant, and surgery are required to draw more robust conclusions.

Stresses in the femoral component

The PEEK implant was more heavily subjected to compressive stresses than the CoCr component, but both remained within the mechanical limits. We analyzed case reports of fractured femoral components to find indications of fatigue and to compare crack initiation sites to stress intensities found in the current study³⁹⁻⁴⁵. All implant fractures, metal or ceramics, were attributed to either trauma³⁹ or tensile fatigue³⁹⁻⁴⁵. The locations of crack initiation were reported to occur at the edges of the posterior chamfers^{40-42,45} or at the apex of the intercondylar notch^{39,43,44}. These initiation sites correspond well with our findings for the tensile stress intensities in the CoCr component, while the same patterns in the PEEK implant were of a substantially lower magnitude.

Stresses in the cement mantle

Neither of the reconstructions were largely subjected to critical stress levels, although there were notable differences between CoCr and PEEK. Compressive stresses in the cement mantle were higher for the PEEK implant. Increased cement loading could potentially lead to earlier fatigue failure of the PMMA, although the main difference between the two materials was found for the compressive stress distribution which probably plays a negligible role in fatigue if no pre-existing plastic damage is present^{29,30}. Conversely, it is known that metal femoral components can loosen and that this is most likely to be initiated at the anterior flange^{18,46}. Stress intensities in these areas may thus be considered as a precursor of implant loosening. In the PEEK implant the tensile stresses in these regions were lower than with CoCr. Moreover, the CoCr component showed a tensile stress intensity at the proximal tip suggesting local loosening or failure may occur in this small region.

Stress shielding of the periprosthetic femur

This study further corroborates the idea that the compliant PEEK implant is capable of lowering periprosthetic stress shielding. This study furthermore suggests that patellofemoral loading at high flexion may prevent loss of anterodistal bone stock in the PEEK implanted case. This effect was visible already at 90° of flexion, making it relevant for the majority of TKA patients who are usually not able to flex beyond 120°³³⁻³⁵, but can walk the stairs or stand up from a chair or bed. The stress shielding patterns that the CoCr implant imposes on the femur correspond to the areas of bone resorption that have been previously published^{11-16,47,48}. This is a strong indicator that there is a correlation between the stress shielding that is presented in the current study and bone resorption following remodeling studies, where both clinical DEXA studies¹¹⁻¹⁶ and FE bone remodeling simulations^{47,48} showed the expected loss of bone mineral density to be most prominent in the anterodistal area and, to a lesser but substantial extent, the posterodistal femur.

Conclusions

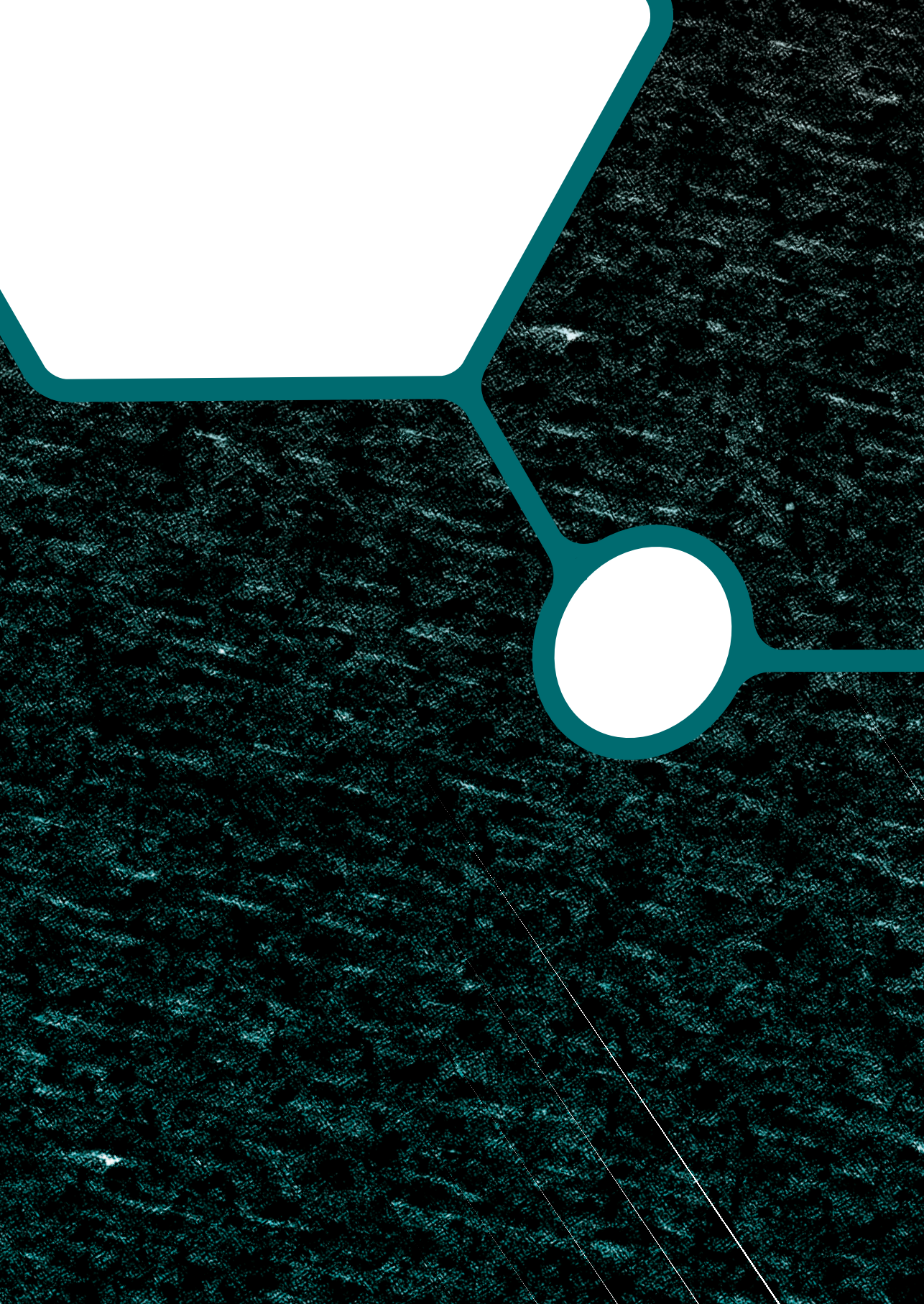
This finite element study has identified differences and similarities between CoCr and PEEK TKA reconstructions during high-demand squatting. The current findings demonstrate that 1) a PEEK femoral implant is strong enough to endure high-demand loading, and that 2) with a PEEK implant compressive cement stresses were higher, while tensile cement stresses were reduced. Moreover, the current results suggest that 3) the PEEK device has potential for periprosthetic bone stock retention. Future research should be aimed at corroboration of the data presented in this paper via experimental and clinical studies.

References

1. Boudeau N, Liksonov D, Barriere T, et al. Composite based on polyetheretherketone reinforced with carbon fibres, an alternative to conventional materials for femoral implant: Manufacturing process and resulting structural behaviour. *Mater Des* 2012; 40: 148–156.
2. Scholes SC, Unsworth A. The wear performance of PEEK-OPTIMA based self-mating couples. *Wear* 2010; 268: 380–387.
3. East RH, Briscoe A, Unsworth A. Wear of PEEK-OPTIMA® and PEEK-OPTIMA®-Wear Performance articulating against highly cross-linked polyethylene. *Proc Inst Mech Eng H* 2015; 229: 187–93.
4. Joyce TJ. The wear of two orthopaedic biopolymers against each other. *J Appl Biomater Biomech* 2005; 3: 141–6.
5. Akay M, Aslan N. Numerical and experimental stress analysis of a polymeric composite hip joint prosthesis. *J Biomed Mater Res* 1996; 31: 167–182.
6. Rankin KE, Dickinson AS, Briscoe A, et al. Does a PEEK Femoral TKA Implant Preserve Intact Femoral Surface Strains Compared With CoCr? A Preliminary Laboratory Study. *Clin Orthop Relat Res* 2016; 474: 2405–2413.
7. Cowie RM, Briscoe, Fisher, et al. PEEK-OPTIMA™ as an alternative to cobalt chrome in the femoral component of total knee replacement: A preliminary study. *Proc Inst Mech Eng H* 2016; 230: 1008–1015.
8. Dickinson A, Taylor A, Browne M. The influence of acetabular cup material on pelvis cortex surface strains, measured using digital image correlation. *J Biomech* 2012; 45: 719–23.
9. Kurtz S, Devine J. PEEK biomaterials in trauma, orthopedic, and spinal implants. *Biomaterials* 2007; 28: 4845–69.
10. Lee W, Koak J, Lim Y, et al. Stress shielding and fatigue limits of poly-ether-ether-ketone dental implants. *J Biomed Mater Res Part B* 2012; 100B: 1044–52.
11. Järvenpää J, Soininvaara T, Kettunen J, et al. Changes in bone mineral density of the distal femur after total knee arthroplasty: a 7-year DEXA follow-up comparing results between obese and nonobese patients. *Knee* 2014; 21: 232–5.
12. Lavernia CJ, Rodriguez J a, Iacobelli D a, et al. Bone mineral density of the femur in autopsy retrieved total knee arthroplasties. *J Arthroplasty* 2014; 29: 1681–6.
13. Mintzer CM, Robertson DD, Rackeman S, et al. Bone loss in the distal anterior femur after total knee arthroplasty. *Clin Orthop Relat Res* 1990; 260: 135–43.
14. Petersen MM, Olsen C, Lauritzen JB, et al. Changes in bone mineral density of the distal femur following uncemented total knee arthroplasty. *J Arthroplasty* 1995; 10: 7–11.
15. Seki T, Omori G, Koga Y, et al. Is bone density in the distal femur affected by use of cement and by femoral component design in total knee arthroplasty?. *J Orthop Sci* 1999; 4: 180–186.
16. Loon C Van, Oyen W. Distal femoral bone mineral density after total knee arthroplasty: a comparison with general bone mineral density. *Arch Orthop Trauma Surg* 2001; 282–285.
17. de Ruitter L, Janssen D, Briscoe A, et al. A preclinical numerical assessment of a

- polyetheretherketone femoral component in total knee arthroplasty during gait. *J Exp Orthop* 2017; 4: 3.
18. Zelle J, Janssen D, Van Eijden J, et al. Does high-flexion total knee arthroplasty promote early loosening of the femoral component?. *J Orthop Res* 2011; 29: 976–983.
 19. Bollars P, Luyckx J, Innocenti B, et al. Femoral component loosening in high-flexion total knee replacement. *J Bone Joint Surg Br* 2011; 93: 1355–1361.
 20. Zelle J, Barink M, De Waal Malefijt M, et al. Thigh-calf contact: does it affect the loading of the knee in the high-flexion range?. *J Biomech* 2009; 42: 587–93.
 21. Ashman RB, Rho JY. Elastic modulus of trabecular bone material. *J Biomech* 1988; 21: 177–181.
 22. Cuppone M, Seedhom BB, Berry E, et al. The Longitudinal Young's Modulus of Cortical Bone in the Midshaft of Human Femur and its Correlation with CT Scanning Data. *Calcif Tissue Int* 2004; 74: 302–309.
 23. Turner CH, Rho J, Takano Y, et al. The elastic properties of trabecular and cortical bone tissues are similar: results from two microscopic measurement techniques. *J Biomech* 1999; 32: 437–441.
 24. Lewis G. Properties of acrylic bone cement: state of the art review. *J Biomed Mater Res* 1997; 38: 155–82.
 25. Zebarjad SM. A Study on Mechanical Properties of PMMA/Hydroxyapatite Nanocomposite. *Engineering* 2011; 03: 795–801.
 26. Okazaki Y. Comparison of Fatigue Properties and Fatigue Crack Growth Rates of Various Implantable Metals. *Materials (Basel)* 2012; 2981–3005.
 27. Sobieraj MC, Murphy JE, Brinkman JG, et al. Biomaterials Notched fatigue behavior of PEEK. *Biomaterials* 2010; 31: 9156–9162.
 28. Murphy BP, Prendergast PJ. On the magnitude and variability of the fatigue strength of acrylic bone cement. *Int J Fatigue* 2000; 22: 855–864.
 29. Dai P, Li Z. A plasticity-corrected stress intensity factor for fatigue crack growth in ductile materials. *Acta Mater* 2013; 61: 5988–5995.
 30. Eliáš J, Le JL. Modeling of mode-I fatigue crack growth in quasibrittle structures under cyclic compression. *Eng Fract Mech* 2012; 96: 26–36.
 31. Huiskes R, Weinans H, Grootenboer HJ, et al. Adaptive Bone-Remodeling Theory Applied to Prosthetic-Design Analysis. *J Biomech* 1987; 20: 1135–1150.
 32. Carter DR, Fyhrie DP, Whalen RT. Trabecular bone density and loading history: regulation of connective tissue biology by mechanical energy. *J Biomech* 1987; 20: 785–794.
 33. Bade MJ, Kittelson JM, Kohrt WM, et al. Predicting Functional Performance and Range of Motion Outcomes After Total Knee Arthroplasty. *Am J Phys Med Rehabil* 2014; 93: 579–585.
 34. Matassi F, Duerinckx J, Vandenuecker H, et al. Range of motion after total knee arthroplasty: the effect of a preoperative home exercise program. *Knee Surg, Sport Traumatol Arthrosc* 2014; 22: 703–9.
 35. Horikawa A, Miyakoshi N, Shimada Y, et al. Comparison of clinical outcomes between total knee arthroplasty and unicompartmental knee arthroplasty for osteoarthritis of the knee: a retrospective analysis of preoperative

- and postoperative results. *J Orthop Surg Res* 2015; 10: 168.
36. Ashman RB, Cowin SC, Van Buskirk WC, et al. A Continuous Wave Technique for the Measurement of the Elastic Properties of Cortical Bone. *J Biomech* 1984; 17: 349–361.
 37. Stolk J, Verdonschot N, Mann KA, et al. Prevention of mesh-dependent damage growth in finite element simulations of crack formation in acrylic bone cement.. *J Biomech* 2003; 36: 861–71.
 38. Howard K, Miller M, Damron T, et al. The distribution of implant fixation for femoral components of TKA: A postmortem retrieval study. *J Arthroplasty* 2014; 29: 1863–1870.
 39. Krueger AP, Singh G, Beil FT, et al. Ceramic femoral component fracture in total knee arthroplasty: an analysis using fractography, fourier-transform infrared microscopy, contact radiography and histology.. *J Arthroplasty* 2014; 29: 1001–4.
 40. Swarts E, Miller SJ, Keogh C V, et al. Fractured Whiteside Ortholoc II knee components.. *J Arthroplasty* 2001; 16: 927–934.
 41. Lemaire R. Fatigue fracture of the femoral component in a mobile bearing knee prosthesis. *Acta Orthop Belg* 2010; 76: 274–281.
 42. Duffy GP, Murray BE, Trousdale RR. Hybrid Total Knee Arthroplasty. Analysis of Component Failures at an Average of 15 Years. *J Arthroplasty* 2007; 22: 1112–1115.
 43. Han HS, Kang S-B, Yoon KS. High incidence of loosening of the femoral component in legacy posterior stabilised-flex total knee replacement.. *J Bone Joint Surg Br* 2007; 89: 1457–1461.
 44. Huang C, Yang C, Cheng C. Fracture of the femoral component associated with polyethylene wear and osteolysis after total knee arthroplasty. *J Arthroplasty* 1999; 14: 375–379.
 45. Sarraf KM, Wharton R, Abdul-jabar HB, et al. Fatigue Fractures of Total Knee Prostheses. *Bull Hosp Joint Dis* 2014; 72: 242–246.
 46. Zelle J, van de Groes S, de Waal Malefijt M, et al. Femoral loosening of high-flexion total knee arthroplasty: the effect of posterior cruciate ligament retention and bone quality reduction.. *Med Eng Phys* 2014; 36: 318–24.
 47. Lenthe G Van, Willems M, Verdonschot N, et al. Stemmed femoral knee prostheses: effects of prosthetic design and fixation on bone loss. *Acta Orthop Scand* 2002; 73: 630–637.
 48. Lenthe G Van, de Waal Malefijt MC, Huiskes R. Stress shielding after total knee replacement may cause bone resorption in the distal femur.. *J Bone Joint Surg Br* 1997; 79: 117–122.



Chapter 4

Decreased stress shielding with a PEEK femoral total knee prosthesis measured in validated computational models

de Ruiter L, Rankin K, Browne M, Briscoe A, Janssen D, Verdonschot N. Decreased stress shielding with a PEEK femoral total knee prosthesis measured in validated computational models. *Submitted*

Introduction

In total knee arthroplasty (TKA), change in mechanical loading of the bone is the main stimulus driving remodelling and periprosthetic bone density changes, which is influenced by the relatively stiff implant materials being used, such as Cobalt-Chromium (CoCr)¹⁻⁸. A reduced stimulus may lead to disturbed bone remodeling and osteopenia, which in turn increases the risk of periprosthetic bone fractures^{1,9,10}. At other locations the stiff TKA materials may generate peak stresses in the underlying bone, which further increases the risk of fractures^{11,12}. These fractures occur in up to 5% of TKA patients, depending on service time, and are often the result of trauma, in combination with a weakened bone stock¹³⁻¹⁵. Therefore, alternative, more compliant materials that have the potential to reduce stress shielding have been considered for femoral TKA components, such as polyacetal implants that were evaluated in a clinical trial¹⁶.

Recently, the potential benefit of a polyetheretherketone (PEEK) femoral component in TKA was studied in computational studies^{11,12}. Those studies demonstrated that a PEEK knee implant may improve the periprosthetic bone remodeling stimulus. During a squatting exercise the PEEK material reduced the stress shielding by 55 percent points compared to a CoCr device. A study by Rankin *et al.* (2016) demonstrated this potential in in vitro experiments with a bone-analogue model¹⁷. Both the computational and in vitro studies confirmed the hypothesis that a more compliant material can distribute forces more physiologically than when using a stiff metal implant.

The in vitro study as performed by Rankin *et al.* (2016) used digital image correlation (DIC) to measure surface strains on the cortical surface during loads equivalent to level gait. This technique provides a robust quantification of small two- or three-dimensional displacements and strains¹⁸. However, it can only measure on visible surfaces and, as such, can only identify stress shielding at the cortical surface. Finite element (FE) modeling does have the capability to determine internal bone strains^{11,12}. In the current study, experimental measurements using DIC were therefore combined with FE modeling to investigate the effect of femoral TKA with PEEK and CoCr components on peri-prosthetic bone strains.

We hypothesized that a PEEK femoral component would cause a bone strain distribution that more closely resembles the intact situation compared to a reconstruction with a CoCr component.

Materials and methods

The current study combined experimental DIC analysis, to quantify the change in surface bone strains following reconstruction with either a PEEK or a CoCr component, with FE analyses for evaluation of the surface and internal bone strain changes.

Study design

Experiments were conducted with three pairs of human cadaveric femurs. DIC strain measurements were first taken from the intact femurs to serve as a control after implantation. Left femurs were implanted with PEEK implants, and right femurs with CoCr implants, assuming similarity in geometry and mechanical properties¹⁹. Comparison of the intact and post-implantation situations illustrated the effect of TKA on the changes in load transfer, while comparing between the left and right reconstructed femurs provided information on the effect of implant material. Specimen-specific FE models were created and validated against the experimental surface strains, and subsequently used to investigate the internal periprosthetic bone strain distribution.

Specimen preparation

Six fresh-frozen human cadaveric femurs (three pairs, female donors, 76-83 years) were CT-scanned to exclude the presence of foreign materials, or signs of pathology or severe osteoporosis. The femurs were dissected distally, thawed at room temperature and cleaned from soft tissues. Special care was given to the lateral epicondylar region to facilitate DIC measurements. A polyurethane resin mould (Smooth-Cast 60D, Smooth-On Inc. USA), potted in polymethylmethacrylate (PMMA), was created from the femoral articulating surface to form a custom load applicator for the intact femur measurement (Figure 1). Next, the intercondylar entry point into the intramedullary canal was drilled for placement of the surgical tools. Each specimen was then potted in PMMA 100 mm proximally from the distal femur. To ensure a reproducible load application between the intact and implanted femurs, femoral alignment was controlled by inserting the surgical alignment tool into the intramedullary canal, which subsequently was equipped with a customized planar spirit level. This ensured horizontal alignment of the (future) distal cut and resulted in the correct flexion angle during potting. After curing of the bone cement a Perspex rod was inserted into the intramedullary canal to keep it open and visible on the computed tomography (CT) scans that followed. All specimens were then submerged in a water-basin to simulate peripheral soft tissues, and were CT-scanned (530 mA, 120 kV, 0.5x0.5 mm in-plane resolution, 1.0 mm slice thickness, Siemens Somatom Sensation 64, Siemens AG, Germany) along with a calibration phantom (Image Analysis Inc., Columbia, KY, USA)²⁰⁻²⁴. After scanning all specimens were re-frozen.

Experimental procedure

Before testing, specimens were thawed at room temperature for at least 12 hours. After drying in ambient air, the surface was coated with matt white spray paint (Plastikote Ltd, UK). Once dry, a matt black speckle pattern was applied onto the white surface by an experienced DIC operator. Then, the specimen was placed in the unidirectional servo-hydraulic loading apparatus with a 15kN load cell (MTS45820, MTS Systems Corp., USA). The specimen-specific polyurethane mould was positioned onto the femoral cartilage, aligned using a laser spirit level, and then potted in PMMA for fixation to the loading apparatus. After curing of the PMMA and seating of the load applicator onto the specimen, ambient and focal light sources were positioned to obtain optimal lighting of the specimen (Figure 1). The experimental load for the specimens was not predefined as a fixed value, to avoid femoral fractures. Alternatively, the specimen-specific load was determined using the left femur by first measuring the unloaded baseline noise in the DIC setup, after which the femoral load was increased incrementally until a 10:1 signal-to-noise ratio (SNR) was achieved. A 10:1 SNR provides good accuracy of the captured data, accounts for potential noise increase and reduces any measurement error to an acceptable level. The resulting loads were 3.5 kN, 2.5 kN and 3.5 kN for specimens 1, 2 and 3, respectively. These loads were then applied to both the left and right femurs. The load applicator allowed for free translations in the horizontal plane free varus/valgus rotations, while other degrees of freedom were constrained. Six cycles of loading/unloading were executed. Of each loaded and unloaded state six DIC image arrays were captured, resulting in a total of $2 \times 6 \times 6 = 72$ images per (intact or implanted) specimen.

Following the intact femur measurements, either a CoCr (Maxx Freedom Knee) or PEEK (adopted from Maxx Freedom Knee) implant was cemented (Palacos R, Palamix system, Heraeus Medical GmbH, Germany) onto the femur according to surgical guidelines. After implantation, one hour was allowed for cement curing, after which the specimen was placed back into the tensile testing rig and the experimental procedure as described above was repeated.

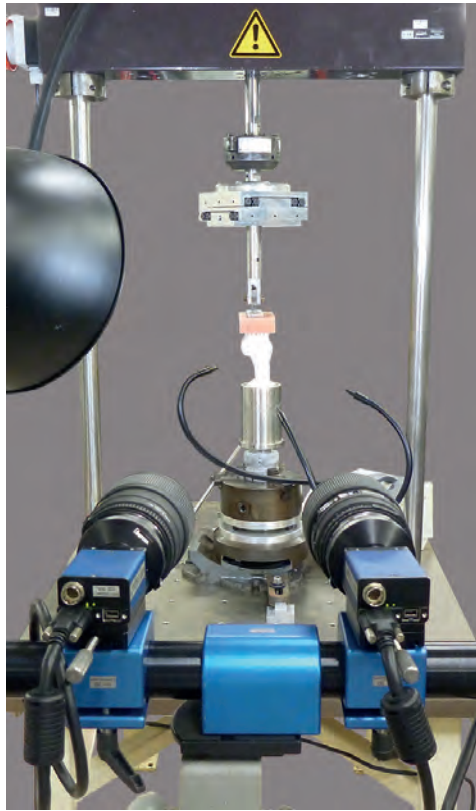


Figure 1. Experimental setup with a) the load cell, b) planar x/y bearing, c) varus/valgus hinge, d) custom load applicator, e) painted specimen, f) ambient light source, g) focal light source, h) dual camera setup.

Digital image correlation

A dual-camera DIC setup using Sigma 105mm lenses was used (Limess GmbH, 2 megapixel) to capture 3-D femur strain data (Figure 1). Prior to a measurement series, the corresponding rigid DIC-calibration tool (12 x 9 grid of 5 mm targets) was used to calibrate the position of the cameras relative to one another via triangulation to define the 3D coordinate system for the bone surface. The camera setup was placed at approximately one meter from the specimens for optimal focal depth, with a relative pan angle of 10 degrees for 3-D capturing. As the region of interest (ROI – Figure 2) must be visible for both cameras, higher angles could lead to loss of field of view. Images were captured using Vic3D software (Correlated Solutions Inc., Irmo, SC, USA). Lighting was arranged such that maximal contrast was reached while avoiding pixel saturation. The Vic3D software indicated when image conditions were sufficient for accurate analysis, indicating a suitable spread in the grey scale histogram (i.e. not oversaturated, nor too dark), which was obtained by adjusting lighting. This baseline assessment was performed on unloaded specimens and revealed if the agreement between

the two cameras was adequate for the experimental procedure. The same interrogation area was used across each bone surface with a subset size of 41 and step size of 7, with normalised sum of square differences (NSSD) correlation criterion.

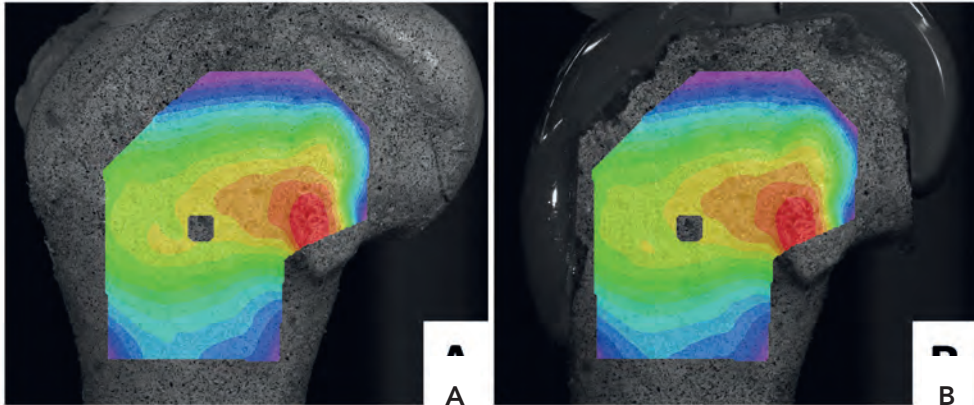


Figure 2. DIC region of interest indicated on (A) the intact femur and (B) the implanted femur. The regions were chosen such that the speckle patterns were visible in both trials, and were kept constant between the intact and implanted cases (displacement maps are shown for illustrative purposes only).

Finite element models

Geometry

FE models were based on the CT scans of the intact, potted femurs. CT-scans were exported with a bone filter and with a soft tissue filter for better visibility of the femoral cartilage. The femurs were segmented based on the bone scan, while the differences between scans in the condylar area were assumed to represent the cartilage layer, which were then added to the femur. A surface representation was created using Mimics 14 (Materialise, Leuven, Belgium), which was then used to create a solid mesh (Patran, MSC Software, Newport Beach, CA, USA). The models were meshed with tetrahedral elements with an average edge length of 2 millimetres, based on previous FE studies with a similar loading configuration (de Ruyter et al., 2017b). The PMMA fixation was segmented as a vertical reference, while the Perspex rod was segmented as a reference for the distal cut. Two pins of the distal femoral cutting guide left indents in the femur during implantation, which were identified on the CT scans and used as reference for the final alignment of the distal cut. The custom load applicators were digitized by a white-light scanner (Creaform Go!SCAN 3D 2012). The bearing surface mesh was positioned on the femoral condylar cartilage via a customized positioning algorithm with the constraints of horizontal alignment and varus/valgus rotation, according to the experimental degrees of freedom. The placement was then compared to anteroposterior and mediolateral pictures taken during the experiment to verify the positioning in the models.

Material properties

To assign material properties to the femurs, the Hounsfield units were first converted to bone mineral density (BMD) using the calibration phantom. The BMD was subsequently used to calculate the local Young's modulus for the femurs using equations by Keyak et al. (2005)²⁰. All other materials were given homogeneous material properties as provided by manufacturers (Table 1). The comparison between DIC strain data and FE strain data on the lateral epicondylar surface was facilitated by connecting zero-thickness surface elements to the tetrahedrons' vertices on the surface in the region of interest, which was meshed with a higher density (average edge length of 1 mm). These surface elements were given a near-zero stiffness to ensure they followed the deformation of the underlying bone elements, and provided strains metrics identical to the DIC measurements.

Table 1. Material properties.

Material	Young's modulus (MPa)	Poisson's ratio	Yield strength (MPa) *
CoCr	210,000	0.3	600/600
PEEK-Optima®	3,700	0.362	117/90
Polyurethane	800	0.3	n/a
PMMA	2,866	0.3	97/40
Femur	1-20,000	0.3	n/a

* Compressive/Tensile

Loading

The experimental load was replicated via one node connected to the load applicator via stiff springs, simulating the experimental load transfer and degrees of freedom. The models were fixed at the elements representing the PMMA pot.

Outcome measures

Experimental surface strain comparison and FE strain validation

The surface strain measured by the DIC software was a Von Mises strain for zero-thickness surfaces as defined by Equation 1. The equation was implemented in the ROI surface elements of the FE models for direct DIC/FE comparison. DIC data was averaged twice: first, over the image arrays within one load instance, and second the mean over the six load instances was taken. The resulting strain map was assessed qualitatively for patterns, and quantitatively by analysing the strain distribution in the DIC region in 500-microstrain intervals. These were subsequently compared to the FE strain map, providing a measure for the accuracy of the FE models.

$$\varepsilon_{vm} = \sqrt{\varepsilon_1^2 - \varepsilon_1 \varepsilon_2 + \varepsilon_2^2} \quad \text{Equation 1.}$$

Volumetric strain (shielding) assessment

Strain energy density (SED) was calculated in the FE models as a measure for stress shielding in the in the periprosthetic femur. SED has been described in literature as the stimulus for bone remodelling^{2,3}, with a decrease in SED causing loss of bone mass. A comparison between the intact and implanted femur is therefore required to predict postoperative periprosthetic bone changes. To this end, the SED data of the intact femur measurements were subtracted from the CoCr and PEEK reconstructions at each integration point in the periprosthetic volume. The integration point data were then multiplied by their element volume and summed to yield the total strain energy in all five periprosthetic regions of interest (ROI). The ROIs were determined in the sagittal view, according to representations in literature^{7,10}. The condylar ROIs were split for lateral and medial condyle, effectively creating 7 ROIs (Figure 5).

Results

Experimental observations

During the experiment events were observed that were not according to protocol. During capturing of the DIC images, on several occasions one or two out of six image recordings were unsuitable for measurement, leaving 4 or 5 strain maps for strain averaging. Secondly, the load applicator for one pair of implanted femurs (specimen 2) was slightly undersized, which was resolved by moving the load applicator to ensure optimal lateral seating, where DIC data was being recorded. The shift of the load applicator was implemented correspondingly in the FE models of these femurs, based on images of the adjusted set-up, while the loading configuration was unchanged.

Experimental surface strain comparison

The largest strain values were measured in the distal femur, in line with the principal loading direction (Figure 3). Strain distributions were similar between left and right leg intact femurs, confirming similarity between contralateral specimens.

Once implanted, the epicondylar surface strains generally decreased, suggesting stress shielding in both reconstructions. The strain decrease was larger with a CoCr implant than with a PEEK component, which was particularly obvious in specimens 1 and 2, and more subtly in specimen 3. The frequency plots in Figure 4 reflect the stress shielding effect after implantation, as larger portions of the implanted femurs displayed lower strain values as seen by the shift to the left of the curves for the implanted cases.

FE strain validation

In general, the FE simulations showed good agreement with the experimental strain patterns and magnitudes (Figure 3), and thus provided a satisfactory validation of the models. Exceptions were the intact right FE models of specimens 1 and 2, which showed a similar distribution but generally lower strain values, which is also reflected in the strain frequency plots (Figure 4).

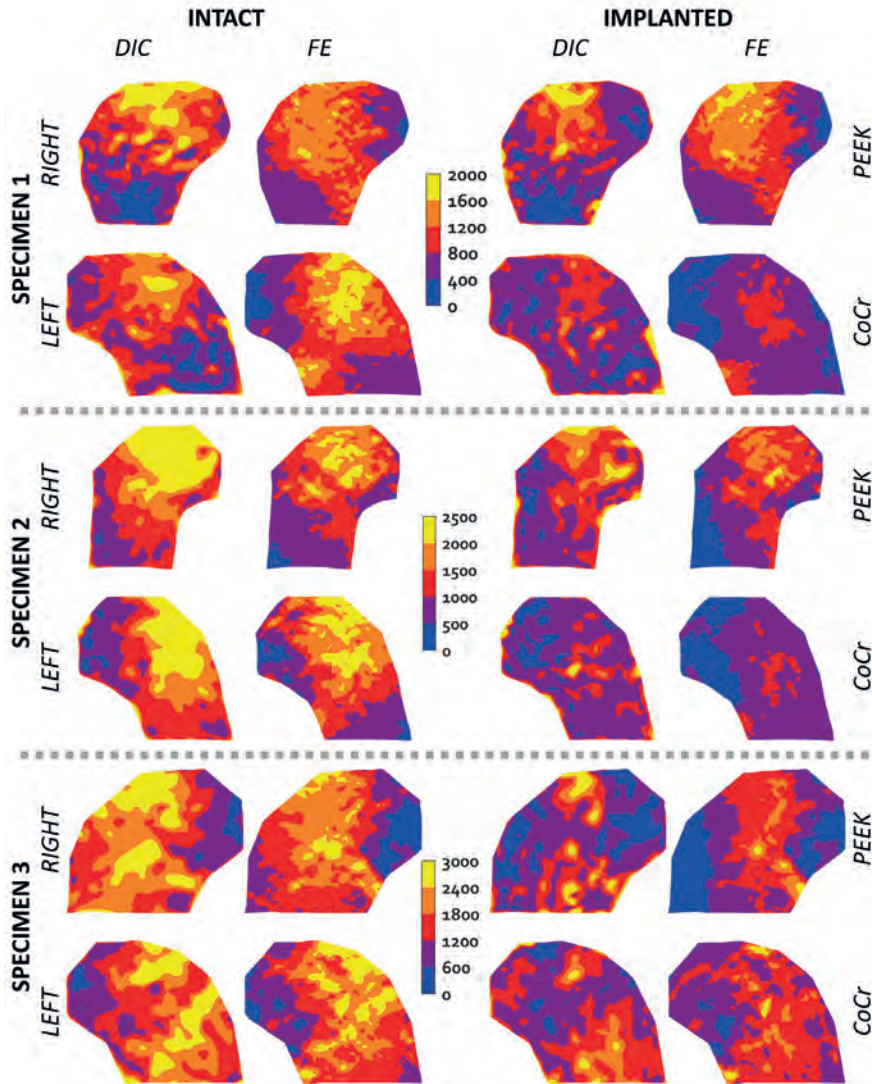


Figure 3. Von Mises strain maps of all specimens for both pre- and postoperative DIC and FE measurements.

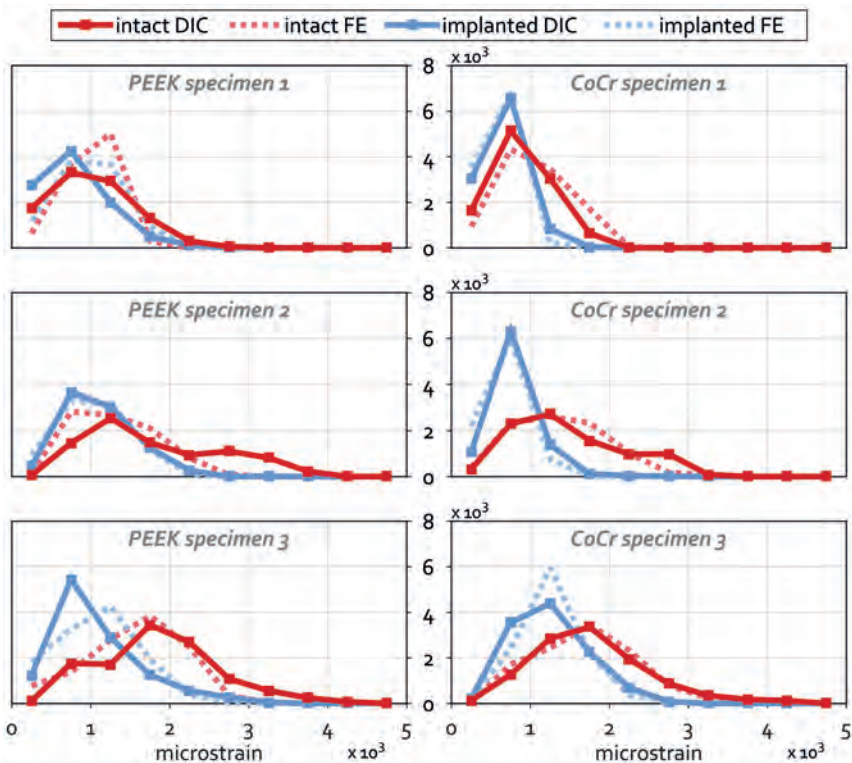


Figure 4. Von Mises strain curves of all specimens for both pre- and postoperative DIC and FE measurements. The strains are accumulated in 500 microstrain intervals.

Volumetric strain (shielding) assessment

For all specimens PEEK led to an overall increase in SED compared to the intact cases, whereas for CoCr a decrease was seen in specimen 1 and slight increases in specimens 2 and 3 (Figure 5). In ROIs 1 and 5, the CoCr implant always showed lower SED values than the intact specimens. In the medial condyles (ROI 5) of the CoCr reconstructions the difference with intact was smaller, while larger strains were found for the PEEK reconstructions in this region. In the anterodistal area (ROI 1), stress shielding was observed in the PEEK reconstructions of specimens 2 and 3, albeit to a lesser extent than CoCr. The proximal regions (ROI 2 and 3) showed only marginal and dispersed differences between the CoCr and PEEK reconstructions. In the posterior region (ROI 4) the differences between intact and implanted were small for both implant materials.

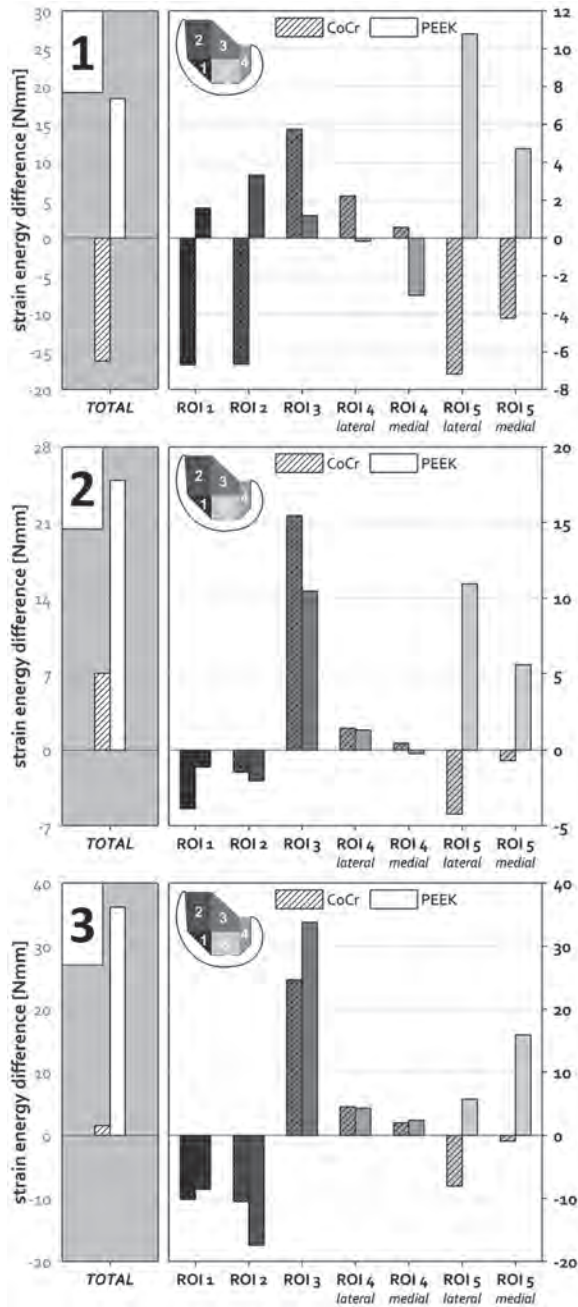


Figure 5. Postoperative volumetric strain energy density differences in all specimens, separated for five periprosthetic regions of interest. The SED values at each integration point in a specific ROI were multiplied by their volume and summed to yield the total strain energy per ROI.

Discussion

We hypothesized a PEEK femoral component would cause a strain distribution more closely resembling the intact situation compared to a reconstruction with a CoCr component. Our DIC results on the surface strains indeed confirmed this hypothesis. Similarly, internal strain energy density distributions calculated by FE were more similar to the intact femurs with PEEK in regions 1 and 5.

Validation

From a qualitative perspective, the FE models displayed surface strain distributions that were very similar to the experimental DIC measurements. The largest strain mismatch was observed in the right intact femur of specimen 2. Although the patterns were similar, the magnitude of the DIC strain was substantially larger. This may have been caused by the experimental loading configuration, in which the varus/valgus rotation that was allowed may have led to a load imbalance, with an increased portion of the load acting on the lateral femur. This was confirmed in additional FE simulations in which, in addition to the change in the positioning of the load applicator, this assumed load imbalance was incorporated. The results of that simulation showed a similar increase in strain in the lateral femur.

Stress shielding

Reduced stress shielding was seen in the PEEK reconstructions, particularly due to a more favorable strain energy distribution in the (antero)distal area. Conversely, stress shielding was always observed with a CoCr implant in this region. Interestingly, the PEEK implant showed an increase in strain energy density, leading to the expectation for increased bone formation. Although it is desirable to increase bone quality in generally osteopenic bones, an increase in bone loading may also increase the risk of periprosthetic fractures. The current FE results show the same trend as previous studies where the bone remodeling stimulus of a PEEK femoral TKA was analyzed^{11,12,17}. Both during simulated level gait¹¹ and squatting¹², a clear reduction in stress shielding was seen with a PEEK component, although these studies only included a single bone geometry and simplified bone material properties. Experimental data on standardized analogue femurs with PEEK and CoCr femoral prostheses demonstrated a similar trend¹⁷.

Limitations

This study has several limitations with regard to the design, statistics and analysis. First, only three pairs of femurs were used for testing and analysis. Cadaver studies are rarely sizable enough to establish statistical support for a conclusion due to, amongst others, variability in specimen size and bone quality¹⁹, and limited specimen availability. Consequently, the data that were obtained in this small-sample study were intended to support hypothesized

trends, build confidence and improve on previously generated data. The FE models that were created during this study proved to be robust and an accurate representation of the experiment, generating the desired confidence.

Only a single loading configuration was analysed in the experimental set-up, whereas load variations could have revealed difference in the femoral strain, as shown in our previous FE simulations of PEEK and CoCr reconstructions^{11,12}.

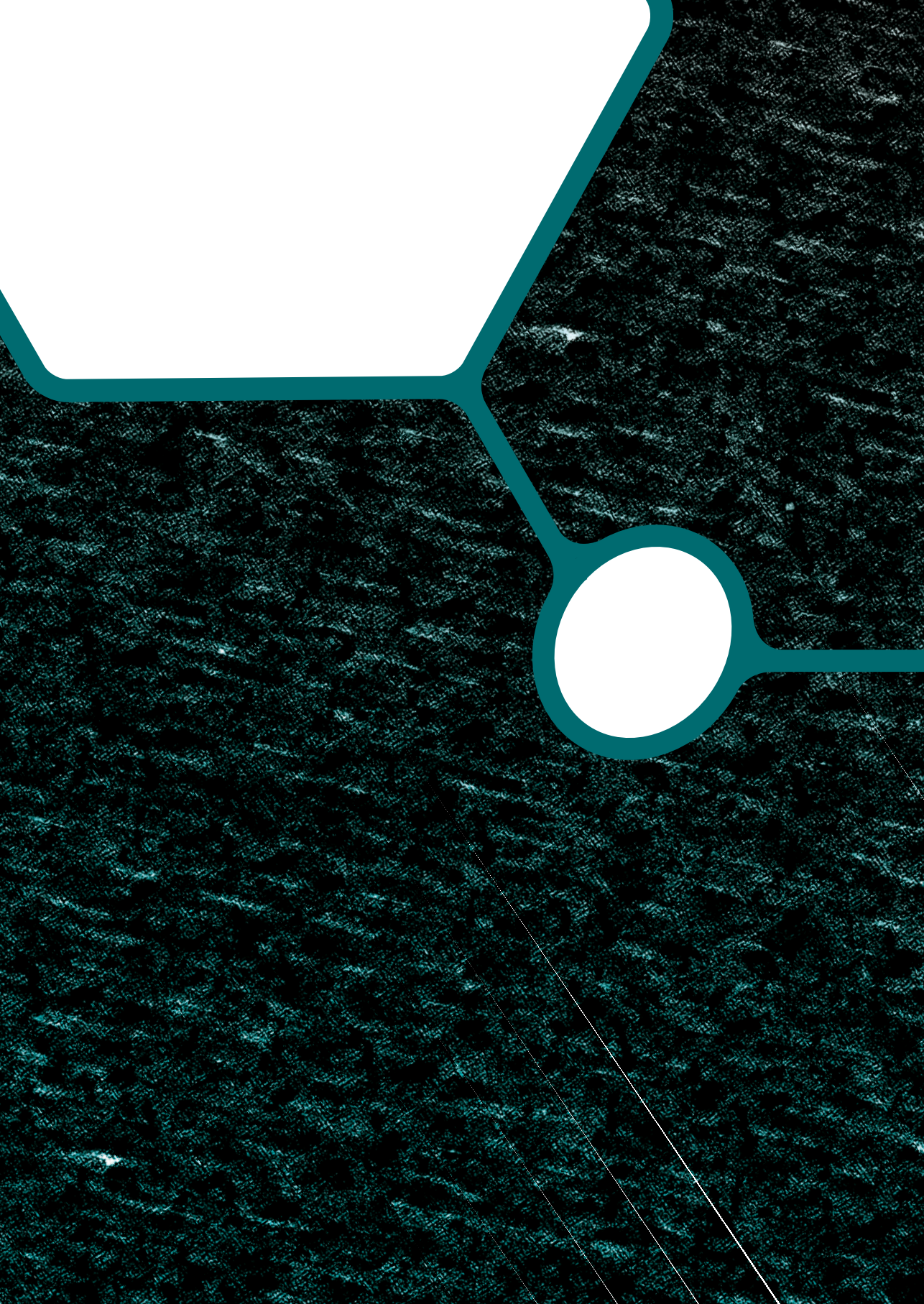
Conclusion

This cadaveric study demonstrates the potential for PEEK femoral components to reduce periprosthetic stress when compared to CoCr.

References

1. Mintzer CM, Robertson DD, Rackeman S, et al. *Bone loss in the distal anterior femur after total knee arthroplasty.* Clin Orthop Relat Res 1990; 260: 135–43.
2. Carter DR, Fyhrie DP, Whalen RT. *Trabecular bone density and loading history: regulation of connective tissue biology by mechanical energy.* J Biomech 1987; 20: 785–794.
3. Huiskes R, Weinans H, Grootenboer HJ, et al. *Adaptive Bone-Remodeling Theory Applied to Prosthetic-Design Analysis.* J Biomech 1987; 20: 1135–1150.
4. Wolff J. *Über die Bedeutung der Architektur der spongiosen Substanz.* Zentralblatt für die medizinische Wiss 1869; 223–234.
5. Frost H. *The Laws of Bone Structure.* Springfield, IL: Charles C. Thomas, 1964.
6. Kummer B. *Biomechanics of bone: Mechanical properties, functional structure, and functional adaptation.* In: Fung Y, Perrone N, Anliker M (eds) *Biomechanics: Its Foundations and Objectives.* Englewood Cliffs, NJ: Prentice-Hall, 1972, p. 237:271.
7. Lenthe G Van, de Waal Malefijt MC, Huiskes R. *Stress shielding after total knee replacement may cause bone resorption in the distal femur.* J Bone Joint Surg Br 1997; 79: 117–122.
8. Lenthe G Van, Willems M, Verdonshot N, et al. *Stemmed femoral knee prostheses: effects of prosthetic design and fixation on bone loss.* Acta Orthop Scand 2002; 73: 630–637.
9. Järvenpää J, Soininvaara T, Kettunen J, et al. *Changes in bone mineral density of the distal femur after total knee arthroplasty: a 7-year DEXA follow-up comparing results between obese and nonobese patients.* Knee 2014; 21: 232–5.
10. Lavernia CJ, Rodriguez J a, Iacobelli D a, et al. *Bone mineral density of the femur in autopsy retrieved total knee arthroplasties.* J Arthroplasty 2014; 29: 1681–6.
11. de Ruiter L, Janssen D, Briscoe A, et al. *A preclinical numerical assessment of a polyetheretherketone femoral component in total knee arthroplasty during gait.* J Exp Orthop 2017; 4: 3.
12. de Ruiter L, Janssen D, Briscoe A, et al. *The mechanical response of a polyetheretherketone femoral knee implant under a deep squatting loading condition.* Proc Inst Mech Eng H 2017; 231: 1204–1212.
13. Schroer W, Berend K, Lombardi A, et al. *Why are total knees failing today? Etiology of total knee revision in 2010 and 2011.* J Arthroplasty 2013; 28: 116–9.
14. Seki T, Omori G, Koga Y, et al. *Is bone density in the distal femur affected by use of cement and by femoral component design in total knee arthroplasty?* J Orthop Sci 1999; 4: 180–186.
15. Canton G, Ratti C, Fattori R, et al. *Periprosthetic knee fractures. A review of epidemiology, risk factors, diagnosis, management and outcome.* Acta Biomed 2017; 88: 118–128.
16. Moore D, Freeman M, Revell P, et al. *Can a total knee replacement prosthesis be made entirely of polymers?* J Arthroplasty 1998; 13: 388–395.
17. Rankin KE, Dickinson AS, Briscoe A, et al. *Does a PEEK Femoral TKA Implant Preserve Intact Femoral Surface Strains Compared*

- With CoCr? A Preliminary Laboratory Study.* Clin Orthop Relat Res 2016; 474: 2405–2413.
18. Dickinson A, Taylor A, Ozturk H, et al. *Experimental validation of a finite element model of the proximal femur using digital image correlation and a composite bone model.* J Biomed Eng 2011; 133: 014504.
 19. Pierre MA, Zurakowski D, Nazarian A, et al. *Assessment of the bilateral asymmetry of human femurs based on physical, densitometric, and structural rigidity characteristics.* J Biomech 2010; 43: 2228–2236.
 20. Keyak JH, Kaneko TS, Tehranzadeh J, et al. *Predicting Proximal Femoral Strength Using Structural Engineering Models.* Clin Orthop Relat Res 2005; 219–228.
 21. Keyak JH, Falkinstein Y. *Comparison of in situ and in vitro CT scan-based finite element model predictions of proximal femoral fracture load.* Med Eng Phys 2003; 25: 781–787.
 22. Carballido-Gamio J, Bonaretti S, Saeed I, et al. *Automatic multi-parametric quantification of the proximal femur with quantitative computed tomography.* Quant Imaging Med Surg 2015; 5: 552–568.
 23. Cuppone M, Seedhom BB, Berry E, et al. *The Longitudinal Young's Modulus of Cortical Bone in the Midshaft of Human Femur and its Correlation with CT Scanning Data.* Calcif Tissue Int 2004; 74: 302–309.
 24. Lenaerts L, van Lenthe GH. *Multi-level patient-specific modelling of the proximal femur. A promising tool to quantify the effect of osteoporosis treatment.* Philos Trans R Soc A Math Phys Eng Sci 2009; 367: 2079–2093.



Chapter 5

Fixation strength of a polyetheretherketone femoral component in total knee arthroplasty

de Ruiter L, Janssen D, Briscoe A, Verdonchot N.
Fixation strength of a polyetheretherketone femoral component
in total knee arthroplasty. *Medical Engineering and
Physics* 2017; 49: 157–162

Introduction

The initial fixation of the femoral component after total knee arthroplasty (TKA) is an important outcome measure for the success of the procedure. The research and development in cementless TKA is focused on primary stability through mechanical fixation (e.g. press-fit or pin/screw fixation) to allow the biological process of bone ingrowth to provide long-term fixation¹⁻⁵. In cemented fixation there are two interfaces at which failure can occur; the cement-bone and cement-implant interface. Studies that focused on the integrity of the cement-bone interface concluded that of the two this one was the most vulnerable, especially when the counterface was cortical bone^{6,7}. The interdigitation of bone cement (PMMA) with trabecular bone provides the strength through mechanical interlock. However, in time the strength of this interface decreases as a result of bone resorption caused by stress shielding, wear particle induced osteolysis or thermal necrosis⁸⁻¹⁰.

The fixation of the cement-implant interface relies on the implant bonding surface geometry (recesses and undercuts; i.e. cement pockets) to obtain long-term mechanical interlock with the cement. Additional efforts have been made to improve cement-to-implant adhesion to further improve fixation. This led to the enhancement of the cement-bonding interfaces from the early metal components to the current designs¹¹⁻¹⁴. Studies showed that smooth implant surfaces had low interface adhesive strength, whereas a roughened interface appeared significantly stronger by adding a level of micro-mechanical interlock^{15,16}. Chemical agents have also been studied, including the use polymethylmethacrylate (PMMA) pre-coatings or primers known from applications in hip arthroplasty and dentistry^{5,17}.

The fact that implant fixation is primarily a consequence of macro- and/or micro-mechanical interlock means that the cemented femoral component is inherently well fixated directly postoperative if adequate surface roughness and undercuts (or cement pockets) are available. This was also shown for polyethylene acetabular liners that clearly benefitted from the addition of profiles on the cement-implant interface since the interface had negligible strength without profiles¹⁸.

Early TKA failures with a mechanical cause are usually related to implant sizing and positioning rather than suboptimal fixation¹⁹. The apparent absence of early clinical problems related to the cement mantle has probably led to only a short list of studies focusing on initial fixation issues of cemented femoral knee implants. Those that did evaluate the strength of the bone-implant or cement-implant interface used pull-out or push-off experiments. Most studies used coupon samples^{5,11,12,14-16} and surprisingly few have studied the effect of the entire femoral implant geometry^{20,21}. Bergschmidt *et al.* (2015) performed high-flex pull-out tests on synthetic femurs and reported an average pull-out force of 2,322 N for ceramic

implants compared to 4,769 N for metallic ones. This reduction in fixation strength may not be problematic as a 5-year clinical follow-up study of the component showed outcomes similar to CoCr devices²². Hence, it seems that cemented fixation of a standard CoCr femoral component has a considerable factor of safety against mechanical debonding and that components with a 49% (2,322 N/4,769 N) lower fixation strength perform adequately under in-vivo conditions.

The studies above all make use of stiff metal or ceramic implants^{11,21} and thus share the fact that the material hardly deforms under the loading conditions. The object of the current study is a polyetheretherketone (PEEK) femoral TKA component. It is a polymer known for its wear resistance, strength and biocompatibility²³, but is weaker and substantially more compliant compared to metals and ceramics. These features may have potential benefits for application in TKA²⁴, but could also jeopardize the fixation strength and failure mechanisms of the femoral implant.

Prior experiments on the fixation of PEEK to PMMA have been conducted in-house to assess the influence of cement-bonding surface finish on the bond strength. These tests were performed on coupon specimens under tensile and under shear loads. A smooth PEEK coupon was easily debonded and did not provide any noteworthy strength. Based on these findings surface features were added, comprising of a large rib macrotecture and laser etched microtexture. This greatly improved the fixation strength, but those data were difficult to relate to either pure tensile or shear strengths as the multidimensional interface features provided interlock between the coupon and cement layer. Therefore, we decided to perform strength tests with the entire implant geometry to be able to relate findings of one implant to the other.

The current study was designed to assess the primary fixation strength and failure mechanisms of a cemented TKA femoral component made of PEEK and compare that with the same design made of CoCr. Three designs of the PEEK implant were considered; a smooth cement pocket design, a design with enhanced cement bonding features, and the latter with additional primer.

Materials and methods

Study design

The present study was set up as a controlled experimental design with four groups. Group 1 consisted of CoCr (N=4) implants (Maxx Orthopedics Inc., US), which served as a control for the other three groups because of its present clinical applications (Figure 1A). Group 2 was a regular PEEK implant (N=5) with the exact same geometry as the CoCr component

and identical cement pockets, yet lacking the surface roughness of CoCr (Figure 1B). They were machined from a block of annealed PEEK-OPTIMA® (Invivo Ltd, Thornton-Cleveleys, UK). Group 3 was the injection molded PEEK-OPTIMA® (N=5) with enhanced cement-bonding features (ribs and laser-etching, Figure 1C). Group 4 was added which were the same implants as Group 3 but included a primer on the PEEK surface prior to implantation (N=4). This primer (Scotchbond Universal, 3M ESPE, Neuss, Germany) is commonly used in dental applications with positive results when tested with PEEK²⁵.

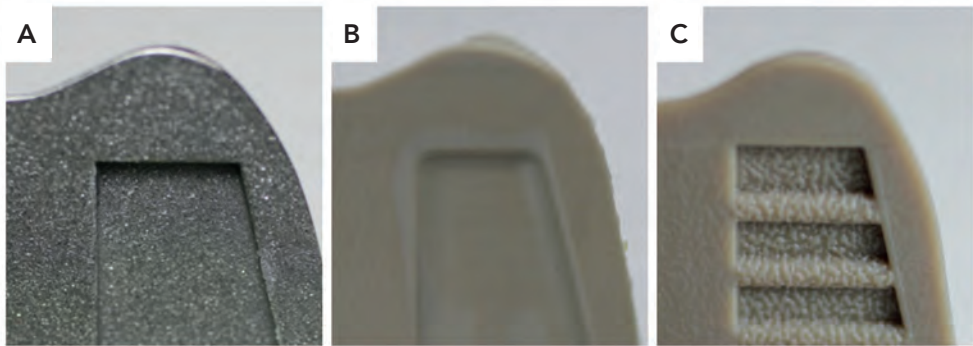


Figure 1. Cement-bonding interface morphology of A) CoCr, B) regular PEEK and C) enhanced PEEK femoral component.

Experimental set-up

All groups were cemented onto biomechanical testing foam blocks, analogue to trabecular bone (Sawbones Europe AB, Malmö, Sweden). A cellular foam block was chosen (0.32 g/cm^3) as the mechanical properties are similar to healthy trabecular bone with regard to stiffness (137 MPa) and strength (5.4 MPa) and allowed cement penetration²⁶. To minimize differences between samples the foam blocks were machined to geometrical cutting specifications. Milling residue was removed with vacuum suction and any remaining particles were cleaned off with pressurized air. Heraeus Palacos-R bone cement was used in combination with the Palamix vacuum mixing system (Heraeus Medical, Wehrheim, Germany). The implants were cemented according to the protocol described by Vaninbroux *et al.* (2009) to achieve maximum fixation²⁷. Prior to cementation Group 4 received the adhesive primer. A fine brush was used to apply the adhesive to the implant surface. Subsequently, the adhesive (in liquid state) was distributed with pressurized air to form a constant thin film after which it was left under a UV light source for 10 minutes.

The reconstructions were pre-conditioned by subjecting them to 24 h of 1 Hz cyclic compressive, slightly medially biased loading on a hydraulic uni-axial testing rig, between 2,600-260 N. The maximum load of 2,600N was based on the ISO-14243 standard for knee

replacement²⁸. The cyclic loading was applied in extension through a modified matching tibial component (Figure 2A). After preconditioning the foam blocks were firmly clamped onto a platform. A customized surgical extractor was placed over the medial and lateral recesses in the distal flange of the femoral component to apply the tensile load from the hydraulic testing rig (Figure 2B). The machine was set to displacement control at a rate of 0.5 mm/min. This resulted in a pure axial tensile load with respect to the implant alignment. During preconditioning and the pull-off test a planar xy-bearing was mounted to maintain axial alignment.

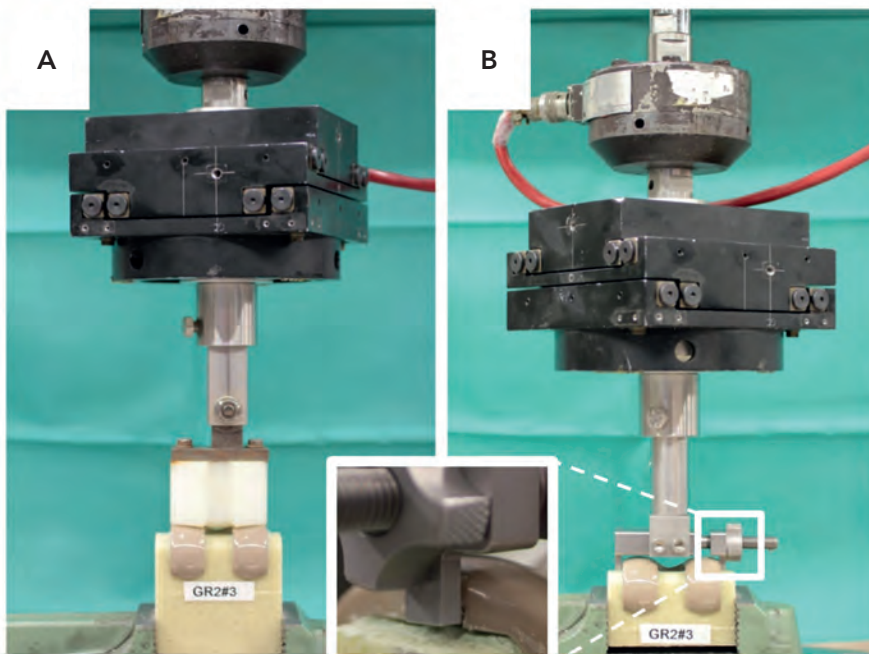


Figure 2. Testing rig set-up for A) preconditioning and B) pull-off, with planar xy-bearing (black).

Outcome measures

During the pull-off phase observations of debonding, cracking, deformations and total failure were recorded. Displacements and loads were recorded throughout the test. The outcome measures were the maximum pull-off load and failure patterns. The main failure mode was defined as the damage corresponding to the greatest loss of strength after the peak force, i.e. cement-foam debonding, cement-implant debonding or foam fracture.

Statistics

Results were described with the mean and standard deviation for each group. A one-way ANOVA with post-hoc Bonferroni correction was employed to calculate the two-sided statistical significance of differences between groups ($\alpha=0.01$).

Finite Element Analysis of the experiment

The differences between the stress distributions in the CoCr and PEEK reconstructions were further analyzed using finite element analysis (FEA). For this purpose, an FEA model was created consisting of the foam block, a cement layer (1 mm thickness), the femoral component and the extractor. The femoral component was assigned with a Young's modulus either representing CoCr (210 GPa) or PEEK (3.7 GPa). The cement, foam block and extractor were assigned with a Young's Modulus of 2.886 GPa, 0.137 GPa and 150 GPa, respectively. The cement-bone and implant-cement interfaces were assumed to be fully bonded.

The model was fixed at its distal end, while the extractor was loaded at a force of 2,525 N for both models. To compare regional differences between the CoCr and PEEK implants, the foam Von Mises stresses were binned in anterior-posterior and medio-lateral sections with a size of 3 mm.

Results

Pull-off force

Group 1 with the CoCr implants showed the highest fixation strength, while regular PEEK was the weakest (Figure 3). The design features of the enhanced PEEK implant improved the fixation of the device, while the primer did not result in additional fixation strength relative to the enhanced PEEK implant. All groups were significantly different from each other ($p<0.01$) with the exception of Groups 3 and 4 ($p=0.4$).

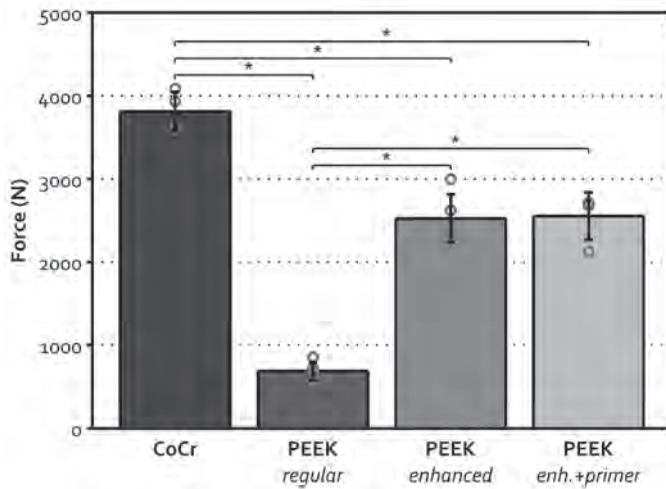


Figure 3. Mean (SD) pull-off force for the femoral components. Circles depict the separate observations. Significant levels are indicated (* $p < 0.01$).

Failure mechanisms

During the pull-off of the CoCr implants in Group 1 the first signs of failure occurred at the distal interface. While the measured force kept increasing a gap was visible between the cement and foam or cement and implant, varying between samples. This gap propagated to the posterior chamfers after which it only increased in gap opening size. This was followed by increased audible cracking and eventually a brief snap indicating the foam and/or cement mantle had cracked (Figure 4). Failure was simultaneous over the majority of the implant, leaving small sections of the anterior flange still fixed. The main failure mode was foam fracture combined with cement-bone interface failure and initiated at the posterior condyles. The bulk of the CoCr implant surface after pull-off was still covered with cement and foam remnants. Although during the test it appeared that there was some amount of cement-implant debonding on the distal condyles this did not lead to loss of fixation of the implant as the final failure occurred at the cement-bone interface (Figure 5A).

Regular PEEK implants in Group 2 showed markedly different failure mechanisms from the CoCr constructs. Immediately from the start of the extraction audible cracking/squeaking was present. Increased force soon led to a gap opening of the distal flange and both anterior and posterior chamfers, similar to CoCr. Unlike the CoCr components this was a clean debonding of the cement-implant interface. Further displacement initiated an elastic 'opening' deformation of the implant increasing while the cement pocket edges were pulled over the angled cement mantle edge. It is suspected that this is associated with the peak pull-off force as forces dropped after maximum implant opening (Figure 4). After that, the

residual fixation strength was primarily due to frictional forces the aforementioned elastic opening of the implant returned to the foam-cement construct. The main failure mode was complete cement-implant debonding (Figure 5B).

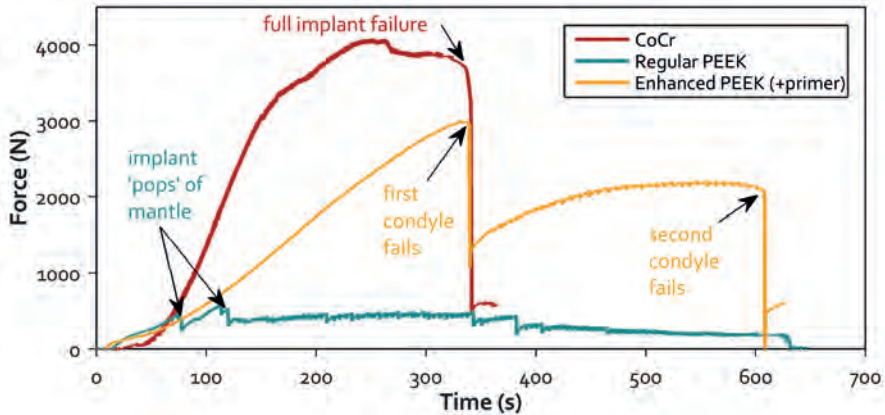


Figure 4. Typical force curves for the different implant designs with crucial events identified.

In Group 3, the enhanced PEEK implant design, was highly similar to CoCr in terms of primary failure pattern. Again, a distal flange gap opening was visible. This gap increased in width, eventually followed by fracturing of the foam behind the posterior condyles toward the pegs. The axial displacement led to the elastic deformation of the condyles resulting in failure in the condyles, but left the anterior flange still firmly attached to the foam. In contrast to CoCr, initial failure in this group occurred on either the medial or the lateral condyle, slightly later followed by the other (Figure 4). Further axial displacement initiated cement-implant debonding as the implant was being peeled off from the cement mantle. Similar to regular PEEK was the audible cracking/squeaking during the extraction, although this did not result in visible changes to the construct. The peak pull-off force was found at the initial condylar foam fracture which was deemed the main failure mode for this design. Similar to the CoCr group, the PEEK implant surface was still covered with cement and foam remnants after pull-off (Figure 5C).

The additional PEEK surface primer in Group 4 did not lead to increased fixation strength and also did not alter the failure patterns as seen in the enhanced PEEK implants in Group 3 (Figure 5D).

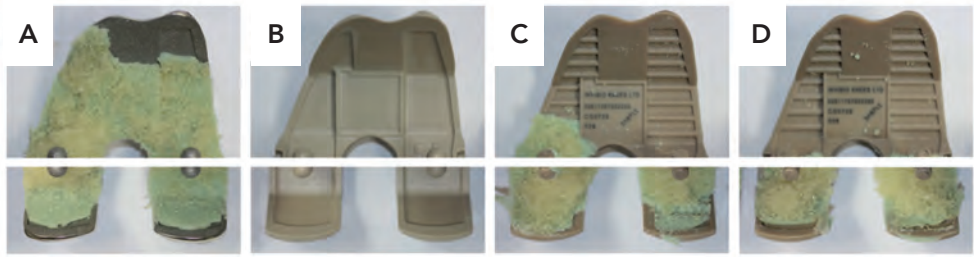


Figure 5. Implants after extraction for A) CoCr, B) regular PEEK, C) enhanced PEEK and D) enhanced PEEK+primer.

FEA model of the experiment

The results of the FEA model indicated that the stresses in the foam were substantially higher in combination with a PEEK implant than with a CoCr implant, particularly in the distal implant region (Figure 6). More proximally, the Von Mises stresses were higher in the CoCr reconstruction, due to the stiffer anterior flange.

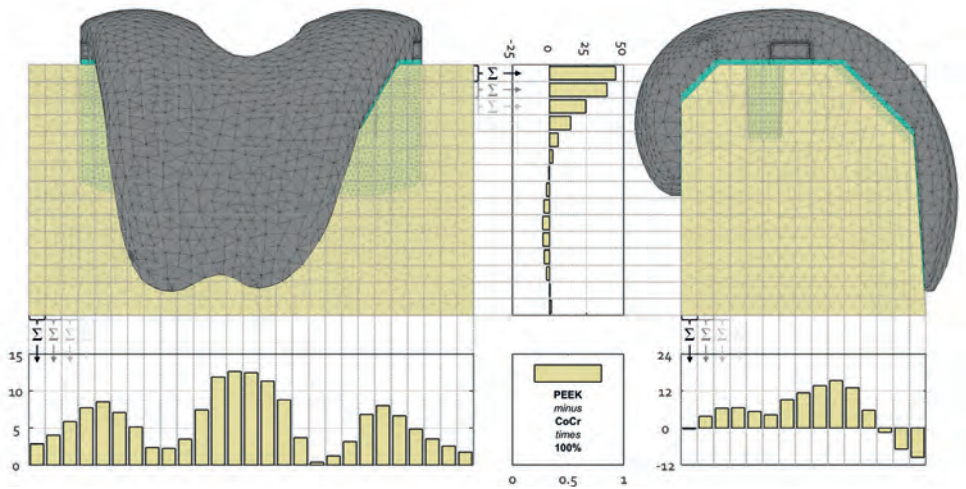


Figure 6. Increase in Von Mises stress (percentage) in the foam block underneath the enhanced PEEK implant relative to CoCr. Data are summed in 3 mm thick slices in three different planes: medial-lateral (bottom left), proximal-distal (top center), anterior-posterior (bottom right). For example: in the medial-lateral direction stresses in the foam are increased most in the slices between the condyles. In the proximal-distal direction foam stresses are increased by about 50% in the most distal slice, underneath the implant. In the anterior-posterior direction stresses in the anterior flange are decreasing when using a PEEK implant.

Discussion

The goal of this study was to determine the fixation strength and failure mode of a cemented PEEK femoral TKA component and to put this in the perspective of a conventional CoCr design. The results for the initial regular PEEK implant were such that a redesign of the cement bonding surface was necessary. Large ribs were added to the anterior and posterior flanges and chamfers, combined with a laser-etched microtexture. This led to a substantial improvement in fixation strength. More importantly, the main failure scenario of the enhanced implant was similar to that of the conventional CoCr component, namely foam fracturing and cement-bone interface failure in the posterior condyles/chamfers. In an effort to even further improve the fixation between implant and bone cement the redesigned implants were tested with an additional surface primer. This did not provide additional fixation in the current application.

Failure mechanisms

The most interesting similarities and differences were those between CoCr and PEEK with added surface features. Most notable was the fact that initial failure occurred at the same place as with CoCr, but at a lower force with the PEEK implant (3,814 N vs. 2,525 N). The foam was chosen for its consistency in material properties and hence, it was expected that the foam underneath both CoCr and PEEK implants experienced similar stresses at failure. The observation that failure of the PEEK reconstructions always initiated in one condyle, in contrast to both condyles simultaneously with CoCr, suggested that the force applied by the rig was biased toward the medial or lateral condyle in the PEEK construct. This effectively increased the stress in the foam to levels similar to the CoCr construct, initiating failure at a lower applied force. This was further corroborated by the observation that after the first condyle had failed, a similar but slightly lower force was needed to loosen the other condyle. This phenomenon was attributed to the more compliant PEEK compared to the stiff CoCr, which makes the whole reconstruction more rigid. The PEEK implant deforms under the forces implicated with the set-up and consequently distributes loads differently throughout the implanted construct. The FEA model mimicking the experiment further confirmed that at the same load the stresses in the foam were substantially higher in the PEEK configuration.

The forces required to loosen the enhanced PEEK implants were higher than those from measurements in a push-off setup for cementless CoCr femoral components²⁹ or pull-out experiments from cemented ceramic implants²¹. Although the nature of primary fixation or differences in loading configuration do not allow for a direct comparison they do provide a benchmark for fixation strength to which our measurements agree. These results further stress the importance of the surface features for providing further fixation strength.

Limitations

The number of specimens tested in each group was based on availability. Therefore, no power study was performed to determine the optimal group size. Statistically significant differences were detectable due to the small variation within groups and large variations between groups.

The regular PEEK implants in Group 2 were produced differently from those in Groups 3 and 4. Group 2 implants were machined from a block of PEEK against injection molding of Groups 3 and 4 implants. Although this impacts the material properties of the implants slightly, these differences are more likely to play a role in strength and fatigue testing and not the current fixation experiment.

The use of trabecular bone analogue foam prevented the wide variety of bone quality and cement penetration capacity from biasing our findings. There are some limitations to the extrapolation of the fixation strength to an in-vivo situation, however. First, the simulated bone quality of the foam is relatively high for the expected bone quality of patients receiving TKA³⁰. Also, the cement penetration of the foam that was used was lower than can be expected in-vivo as the cellular structure does not fully compare to the open cell structure of trabecular bone³¹. Furthermore, the entire cement-bone interface was trabecular bone. It is known that the cement-bone interface has two components, cortical and trabecular bone, and that the former provides substantially weaker fixation⁶. The (foam) bone quality and lack of cortical fixation are likely to overestimate the strength of this study's cement-bone interface, whereas foam cell structure is likely to underestimate it. The machined foam provided reproducibility though, which is vital to the comparative nature of this study.

Finally, the extraction direction that was used in the set-up does not replicate a physiological loosening mode. A caudal oriented axial force is only found in high flexion angle activities but is always accompanied by an anterior-directed force component and opposite patellofemoral force. In that respect, this study utilizes a substitute measure for fixation in absence of a physiological one. The absence of compressive forces in this study implies that an even higher failure force may be found in a high-flex push-off setup.

Conclusions

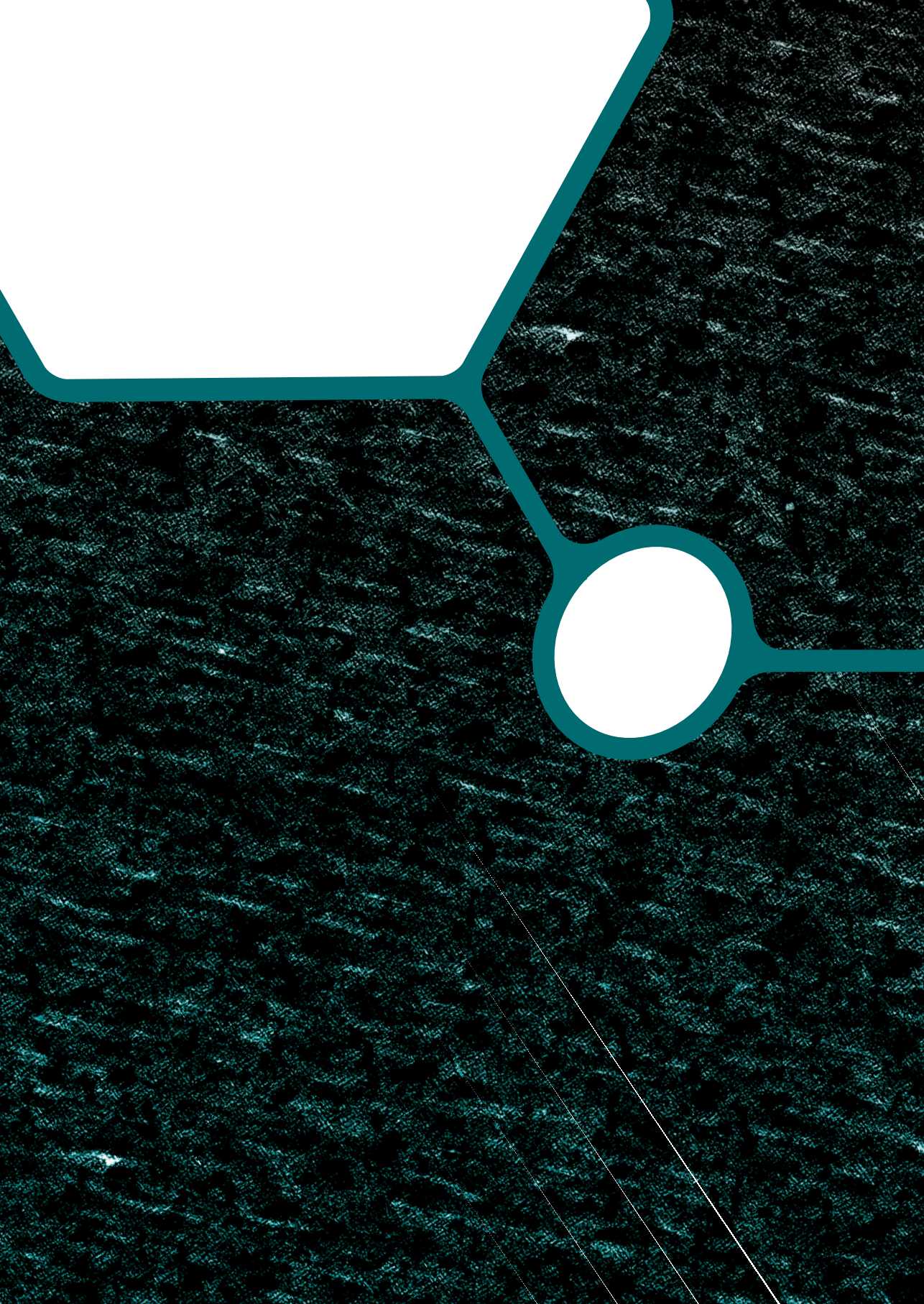
This study showed that a PEEK femoral TKA component is able to replicate the main failure mechanism of a conventional CoCr femoral implant but that the fixation strength is lower than that of a CoCr device. A strong improvement was made when profiles were added to the cement-bonding interface of the PEEK implant. This resulted in a fixation strength that seems higher than in-vivo loads as it outperforms the fixation strength of clinically well-performing ceramic femoral components when compared to standard metallic control implants; strength

reductions were 33% (2,525 N vs. 3,814 N) for the PEEK component (this study) and 50% (2,322 N vs. 4,769 N) for the ceramic implant^{21,22}. Therefore, this study indicates that adequate fixation can be obtained with a PEEK femoral component which should be corroborated in clinical studies.

References

1. Pilliar R. *Power metal-made orthopedic implants with porous surface for fixation by tissue ingrowth.* Clin Orthop Relat Res 1983; 176: 42–51.
2. Kienapfel H, Sprey C, Wilke A, et al. *Implant fixation by bone ingrowth.* J Arthroplasty 1999; 14: 355–368.
3. Berahmani S, Janssen D, van Kessel S, et al. *An experimental study to investigate biomechanical aspects of the initial stability of press-fit implants.* J Mech Behav Biomed Mater 2015; 42: 177–185.
4. Matassi F, Carulli C, Civinini R, et al. *Cemented versus cementless fixation in total knee arthroplasty.* Joints 2013; 1: 121–5.
5. Ahmed A, Raab S, Miller J. *Metal/cement interface strength in cemented stem fixation.* J Orthop Res 1984; 2: 105–18.
6. van de Groes S, de Waal Malefijt M, Verdonschot N. *Influence of preparation techniques to the strength of the bone-cement interface behind the flange in total knee arthroplasty.* Knee 2012; 20: 186–190.
7. van de Groes S, de Waal-Malefijt M, Verdonschot N. *Probability of mechanical loosening of the femoral component in high flexion total knee arthroplasty can be reduced by rather simple surgical techniques.* Knee 2014; 21: 209–15.
8. Howard K, Miller M, Damron T, et al. *The distribution of implant fixation for femoral components of TKA: A postmortem retrieval study.* J Arthroplasty 2014; 29: 1863–1870.
9. Miller M, Goodheart J, Izant T, et al. *Loss of cement-bone interlock in retrieved tibial components from total knee arthroplasties.* Clin Orthop Relat Res 2014; 472: 304–13.
10. Mann K, Miller M, Pray C, et al. *A new approach to quantify trabecular resorption adjacent to cemented knee arthroplasty.* J Biomech 2012; 45: 711–715.
11. Welsh R, Pilliar R, Macnab I. *The role of surface porosity in fixation to bone and acrylic.* J Bone Joint Surg Am 1971; 53: 963–977.
12. Stone M, Wilkinson R, Stother I. *Some factors affecting the strength of the cement-metal interface.* J Bone Joint Surg Br 1989; 71: 217–21.
13. Gardiner R, Hozack W. *Failure of the cement-bone interface.* J Bone Joint Surg Br 1994; 76: 49–52.
14. Raab S, Ahmed A, Provan J. *The quasistatic and fatigue performance of the implant/bone-cement interface.* J Biomed Mater Res 1981; 15: 159–182.
15. Crowninshield R, Jennings J, Laurent M, et al. *Cemented femoral component surface finish mechanics.* Clin Orthop Relat Res 1998; 90–102.
16. Keller J, Lautenschlager E, Marshall GJ, et al. *Factors affecting surgical alloy/bone cement interface adhesion.* J Biomed Mater Res 1980; 14: 639–51.
17. Yerby S a, Paal AF, Young PM, et al. *The effect of a silane coupling agent on the bond strength of bone cement and cobalt – chrome alloy.* J Biomed Mater Res 2000; 49: 127–133.
18. Haft GF, Heiner AD, Dorr LD, et al. *A biomechanical analysis of polyethylene liner cementation into a fixed metal acetabular shell.* J Bone Joint Surg Am 2003; 85-A: 1100–10.

19. Rousseau M-A, Lazennec J-Y, Catonné Y. *Early mechanical failure in total knee arthroplasty.* Int Orthop 2008; 32: 53–6.
20. Bollars P, Luyckx J, Innocenti B, et al. *Femoral component loosening in high-flexion total knee replacement.* J Bone Joint Surg Br 2011; 93: 1355–1361.
21. Bergschmidt P, Dammer R, Zietz C, et al. *Adhesive strength of total knee endoprostheses to bone cement – analysis of metallic and ceramic femoral components under worst-case conditions.* Biomed Tech 2016; 61: 281–289.
22. Bergschmidt P, Bader R, Ganzer D, et al. *Prospective multi-centre study on a composite ceramic femoral component in total knee arthroplasty: Five-year clinical and radiological outcomes.* Knee 2015; 22: 186–191.
23. Kurtz S, Devine J. *PEEK biomaterials in trauma, orthopedic, and spinal implants.* Biomaterials 2007; 28: 4845–69.
24. de Ruiter L, Janssen D, Briscoe A, et al. *A preclinical numerical assessment of a polyetheretherketone femoral component in total knee arthroplasty during gait.* J Exp Orthop 2017; 4: 3.
25. Kolbeck C, Lang R, Platzer K, et al. *Shear bond strength of composite cements on polyetheretherketone (PEEK) combined with various surface treatments.* In: *Conference Proceedings of the 23rd European Dental Materials Conference, Nuremberg, Germany.* 2015.
26. Li B, Aspden RM. *Composition and mechanical properties of cancellous bone from the femoral head of patients with osteoporosis or osteoarthritis.* J Bone Miner Res 1997; 12: 641–51.
27. Vaninbroux M, Labey L, Innocenti B, et al. *Cementing the femoral component in total knee arthroplasty: which technique is the best?.* Knee 2009; 16: 265–268.
28. International Organization for Standardization. *ISO 14243-1: Implants for surgery - Wear of total knee-joint prostheses - Part 1: Loading and displacement parameters for wear-testing machines with load control and corresponding environmental conditions for test.* 2009.
29. Berahmani S, Janssen D, Wolfson D, et al. *The effect of surface morphology on the primary fixation strength of uncemented femoral knee prosthesis: a cadaveric study.* J Arthroplasty 2014; 30: 300–307.
30. Patel P, Shepherd D, Hukins D. *Compressive properties of commercially available polyurethane foams as mechanical models for osteoporotic human cancellous bone.* BMC Musculoskelet Disord 2008; 9: 137.
31. Walker P, Soudry M, Ewald F, et al. *Control of cement penetration in total knee arthroplasty.* Clin Orthop Relat Res 1984; 185: 155–164.



Chapter 6

The effects of cyclic loading and motion on the implant-cement interface and cement mantle of PEEK and cobalt-chromium femoral total knee arthroplasty implants: a preliminary study

de Ruiter L, Cowie R, Jennings L, Briscoe A, Janssen D, Verdonchot N. The effects of cyclic loading and motion on the implant-cement interface and cement mantle of PEEK and cobalt-chromium femoral total knee arthroplasty implants: a preliminary study. *Materials* 2020; 13(15): E3323

Introduction

In cemented total knee arthroplasty (TKA) fixation is achieved by mechanical interlock of the implant with the bone via a layer of polymethylmethacrylate (PMMA) bone cement. During surgery, the doughy cement is typically applied to bone and/or implant surfaces after which the implant is pushed into place. The result is an implant that is well-fixed to the underlying structure, which clinically has demonstrated good long-term survival¹⁻⁴. To ensure adequate long-term fixation, the implant-cement interface can be strengthened by a number of options. Femoral components are usually designed with cement pockets for macro-interlock and a surface texture is added to enhance the fixation strength through micro-interlock. Standard application of these features has amounted to decades of evidence of firm and reliable fixation¹⁻⁴. Additional efforts have been made in the past to further enhance implant fixation by making the material adhere to the cement via chemical bonds rather than just shape-match at a macro- and microscale⁵⁻⁹. However, technologies such as PMMA or silane pre-coatings in cemented arthroplasty have not been largely adopted in conventional implant designs, at least in part due to the absence of evidence on clinical efficacy^{10,11}. Hence, most femoral TKA implants on the market rely on mechanical interlock of the implant to the cement and consequent fixation of the cement to the bone¹²⁻¹⁵.

For conventional femoral component materials (cobalt chrome, CoCr), a microtexture is often applied to the fixation surface (Figure 1) and with this modification, there have been few clinical reports of debonding at the cement-implant interface¹⁶⁻²¹. An increasing interest in the investigation of different materials and different manufacturing techniques for joint replacements however brings about the potential for different failure modes of the implant. PEEK-OPTIMA™ for example has been considered as an alternative to CoCr in the femoral component of a TKA to give a metal-free implant²²⁻²⁸. The lower modulus of a PEEK implant compared to CoCr may help to reduce stress shielding but may also change the distribution of forces at the cement-implant interface which may influence implant fixation. There are potential advantages of investigating different implant materials. With PEEK for example, the injection molding process used in manufacturing can apply macro- and micro-textures to the fixation surfaces in a one-stage manufacturing technique (Figure 1). A previous study into fixation strength of a PEEK implant with modifications of the fixation surface including the addition of macro- and micro-textures demonstrated an altered distribution of forces at the cement-implant interface compared to CoCr implants. Despite a decrease in fixation strength of PEEK femoral components, the failure modes of the different implant materials were similar and it was concluded that the bond between implant and cement may be sufficiently strong for clinical use²⁶.

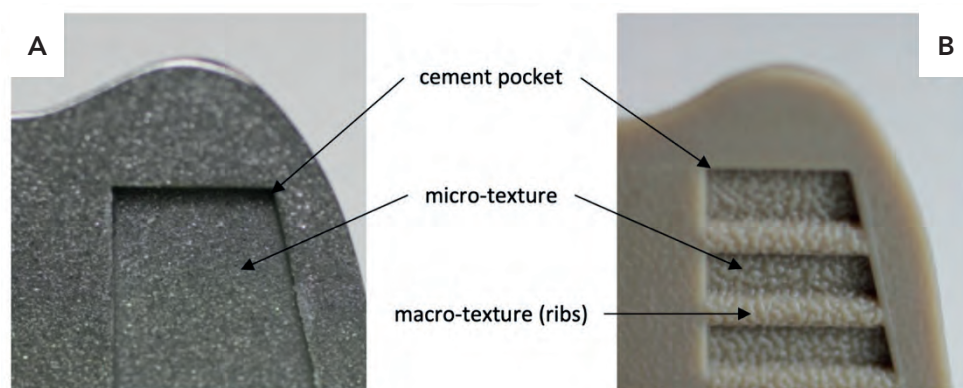


Figure 1. Surface texture of the CoCr (A) and PEEK (B) implants. The additional cement-bonding features of the PEEK implant are visible, comprising a macroscopic rib features within the cement pockets and a microscopic pattern superimposed over the surface.

The fixation at the cement-implant interface is understudied. However, debonding of the femoral component may lead to gross implant loosening, abrasion at the cement-implant interface and failure of the cement mantle. Previous mechanical testing indicated that gross loosening of a PEEK femoral component is very unlikely if the fixation surface has been optimized to provide sufficient mechanical interlock²⁶. However, micromotions of a loosened implant could cause abrasion of the cement-implant interface leading to the subsequent release of PEEK and/or cement particles which may accelerate wear debris induced osteolysis and/or lead to failure of the cement mantle, and could produce cement particles leading to third-body wear^{29,30}. These potential complications underline the importance of understanding the implant-cement interface, particularly for a PEEK femoral TKA component.

The aim of this study was to determine the quality of the implant-cement interface of a PEEK femoral TKA component and compare to a CoCr implant. Implants were subjected to clinically relevant loading and motions for up to 10 million cycles (MC) in a knee simulator and a method was developed to assess the bonding between the implant and cement and the integrity of the cement mantle. It was hypothesized that due to the difference in thermal conductivity and modulus of the implant materials, the bonding at the cement-implant interface and the cracking of the cement would differ between implant materials and that PEEK would show more debonding and cracks in the cement mantle than CoCr. This was a preliminary study to establish a method to evaluate the implant-cement interface and as such was carried out with a small sample size.

Materials and methods

Materials

Mid-size (size C) injection molded PEEK-OPTIMA™ femoral components (collaboration partners Maxx Orthopedics Inc., Plymouth Meeting, PA, USA and Invibio Knee Ltd, Thornton-Cleveleys, UK) and MAXX freedom knee (CoCr) femoral components (Maxx Orthopedics Inc., Plymouth Meeting, PA, USA) were used in this study. The implants had a similar geometry although the macro-features and texture on the fixation surface differed (Figure 1) and was optimized for each femoral component material. The samples were cemented to custom made polyoxymethylene (Delrin®) fixtures using Palacos R&G cement (Heraeus, Hanau, Germany). Delrin was chosen as the substrate due to having mechanical properties suitable for 10 MC wear simulation and a low porosity as the testing was carried out in various liquids. While the machined surface of the Delrin fixture may not be clinically relevant, the fixtures were consistent for all samples and the fixture-implant interface was not of interest in this study. The geometry of the Delrin substrate was designed using CAD and based on the geometry of the implant, allowing for a 1 mm cement mantle. The subsequent CAD model was CNC-machined using a 5-axis machine. The cement used was the same as that used clinically. It was mixed manually, and the doughy cement was applied to the implant in excess. The implant was pressurized onto the Delrin fixture and shims were used to create a cement mantle with a consistent 1 mm thickness. The process was carried out at room temperature with the same technique applied irrespective of the implant material.

When tested under physiological loading and motion, the femoral components were coupled with Size C all-polyethylene tibial components (Maxx Orthopedics Inc., Mahwah, NY, USA). To assess the debonding of the femoral component-cement interface, the implants were immersed and/or tested in a fluorescent penetrant dye (WB200, Sherwin Babbco) in saline solution at [1:10] concentration.

Experimental design

Three experimental groups with three samples in each were defined as shown in Table 1. Group 1 components were soaked in the penetrant dye for 27.8 hours (equivalent to the duration of 100,000 gait cycles carried out at 1 Hz). This was carried out for PEEK implants only, to assess the initial bonding between the cement and implant ('unloaded control'). Only PEEK implants were investigated in this experimental group because a previous in-house cadaveric experiment demonstrated poor initial fixation for PEEK specimens and good initial fixation between the implant and cement for CoCr components. It was assumed that loading of the CoCr device was required to disrupt the fixation at the cement-implant interface and to encourage the dye into the interface. Group 2 ('Gait control') comprised of both PEEK and CoCr femoral components, which, following cementing onto fixtures, underwent

physiological gait loading and motion (Figure 2) in the penetrant dye for 100,000 cycles at 1 Hz (27.8 hours) using a 6-station ProSim electropneumatic knee simulator (Simulation Solutions, Stockport, UK). The simulator has 6 degrees of freedom and 4 axes of motion were controlled during the test; Axial Force (AF), Flexion Extension (FE), Tibial Rotation (TR) and Anterior Posterior displacement (AP). Performing 100,000 cycles facilitated dye uptake in debonded or cracked areas. To determine the number of gait cycles required for the dye to enter the cement-implant interface, an experiment was carried out in which PEEK implants were cemented to a bone-analogue foam and loaded uniaxially (2600N-260N @ 1Hz) in the fluorescent dye for 100,000 cycles. At the conclusion of this preliminary study (Figure 3), for PEEK implants, a fluorescent line could be seen between the cement and implant where the dye had entered the interface. It was assumed that dye uptake would be higher when the sample was loaded in a simulator and subjected to simultaneous loading and motion rather than the uniaxial loading used during method development. It was not feasible to use a bone-analogue foam as the substrate for the 10 MC simulation so to maintain consistency between samples, Delrin was used as the substrate throughout. Group 3 comprised PEEK and CoCr femoral components that had been previously tested for 10 MC in a ProSim knee simulator under physiological loading and motion to represent the kinetics and kinematics at the bearing surface of the tibiofemoral joint during a walking gait cycle. High flexion activities and forces at the patellofemoral joint were not considered in this study. The experimental wear simulation study was carried out under 'Leeds high kinematic' conditions (Figure 2) in a lubricant of 25% bovine serum supplemented with 0.03% sodium azide solution against all-polyethylene tibial components³¹. These test conditions were similar to those previously described by Cowie *et al.* (2016)²³. Following wear simulation, the samples were cleaned using detergent ensuring the PEEK and CoCr implants were treated the same in side-by-side studies. This test group ('10 MC gait') subsequently underwent a further 100,000 cycles under the same loading and motion, while immersed in the penetrant dye. All groups were thus exposed to the dye solution for the same duration.

Table 1. The experimental groups and sample size for each femoral component material.

	Group 1	Group 2	Group 3
	Unloaded control	Gait control	10 MC gait
PEEK	3	3	3
CoCr	-	3	3

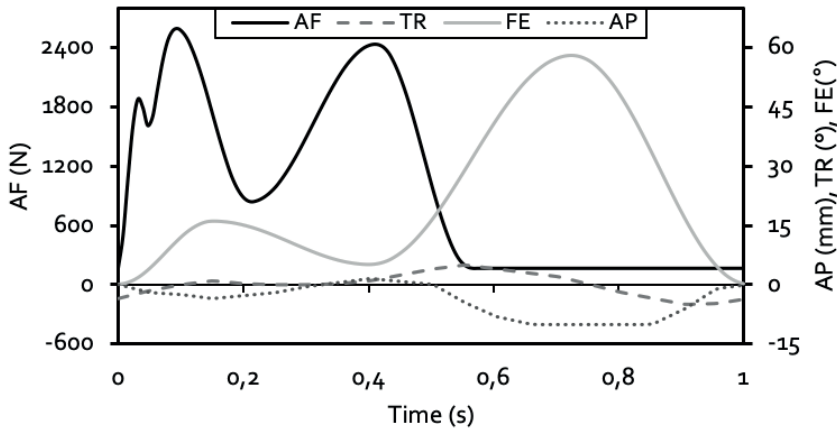


Figure 2. Input profiles for cyclic loading on the knee simulator. The parameters are axial force (AF), tibial rotation (TR), flexion-extension angle (FE) and anterior-posterior displacement (AP).

Analysis of dye penetration (fluorescence)

Having been immersed in the dye, the specimens were sectioned in the sagittal plane through the center of the lateral condyle with a cutting blade under water cooling. The lateral condyle was chosen over the medial condyle because when cross-sectioned, all internal implant faces are visible (Figure 3); for the medial condyle, the geometry of the implant means that when cross-sectioned through the center of the condyle, the anterior chamfer cannot be seen. A UV light was used to excite the fluorescent dye (320–420 μm) and imaging performed using a generic microscope at 1.5×10 magnification. A scoring system was devised to assess whether fluorescent dye was visible at the implant-cement interface. The femoral components were divided into six distinct regions for analysis as shown in Figure 3 namely, the anterior flange, the anterior chamfer, the distal area, the peg, the posterior chamfer and the posterior flange. No differentiation was made for the intensity of the UV-light since debonding was assumed to be complete in regions where fluorescence was observed regardless of the light intensity. Scoring was carried out manually by two scorers and each area was ranked between 0 and 3 (0: no fluorescence; 1: up to 33% of the interface fluorescent; 2: up to 67% and 3: complete fluorescence). There was a high level of inter-observer reliability resulting in few discrepancies between the two scorers. When differences were identified, researchers deliberated and agreed on a final score. Separate area scores were summed for the entire interface and averaged to obtain a single score for each specimen.

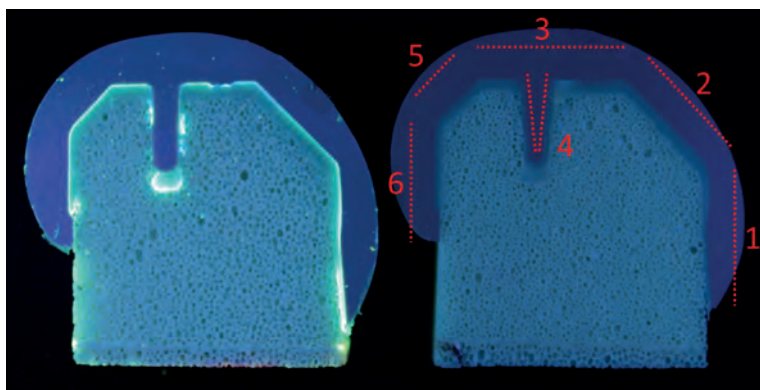


Figure 3. Proof-of-concept lateral condyle PEEK specimens cemented on bone-analogue foam after 100,000 cycles in fluorescent dye. Left: the implant under UV lighting showing complete interface dye fluorescence (score 3), Right: the same sample without UV lighting and how the interface was divided into 6 regions for analysis (1: anterior flange; 2: anterior chamfer; 3: distal area; 4: peg; 5: posterior chamfer; 6: posterior flange).

Analysis of cement damage (full-thickness cracks)

Cement damage was scored for each of the six regions on the femoral component described in Figure 3 by assessing the number and location of cracks that crossed the full-thickness of the cement mantle. Again, two scorers independently examined the implants. Few differences between scorers were identified and were reviewed and debated until a consensus was reached. The dataset was checked and corrected for double hits in overlapping images. The number of cracks in each region were averaged for all specimens in the study group. Average scores were compared between PEEK and CoCr, for both the entire cement mantle and each separate region.

Statistics

The data are presented as the mean (\pm standard deviation) for both fluorescence and full-thickness cracks. Statistical analysis was carried out in SPSS 24.0 (IBM Corp, Armonk, NY, USA) using a t-test to compare PEEK and CoCr for each experimental group, under the hypothesis that PEEK would show more fluorescence and cracks than CoCr. Groups were analyzed with a 0.05 significance level.

Results

Analysis of dye penetration (fluorescence)

Unloaded PEEK control specimens (Group 1) showed high levels of dye penetration at the implant-cement interface without the components undergoing loading and motion (Figure 4). On average, 79% ($\pm 11\%$) of the PEEK-cement interface was fluorescent after being soaked in dye (unloaded) for 28 hours (Figure 5). After 100,000 gait cycles, for the PEEK gait controls (Group 2), the average fluorescence area was 61% ($\pm 23\%$). This was lower than the unloaded controls (Group 1), but with a larger variability between samples. The CoCr Group 2 gait control samples showed limited dye penetration at the interface (13% ($\pm 6\%$)) after 100,000 gait cycles (Figure 4). After an extended number (10 MC) of test cycles under physiological loading and motion (Group 3), the implant-cement interfaces were easily distinguishable for both femoral component materials (Figure 4). For Groups 2 and 3, the PEEK components showed significantly ($p < 0.05$) more fluorescence than the CoCr implants. Comparing the gait controls (Group 2) to the implants loaded for an extended number of cycles (Group 3), the PEEK femoral components showed a slight increase in percentage fluorescence, from 61% ($\pm 23\%$) to 88% ($\pm 5\%$), while the CoCr implants displayed a steep increase after 10 MC of simulation, from 13% ($\pm 6\%$) to 62% ($\pm 6\%$) interface fluorescence (Figure 5). The variability between the samples for the Group 3 implants was lower than the other groups for both material types.

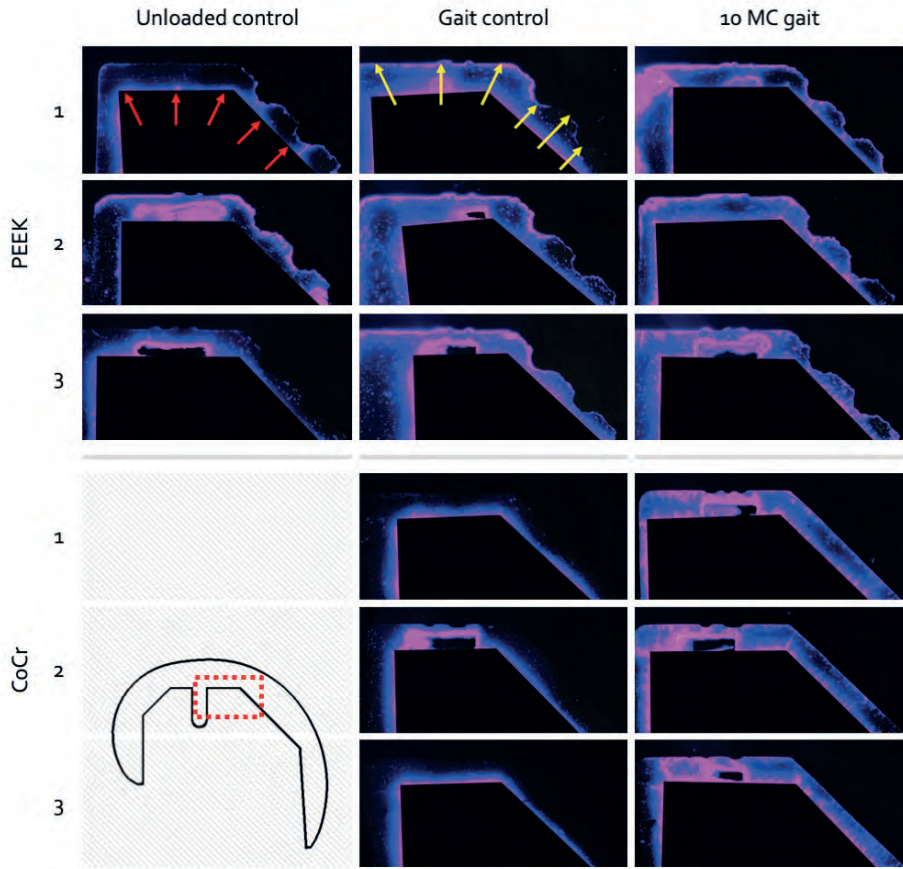


Figure 4. Test specimens under UV lighting show dye fluorescence intensity as blue-to-pink coloration with the pink area highlighting the highest dye uptake. Both cement-Delrin (red arrows) and implant-cement (yellow arrows) interfaces are visible. A section of the anterodistal cement mantle is shown at the three time intervals to demonstrate the appearance of dye penetration in both the PEEK and CoCr group. The variability within the PEEK unloaded control group is noticeable, ranging from near-full bonding (specimen 3) to complete debonding (specimen 2). A clear evolution of dye penetrance in the CoCr can be seen, where no implant-cement interface is visible in the gait control, but full interface fluorescent is visible in the Group 3 samples.

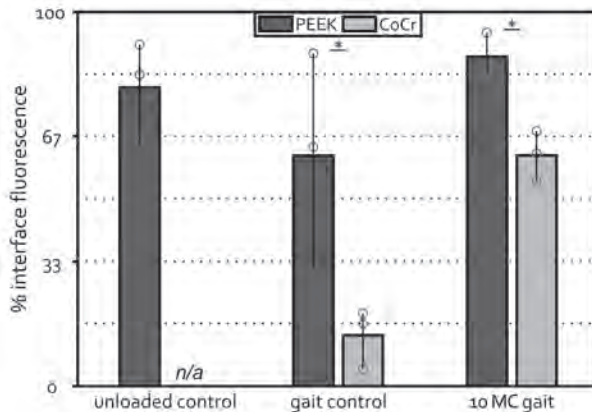


Figure 5. Average interface fluorescence scores of the complete implant-cement interfaces at difference intervals. The bars show the range of observations with the individual specimens shown as circles (statistical analysis compares PEEK to CoCr, * denotes $p < 0.05$).

Analysis of cement damage

Full-thickness cracks were observed in the cement mantles against both the PEEK and CoCr femoral components for the gait controls and 10 MC test groups. The locations of these cracks however were markedly different with cracks at the interface chamfers more often observed with a CoCr component than with a PEEK implant. With CoCr the cracks tended to run the full-thickness of the cement mantle, as opposed to with PEEK where the cracks at the chamfers were mostly incomplete (Figure 6A). In the PEEK femoral components, at the apex of the ridges which were incorporated into the cement pockets to enhance fixation, full-thickness cracks were common in the Group 3 femoral components which had been previously tested for 10 MC (Figure 6B). Both CoCr and PEEK reconstructions showed similar crack patterns in the anterior and posterior flange areas. In this region, the cracks underneath the PEEK components generally resulted in full-thickness cracks, while those underneath the CoCr implants showed both full-thickness and also showed numerous small cracks (Figure 6C).

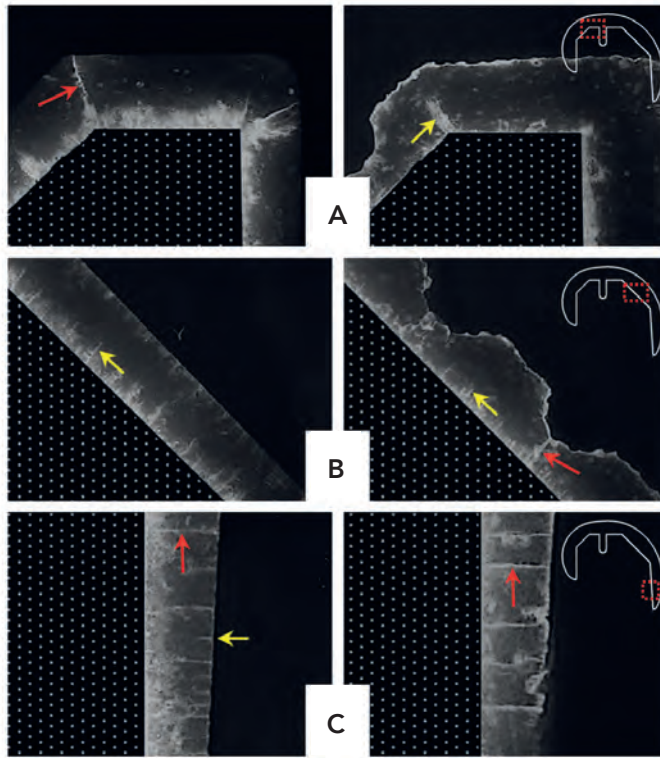


Figure 6. Representative images of CoCr (left) and PEEK (right) reconstructions after 10 MC, showing dye penetration in cement mantle cracks at three locations (A, B and C) around the femoral component as indicated by the red squares in the detail-figures. The red arrows indicate full-thickness cracks in the PMMA cement, the yellow arrows incomplete cracks. The reduced cement mantle thickness, caused by the ridges in the PEEK surface is visible in B (right).

No full-thickness cracks were observed in the unloaded control PEEK femoral components (Figure 7). In the gait control femoral components some full-thickness cracks appeared: $1.3 (\pm 1.9)$ and $0.7 (\pm 0.9)$ cracks on average for PEEK and CoCr respectively. This difference however was not significant ($p > 0.05$). After 10 MC under gait conditions, the number of cracks in both reconstructions had substantially increased. The average number of cracks in the cement layer below the PEEK femoral components was $24 (\pm 4.5)$, whilst the CoCr reconstructions demonstrated a mean of $19 (\pm 3.7)$ full-thickness cracks. Again, this difference was not significant ($p > 0.05$).

Further examination of the crack locations after 10 MC revealed that most cracks occurred in the cement mantle below the anterior flange of the implant (Figure 8). For both femoral component materials, the average number of cracks was 12.7 in this region. For the CoCr components, few cracks were visible around the anterior chamfer, while the PEEK implants

showed cracks in the cement in this area at the apex of the fixation ridges, as shown in Figure 6B. The posterior flange cement area also showed more cracking with the PEEK implant than with CoCr. After 10 MC, the femoral component material did not influence the number of cracks in the distal area, peg or posterior chamfer regions ($p>0.05$).

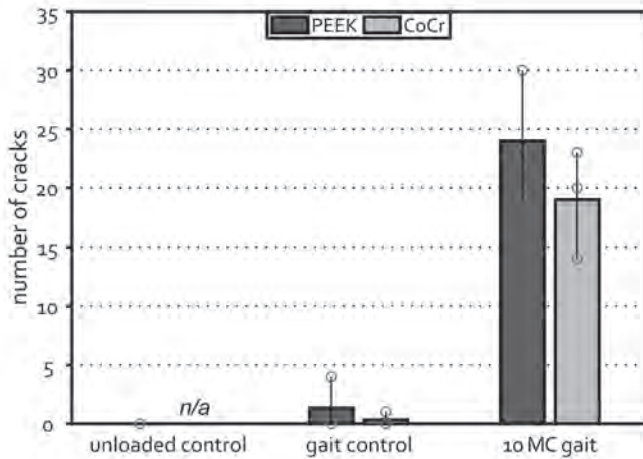


Figure 7. The average number of full-thickness cracks for the three experimental groups. The bars show the range of observations with the individual specimens shown as circles.

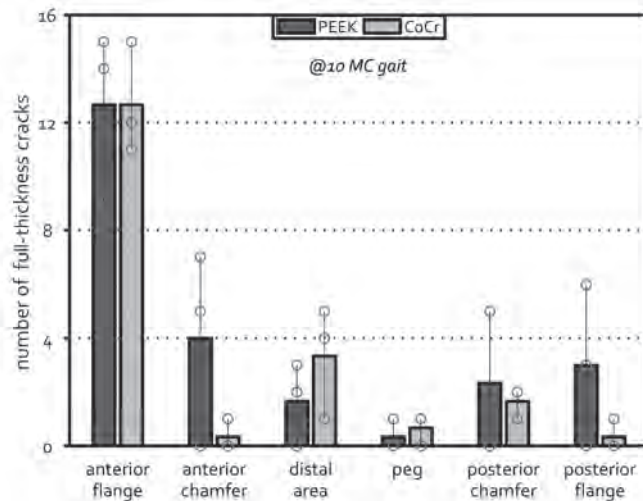


Figure 8. The average number of full-thickness cracks separated for each region after 10 MC. The bars show the range of observations with the individual specimens shown as circles.

Discussion

The aim of this study was to assess and compare the femoral component cement-implant interface for TKA's manufactured from PEEK and CoCr. The two femoral component materials were shown to have different effects on the cement mantle due to differences in the material properties of the components and variations in both the geometry and topography of the fixation surface. In summary, the CoCr implants showed less dye penetration at the cement-implant interface than PEEK components indicating superior adhesion between CoCr and cement. However, debonding of the cement-implant interface was evident for all implants when tested for high numbers of cycles. The integrity of the cement mantle was also analyzed. Cracks were evident in the cement beneath both PEEK and CoCr femoral components. There was no significant difference between the number of cracks in the cement-CoCr or cement-PEEK interface, but the location of the cracks differed depending on the implant material.

Analysis of dye penetration

The PEEK unloaded soaked control specimens showed that PMMA cement did not fully bond to the PEEK implant. Dye penetration did not differ between unloaded (Group 1) PEEK femoral components and those tested for 10 MC, (Group 3) specimens. Therefore, 10 MC experimental simulation had no additional effect on the bonding state of the PEEK implant-cement interface and in no samples was gross implant loosening observed. A previous pull-off fixation study by De Ruiter *et al.* (2017) concluded that PEEK femoral components with the same profile on the fixation surface as used in this study have adequate fixation strength²⁶. The information from these two studies combined suggests that debonding of the PEEK-cement interface does not necessarily limit the long-term mechanical fixation of the construct as a whole, although in both studies, non-physiological bone surrogates were used. This is further emphasized by the fact that substantial interface debonding was seen with CoCr implants following testing for 10 MC. CoCr femoral components are known to be mechanically stable when implanted for periods in excess of 10 years. Clinical evidence from successful polyethylene (PE) implants show similar debonding scenarios. All-polymer PE tibial TKA components for example have been available for several decades and have very positive outcomes, despite PE having no intrinsic bond with the cement³²⁻³⁴. Similarly, cemented all-polymer PE acetabular cups for hip arthroplasty which are dependent on surface textures for fixation also show excellent survival rates^{1,3,35} and a clinical trial of a Delrin femoral component showed a low incidence of loosening after 10 years implantation³⁶.

The cause of the immediate PEEK-cement interface debonding can be attributed to the lack of adhesion between the cement and implant, which means fixation primarily relies on mechanical macro- and micro-interlock with the surface topographical features on the implant fixation surface. The poorer thermal conductivity of PEEK compared to CoCr may reduce the

dissipation of heat produced as the PMMA cement cures which may lead to shrinkage of the cement contributing to debonding of the PEEK-cement interface. In addition, in clinical practice, the bond may be further influenced by contamination of the interface by blood or fat, and poor cementing technique or timing. From that perspective, the clean surfaces and absence of time pressure under which the samples were prepared for this study represent the optimal conditions for obtaining a well-fixed implant-cement interface.

Analysis of cement cracks

Macroscopic damage evaluation showed that full-thickness cracks were present in both CoCr and PEEK reconstructions tested under a gait cycle. Following 10 MC gait simulation, the mean number of full-thickness cracks in the cement mantle was approximately 20% higher for PEEK implants compared to CoCr however, this difference was not significant ($p > 0.05$). With the addition of potential stress risers (ridges in the fixation surface) which lead to a thinner cement mantle at the ridge-locations, the difference between the PEEK and CoCr components was expected to be larger. However, perhaps with the CoCr component, a different failure mechanism occurred. It is postulated that the higher stiffness of CoCr compared to PEEK also gives the potential for higher local stresses in the cement-CoCr implant interface as the femoral component is less compliant. Previous studies have shown the stiff CoCr component to generate high stress peaks in the cement underneath the proximal anterior flange^{24-26,37}. A large number of small cracks were visible in this region. A large number of small cracks were visible in this region. Analysis of these small cracks was beyond the scope of this study but there is potential for these small cracks to grow which may further increase cement damage in the anterior flange^{20,24,25}. The number of cracks in cement at the anterior flange and posterior chamfer areas of the cement mantle were similar in both implants however, there was a greater number of cracks in the PEEK-cement interface in the anterior chamfer and the posterior flange compared to the CoCr-cement interface.

Limitations

There are a number of limitations associated with this study which should be considered in the clinical interpretation of these findings. Firstly, the study was performed on an experimental wear simulator. As such, it is designed to mimic the kinetics and kinematics at the implant bearing surface as opposed to the femoral/fixture (bone) interface. The femoral components were cemented onto custom-shaped Delrin blocks that were mounted into the simulator. This replaced the in-vivo cement-bone interface with a cement-Delrin interface. It is acknowledged that Delrin may not represent bone in terms of its porosity, elastic modulus and surface texture. However, for this study which involved extensive wear simulation (>6 months) in a biological lubricant applying forces up to 2.8 kN, it was considered appropriate and was easy to section to allow analysis of the cement-implant interface. The intention was not to study the Delrin-cement interface and therefore, the surface was consistent (as machined)

for all experimental groups and other than pockets to accommodate the pegs, no additional features were introduced into the surface of the Delrin which provided a shape-lock fixation. The different mechanical properties of Delrin compared to bone may however have changed the load distribution in the cement mantle and how this influenced interface debonding and cement mantle damage is unknown. The 10 MC of gait simulation, equivalent to the loading the implant undergoes following approximately 10 years use in a moderately active patient³⁸ assumes that throughout the duration of implantation, the implant remains fully supported with no resorption of the underlying bone. It is not known whether the relatively sharp corners at the chamfers of the Delrin block may have stimulated crack propagation or whether the smooth Delrin surface may have reduced stress risers created by individual trabeculae, which may play an important role in crack initiation³⁹. Hence, the exact effect of the use of Delrin is unclear and future studies could consider a more physiologically relevant substrate. In terms of the cementing of the implants, there were further limitations as it was prepared using a manual mixing technique, which is inferior to the vacuum mixing process routinely used in the clinic. Manual mixing of cement gives rise to the potential for entrapment of air during cement preparation, which may cause pores. During analysis of the cement mantles, however, no pores were found in the cement layer, which may be attributed to the well-controlled laboratory conditions in which the reconstructions were prepared.

In addition, the simulator included only tibiofemoral contact. When both the tibiofemoral and patellofemoral joints are considered, *in vivo* forces are higher, since patellofemoral contact is a major contributor to the total loads on the femoral component particularly at higher flexion angles²⁵. However, the increased forces due to patellofemoral contact do not necessarily lead to an increased risk of debonding. A study by Berahmani *et al.* (2016) into micromotions behind cementless femoral knee components concluded that the patellofemoral contact decreased the micromotions in the anterior flange up to 22%⁴⁰. The study also investigated a gait cycle only. Although high-flexion activities are carried out less frequently than level gait, more strenuous activities including stair climbing, standing up and squatting may influence the study findings however, the comparative nature of this study comparing the cement-implant interface of PEEK to that of CoCr is a strength.

Furthermore, only 3 samples were investigated in each experimental group, this was limited by the extended duration of the studies within excess of 6 months continual testing required to prepare the 10 MC gait samples. Future work should consider larger implant sizes and perhaps extending the number of timepoints investigated especially for the CoCr implants to gain a better understanding of when debonding of these implants occurs and including a CoCr group 1 investigation to better understand the initial fixation of CoCr implants. However, increasing the sample size may necessitate automation of the analysis protocols to minimize variability between samples. The protocol used merely considers the loading the

implants undergo but not whether degeneration of the cement occurs during ageing. Further method development would be required to understand this and whether the mechanical properties of cement change with time. To minimize errors between experimental groups associated with ageing effects, the PEEK and CoCr implants were tested in parallel.

Finally, the study outcome parameters, dye penetration and cement cracking, are a local 2D representation of the full cement mantle and are thus subject to extrapolation error. The lateral condyle was chosen to represent all areas from anterior to posterior flange which does not cover the entire surface area. However, cracks in this section did propagate further laterally and medially into the cement mantle, and dye visualized at this location must have travelled from external boundaries, which supports the extrapolation applied here. This research did not include a microscopic damage assessment of the implant or cement interface surfaces after 10 MC of experimental simulation. One of the hypothesized results of long-term interface micromotions is the formation of wear particles. Once formed, these could travel into the joint space where they may initiate inflammatory processes which could contribute to wear debris induced osteolysis leading to implant loosening or, if larger particles were to migrate between the articulating surfaces, they could act as a third-body particle and may accelerate bearing surface damage or wear^{29,41,42}.

Conclusions

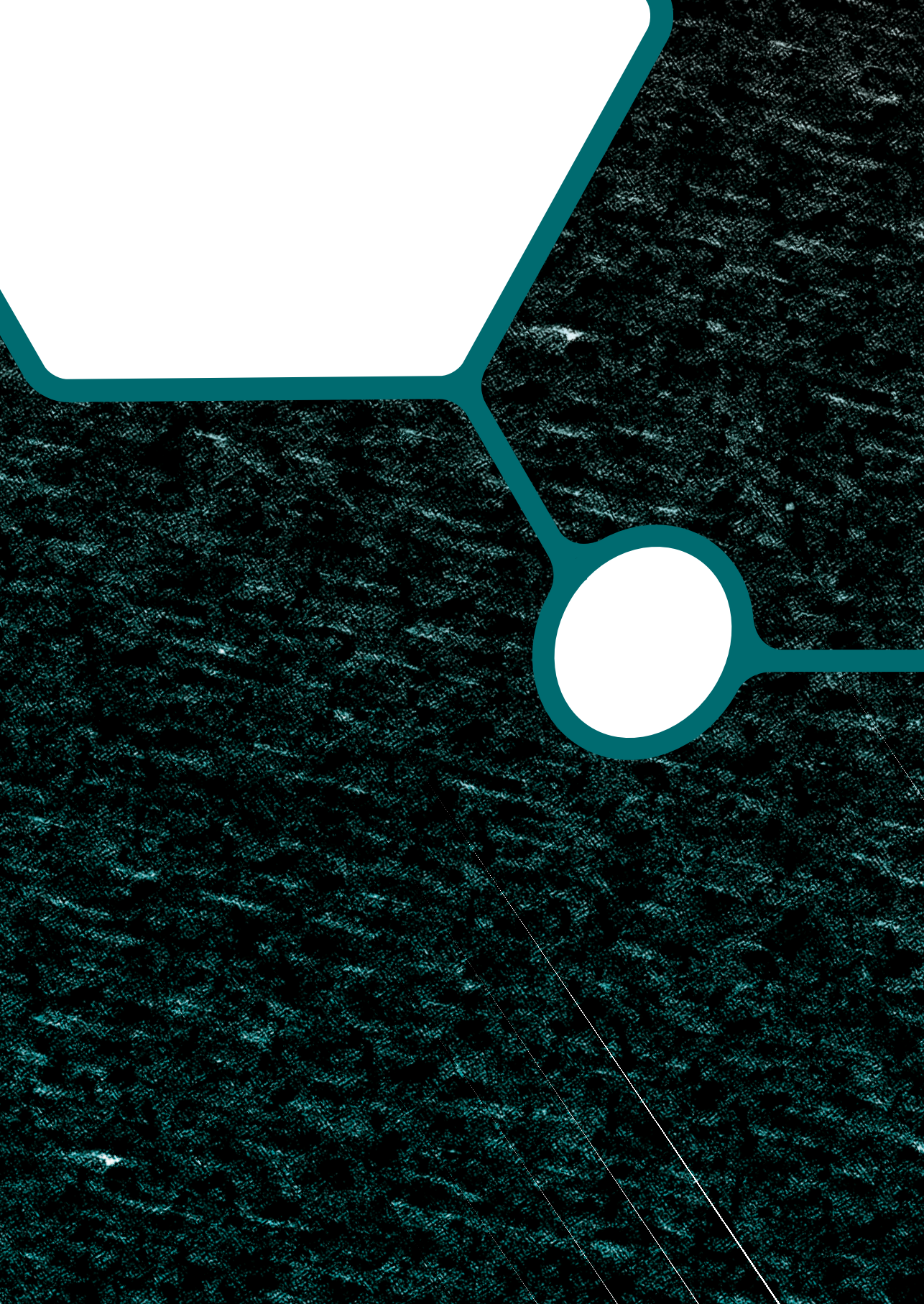
This study aimed to develop a method to assess the cement-implant interface bonding and the integrity of the cement mantle. This was done using a fluorescent penetrant dye and was then used to assess CoCr and PEEK femoral components which had undergone up to 10 million walking gait cycles. The study showed poor initial bonding of the PEEK-cement interface, however, after 10 MC simulation, the bonding of the implant remained similar to that of the controls. For CoCr implants, good fixation was measured for the gait control samples but after 10 MC, substantial implant-cement interface debonding occurred. After 10 MC, there was no significant difference in implant-cement debonding for the femoral component materials investigated, nor were there significant differences in macroscopic damage of the cement mantle. Further investigations using either a more physiologically relevant simulation system or through either animal studies or a clinical trial may be necessary to confirm these findings.

References

1. Australian Orthopaedic Association National Joint Replacement Registry (AOANJRR). *Hip, Knee & Shoulder Arthroplasty: 2017 Annual Report*.
2. Gandhi R, Tsvetkov D, Davey JR, et al. *Survival and clinical function of cemented and uncemented prostheses in total knee replacement: a meta-analysis*. J Bone Joint Surg Br 2009; 91: 889–95.
3. National Joint Registry for England, Wales Northern Ireland and the Isle of Man. *2017 Annual Report*.
4. Hopley CDJ, Dalury DF. *A systematic review of clinical outcomes and survivorship after total knee arthroplasty with a contemporary modular knee system*. J Arthroplasty 2014; 29: 1398–1411.
5. Erli HJ, Marx R, Paar O, et al. *Surface pretreatments for medical application of adhesion*. Biomed Eng Online 2003; 2: 1–18.
6. Marx R, Qunaibi M, Wirtz DC, et al. *Surface pretreatment for prolonged survival of cemented tibial prosthesis components: Full- vs. surface-cementation technique*. Biomed Eng Online 2005; 4: 1–9.
7. Yerby SA, Paal AF, Young PM, et al. *The effect of a silane coupling agent on the bond strength of bone cement and cobalt – chrome alloy*. J Biomed Mater Res 2000; 49: 127–133.
8. Ohashi KL, Yerby SA, Dauskardt RH. *Effects of an adhesion promoter on the debond resistance of a metal–polymethylmethacrylate interface*. J Biomed Mater Res 2001; 54: 419–427.
9. Mann K, Bhashyam S. *Mixed-mode fracture toughness of the cobalt-chromium alloy/polymethylmethacrylate cement interface*. J Orthop Res 1999; 17: 321–328.
10. Ong A, L Wong K, Lai M, et al. *Early failure of precoated femoral components in primary total hip arthroplasty*. J Bone Joint Surg Am 2002; 84-A: 786–792.
11. Bini SA, Chen Y, Khatod M, et al. *Does pre-coating total knee tibial implants affect the risk of aseptic revision?*. Bone Joint J 2013; 95-B: 367–370.
12. Ohashi K, Romero AC, D McGowan P, et al. *Adhesion and reliability of interfaces in cemented total hip arthroplasties*. J Orthop Res 1998; 16: 705–714.
13. Goodheart JR, Miller MA, Mann KA. *In Vivo Loss of Cement-Bone Interlock Reduces Fixation Strength in Total Knee Arthroplasties*. J Orthop Res 2014; 32: 1052–1060.
14. Srinivasan P, Miller MA, Verdonschot N, et al. *Experimental and computational micromechanics at the tibial cement-trabeculae interface*. J Biomech 2016; 49: 1641–1648.
15. van de Groes S, de Waal-Malefijt M, Verdonschot N. *Probability of mechanical loosening of the femoral component in high flexion total knee arthroplasty can be reduced by rather simple surgical techniques*. Knee 2014; 21: 209–15.
16. Bollars P, Luyckx J, Innocenti B, et al. *Femoral component loosening in high-flexion total knee replacement*. J Bone Joint Surg Br 2011; 93: 1355–1361.
17. Bergschmidt P, Dammer R, Zietz C, et al. *Adhesive strength of total knee endoprostheses to bone cement – analysis of metallic and ceramic femoral components*

- under worst-case conditions. *Biomed Tech* 2016; 61: 281–289.
18. Zelle J, Janssen D, Peeters S, et al. *Mixed-mode failure strength of implant-cement interface specimens with varying surface roughness.* *J Biomech* 2011; 44: 780–3.
 19. Arnholt CM, MacDonald DW, Malkani AL, et al. *Corrosion Damage and Wear Mechanisms in Long-Term Retrieved CoCr Femoral Components for Total Knee Arthroplasty.* *J Arthroplasty* 2016; 31: 2900–2906.
 20. Zelle J, van de Groes S, de Waal Malefijt M, et al. *Femoral loosening of high-flexion total knee arthroplasty: the effect of posterior cruciate ligament retention and bone quality reduction.* *Med Eng Phys* 2014; 36: 318–24.
 21. Han HS, Kang S-B, Yoon KS. *High incidence of loosening of the femoral component in legacy posterior stabilised-flex total knee replacement.* *J Bone Joint Surg Br* 2007; 89: 1457–1461.
 22. Rankin KE, Dickinson AS, Briscoe A, et al. *Does a PEEK Femoral TKA Implant Preserve Intact Femoral Surface Strains Compared With CoCr? A Preliminary Laboratory Study.* *Clin Orthop Relat Res* 2016; 474: 2405–2413.
 23. Cowie R M, Briscoe A, Fisher J, et al. *PEEK-OPTIMA™ as an alternative to cobalt chrome in the femoral component of total knee replacement: A preliminary study.* *Proc Inst Mech Eng H* 2016; 230: 1008–1015.
 24. de Ruiter L, Janssen D, Briscoe A, et al. *A preclinical numerical assessment of a polyetheretherketone femoral component in total knee arthroplasty during gait.* *J Exp Orthop* 2017; 4: 3.
 25. de Ruiter L, Janssen D, Briscoe A, et al. *The mechanical response of a polyetheretherketone femoral knee implant under a deep squatting loading condition.* *Proc Inst Mech Eng H* 2017; 231: 1204–1212.
 26. de Ruiter L, Janssen D, Briscoe A, et al. *Fixation strength of a polyetheretherketone femoral component in total knee arthroplasty.* *Med Eng Phys* 2017; 49: 157–162.
 27. Du Z, Zhu Z, Yue B, et al. *Feasibility and Safety of a Cemented PEEK-on-PE Knee Replacement in a Goat Model: A Preliminary Study.* *Artif Organs* 2018; 42: E204–E214.
 28. Meng X, Du Z, Wang Y. *Characteristics of wear particles and wear behavior of retrieved PEEK-on-HXLPE total knee implants: A preliminary study.* *RSC Adv* 2018; 8: 30330–339.
 29. Gallo J, Goodman SB, Konttinen YT, et al. *Osteolysis around total knee arthroplasty: A review of pathogenetic mechanisms.* *Acta Biomater* 2013; 9: 8046–8058.
 30. Cowie RM, Pallem NM, Briscoe A, et al. *Third Body Wear of UHMWPE-on-PEEK-OPTIMA™.* *Materials (Basel)* 2020; 13: 1–15.
 31. McEwen HMJ, Barnett PI, Bell CJ, et al. *The influence of design, materials and kinematics on the in vitro wear of total knee replacements.* *J Biomech* 2005; 38: 357–365.
 32. Ranawat AS, Mohanty SS, Goldsmith SE, et al. *Experience with an all-polyethylene total knee arthroplasty in younger, active patients with follow-up from 2 to 11 years.* *J Arthroplasty* 2005; 20: 7–11.
 33. Gioe TJ, Stroemer ES, Santos ERG. *All-polyethylene and metal-backed tibias have similar outcomes at 10 years: A randomized*

- level II evidence study. *Clin Orthop Relat Res* 2007; 212–218.
- 34.** Gieo TJ, Bowman KR. A randomized comparison of all-polyethylene and metal-backed tibial components. *Clin Orthop Relat Res* 2000; 108–115.
- 35.** Haft GF, Heiner AD, Dorr LD, et al. A biomechanical analysis of polyethylene liner cementation into a fixed metal acetabular shell. *J Bone Joint Surg Am* 2003; 85-A: 1100–10.
- 36.** Moore D, Freeman M, Revell P, et al. Can a total knee replacement prosthesis be made entirely of polymers?. *J Arthroplasty* 1998; 13: 388–395.
- 37.** Zelle J, Janssen D, Van Eijden J, et al. Does high-flexion total knee arthroplasty promote early loosening of the femoral component?. *J Orthop Res* 2011; 29: 976–983.
- 38.** Schmalzried TP, Szuszczewicz ES, Northfield MR, et al. Quantitative assessment of walking activity after total hip or knee replacement. *J Bone Joint Surg Am* 1998; 80: 54–59.
- 39.** Race A, Miller MA, Ayers DC, et al. Early cement damage around a femoral stem is concentrated at the cement/bone interface. *J Biomech* 2003; 36: 489–96.
- 40.** Berahmani S, Janssen D, Wolfson D, et al. FE analysis of the effects of simplifications in experimental testing on micromotions of uncemented femoral knee implants. *J Orthop Res* 2016; 34: 812–819.
- 41.** Lorber V, Paulus AC, Buschmann A, et al. Elevated cytokine expression of different PEEK wear particles compared to UHMWPE in vivo. *J Mater Sci Mater Med* 2014; 25: 141–149.
- 42.** Paulus AC, Haßelt S, Jansson V, et al. Histopathological Analysis of PEEK Wear Particle Effects on the Synovial Tissue of Patients. *Biomed Res Int* 2016; 2: 1–5.



Chapter 7

Clinical imaging protocols for in-vivo assessment of an all-polymer PEEK-on-UHMWPE total knee replacement with magnetic resonance imaging, computed tomography and X-ray radiography

de Ruiter L, Fascia D, Tomaszewski P, Janssen D, Verdonchot N.
Clinical imaging protocols for in-vivo assessment of an all-polymer
PEEK-on-UHMWPE total knee replacement with magnetic resonance
imaging, computed tomography and X-ray radiography.

Manuscript in preparation

Introduction

The ongoing development of all-polymer total knee arthroplasty (TKA) has shed light on the potential benefits of such a device to the reconstructed knee environment. Several studies have investigated the influence of a polyetheretherketone (PEEK) femoral component in TKA, looking amongst others into the effects on wear, fixation, mechanical compatibility and (bio)mechanical bone-implant interplay¹⁻⁹. A yet unreported feature of the PEEK knee replacement is its appearance in clinical imaging. The PEEK, non-metallic knee prosthesis is a first in kind device and as such is an unknown entity with regard to clinical imaging in this part of the body. At this stage, a PEEK knee prosthesis has not been implanted into any patient and has therefore never been scanned *in vivo*. However, PEEK materials have been extensively utilized in spine surgery and, as a consequence, Magnetic Resonance Imaging (MRI), Computed Tomography (CT) and X-ray appearances are well appreciated in this area¹⁰⁻¹³.

In TKA, the established and prevailing method for post-operative assessment of implant positioning and alignment is plain film radiography (X-ray)^{14,15}. X-ray offers a quick and economical evaluation, without the downsides known to CT and MRI, like higher radiation exposure and metal artifacts. On X-ray, the contrast between the knee implant and surrounding tissues is adequately high with radiopaque implant materials, such as metal or ceramics. While clinicians develop experience in implant evaluation using standard radiography, there are limits to what can be detected with the technique. Obviously, an X-ray image is a two-dimensional representation of the reconstruction. Although this can partly be overcome by making both coronal and sagittal images, the complex shape of knee implants cannot be fully represented on the images. Furthermore, obtaining the correct orientation of the knee while scanning is difficult, due to the dependency on anatomy and patient orientation. Divergent X-ray beams further complicate full-plane assessment; features close to the divergent X-ray source cast a shadow over more distant features. Moreover, the radiograph is in essence a representation of radiation absorption accumulated throughout structures. Therefore, a radiopaque structure obscures other adjacent structure and tissues between the source and detector. Consequently, the detail of structures immediately adjacent to and shielded by an implant are obscured, which is unfortunate as most post-operative complications are identified in this zone of interest. Common complications such as loosening, implant migration and osteolysis at the interfaces are consequently not easy, or -at an early stage- difficult to observe on plain X-ray¹⁶⁻¹⁸.

CT imaging solves some of the problems encountered when imaging implants, but introduces additional considerations of increased radiation exposure, metallic artifact and higher cost. It allows surgeons to assess 3-dimensional aspects like alignment, component sizing, overhang,

and increasingly frequently plan for (robotic) navigation^{17,19}. Like many advancements in technology the cost impact of this technique is substantial. It is more expensive than radiographic evaluation and, consequently, less universally available.

MRI imaging does not involve radiation exposure, but merely uses the magnetic properties of hydrogen atoms in structures²⁰. Since the response of a structure is dependent on the hydrogen content, this technique theoretically offers excellent contrast in the reconstructed knee joint, with aqueous tissues and artificial (hydrogen-free) components. As such, it is an excellent tool to assess the state and interactions of soft tissues with the implant²¹. Major drawbacks from MRI arise when metallic implants or ceramic implants containing metal are used. The metal bulk interferes heavily with the magnetic field of the scanner and produces severe metal artifact distortion throughout the image array²². The combination of adaptive scanning sequences (increased slice thickness and bandwidth) and digital post-processing of the obtained imaged can somewhat improve image quality with so-called metal artifact reduction algorithms, but the impact of the large metallic implant cannot yet be fully suppressed²³⁻²⁷. Hence, MRI is a limited modality for the detailed analysis of the metal components and surrounding structures.

Non-metallic polymer does not cause typical metallic artifacts in a magnetic field and consequently does not distort nor obscure the surrounding structures on MRI. Furthermore, PEEK's rigid lattice structure of substance with non-free hydrogen ions means that the substance appears on MRI as signal void (totally black)^{11,13}. In CT imaging, non-metallic PEEK is not expected to cause the blooming and streak artifacts usually encountered when CT-imaging metallic knee prostheses²⁸. Its radiodensity and contrast resolution are lower than metallic implants as observed during explorative standard radiography. The lack of artifacts would be expected to allow more effective imaging of the bone-cement and cement-bone interfaces around the margins of the prosthesis. However, since radiologists are accustomed to current standards in imaging, a significant didactic and cultural education program may be required in centers implanting a PEEK knee to prevent misinterpretation or misrepresentation of findings in postoperative patients, since more structures are visible and the implants are not as outlined as with metal parts.

As we approach the point of real-world clinical application of all-polymer knee implants with a PEEK femoral component, the need arises to explore and document the benefits and compromises created when applying common imaging modalities. Since PEEK is already abundantly in use in spinal surgery, this is by no means the first time that the PEEK material has been subjected to the environment of MR/CT scanning^{10,12,13}. As such, no documented safety concerns have arisen with the scanning of this material from in vivo spinal cases. CT scanning is not expected to have a place in the routine imaging of an uncomplicated PEEK

knee prosthesis. However, it is frequently used in orthopedic practice in the investigation of complicated arthroplasty and trauma^{17,22}. It is therefore important that the expected appearances are documented and a recommended starting point scanning protocol is made available. For MRI, PEEK represents a paradigm shift for postoperative imaging of knee arthroplasty because MRI does not currently play a common role in postoperative imaging of the uncomplicated metallic knee prosthesis. MR assessment around orthopedic implants is becoming more commonplace in clinical practice and therefore knowledge of the expected appearances of a novel product would now seem a prerequisite to clinical application.

In this paper we aim to describe imaging specifics of a PEEK component utilizing MRI (four different sequences), CT and X-ray, thereby highlighting the feasibility of various imaging modalities to assess the postoperative status of a PEEK femoral component. As a reference to current practices with metal implants, these specifics are selectively compared to a simultaneously implanted knee with a CoCr component.

Materials and methods

Cadaver selection and preparation

A cadaveric specimen was acquired and utilized prior to any freezing cycle to ensure the most realistic human tissue condition with regard to CT beam attenuation and measured tissue density and magnetic resonance signal characteristics. Prior to the experiment the two knees were screened with use of a mobile fluoroscopic system for absence of any metallic implants or parts. Based on the positive result of this screening the knees were included in the study. The specimen was prepared according to our standard cadaveric protocol²⁹ and in compliance with relevant local safety guidelines.

Implants and surgical procedure

The bilateral knees were implanted with either the PEEK Optima® Freedom Knee system (Invibio Ltd, UK) or the CoCr Freedom Knee system (Maxx Orthopedics Inc., USA). The Maxx Freedom Knee surgical technique was followed, including incision and exposure, femoral and tibial preparation, trial reduction and gap balancing, implantation and closing the soft tissue envelope. Both implants used in this trial allowed retention of the posterior cruciate ligament and none of the patellas was resurfaced.

The implants were cemented onto the femurs using Palacos R bone cement with radiofillers (Heraeus Medical GmbH, Wehrheim, Germany). The cement was stored at operating room temperature of 19°C prior to use. During the trial the cement was mixed under vacuum for one minute before application. Cement application was performed within a maximum of 4

minutes after the start of the mixing procedure, and after implant positioning the cement was pressurized by positioning the knee in extension for a few minutes.

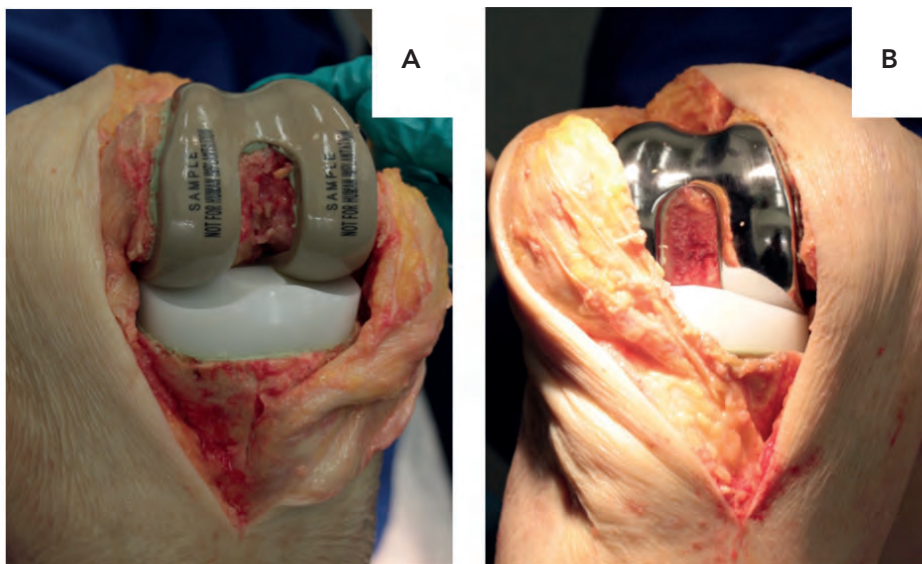


Figure 1. Knees implanted with the PEEK Optima® Freedom Femoral Knee component (A) and the CoCr Freedom Knee (B).

Preparation of cadavers for clinical imaging

Directly after the implantations, the legs were dissected from the cadaver at the hip level and stored at room temperature (19°C) for approximately 7.5 hours before imaging was performed. To simulate the environment of an in-vivo knee joint as accurately as possible, the joint space had to be filled with fluid prior to starting the imaging trial, to replace the synovial fluid that had drained from the knee during surgery. Therefore, just prior to imaging, the joint was injected with 0.9% saline solution and gas was removed from the joint as best as possible. Each knee had in total of 60 mL of liquid injected. At each step the needle was placed in the knee joint via the medial infrapatellar recess and the knee was flexed several times to remove excess gas from the joint. After these injections the knee was scanned.

Clinical imaging

After implantation and preparation, the PEEK and CoCr-alloy reconstructions underwent clinical imaging performed at the Radiology Department of the Radboud university medical center, Nijmegen, The Netherlands. Imaging was done consecutively with MRI, CT and X-ray, following scanning protocols. Protocol design and image assessment were done remotely in the United Kingdom. An experienced radiologist (Dr. Fascia) reviewed and annotated all

scans of which a summary is included in the Results section. DICOM images were archived (ZIP format) for file transport and transferred to the radiologist. The assessing radiologist used OsiriX MD (Pixmeo SARL) to import the (multiplanar reconstructed) DICOM images which were then assessed in a controlled radiology viewing environment on a calibrated monitor.

MRI scanning protocol

The cadaveric trial was carried out on a 1.5 Tesla field strength scanner (Siemens Avanto 1.5 T scanner), as 1.5 Tesla scanners are currently the most ubiquitous machines in clinical practice. Scanning parameters were common to current clinical practice and described in more detail hereafter and in Table 1. The cadaveric knee specimen was placed on the MR table such that it was located in the isocenter of the magnetic field at scan time, with the patella pointed to the sky. The knee joint was fully extended, but alternatively, would be acceptably flexed 5° with underpadding. All foreign bodies and dressings were removed. A dedicated high-resolution knee coil was used and sized appropriately for the limb being scanned. A Field of

View (FOV) of 14 cm was aimed for and adjusted +/- 2 cm based on specimen size to include the anatomical landmarks from proximally 3 cm above the tip of the upper pole of the patella to distally 1 cm beneath the tibial insertion of the patellar tendon. The amount of dead space (air) within the FOV was minimized. Trial imaging was carried out using weak spectral fat saturation which is common in orthopedic MR imaging. Study labelling was carried out as per individual MRI sequence.

Images were assessed for protocol compliance, field of view coverage, signal-to-noise ratio per sequence, artifacts directly caused by prosthesis, contrast resolution, spatial resolution and qualitative observations. Detailed MR sequence analyses were restricted to the PEEK knee, with anecdotal comparison of the metal appearance.

Table 1. MRI sequences and corresponding settings.

Protocol	PD TSE			T1 weighted TSE			T2FS weighted TSE			STIR	
	Axial transverse	Sagittal	Coronal	Axial transverse	Sagittal and Coronal	Coronal	Axial transverse	Sagittal	Coronal	Axial transverse	Sagittal and Coronal
Example TE/TR (ms)	35/3000	30/3000	32/2600	15/400-750	15/400-750	70/5500	110 / 5000				
Slice Thickness / Slice Gap	3 mm / 0.3 mm										
Fat Saturation	None			None			Weak (Fat Sat or SPAIR)			IR (TI = 160ms)	
FOV	140 mm	160 mm	160 mm	140 mm	160 mm	160 mm	140 mm	160 mm	160 mm	140 mm	160 mm
Matrix (Px2)	320 (80% phase FOV)	384 (80% phase FOV)	384 (80% phase FOV)	320 (80% phase FOV)	384 (80% phase FOV)	384 (80% phase FOV)	320 (80% phase FOV)	384 (80% phase FOV)	384 (80% phase FOV)	256 (90% phase FOV)	256 (90% phase FOV)
Bandwidth (Hz/Px)	180										

CT scan protocol

The cadaveric sample was placed in the center of the CT table along the axis of the table, with the patella pointed to the sky. The knee joint was fully extended and all foreign bodies and dressings were removed. The field of view was set from proximally 3 cm above the tip of the upper pole of the patella to distally 1 cm below the insertion of the patellar tendon (Figure 2). CT images were taken from a Toshiba Aquilion Genesis One scanner with parameters set as shown in Table 2.

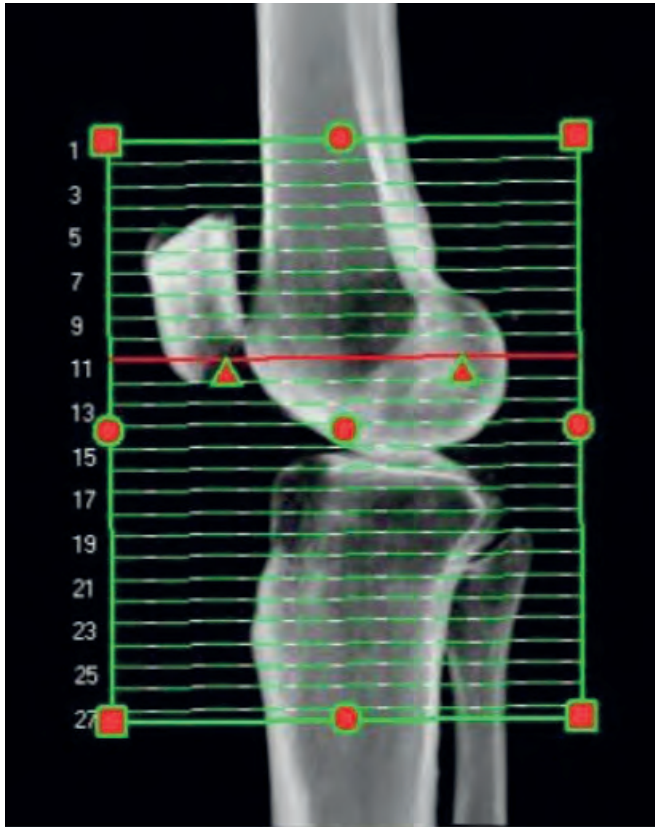


Figure 2. Field of View for the CT protocol.

Table 2. Scanner parameters.

Parameter	Setting
Acquisition slice thickness	0.6 mm isotropic
Output slice thickness	Reconstructed to 1mm
Tube Voltage	120 keV
Tube Current	100 mAs
Reconstruction Planes	Axial, Sagittal, Coronal
Standard output window (Width / Level)	2000 / 250 i.e. bone window
Scan phases	1
Contrast	None
Dose reduction algorithm	Off

No specific image labelling criteria were required for this trial CT since parametric adjustments were not carried out. Images were assessed for protocol compliance, field of view coverage, image noise, artifacts due to prosthesis, contrast resolution, spatial resolution and ability to multiplanar reconstruct.

Plain X-ray protocol

Clinical X-ray images were obtained from the Siemens Ysio system and assessed for visibility of the implants, cement mantle and periprosthetic bone. Placement of the cadaveric sample was dependent on the desired projection and included weight-bearing AP knee, lateral knee and skyline patella. The parameter settings for these projections are shown in Table 3.

Table 3. X-ray projections and parameter settings.

Name of projection	AP knee	Rolled lateral knee in natural extension (5° flexed)	Skyline view of patellofemoral joint (Merchant view,)
Area covered	Distal femur, proximal tibia and fibula centered on knee joint	Distal femur, proximal tibia and fibula centered on knee joint	Patella / patellofemoral joint
Size and orientation	18 x 24 cm portrait or DR equivalent	18 x 24 cm portrait or DR equivalent	18 x 24 cm landscape or DR equivalent
Grid	None	None	None
Filter	None	None	None
Exposure	60kV 5mAS	60kV 5mAS	70kV 12mAS
FFD	100 cm	100 cm	100 – 120 cm
Central Ray	Centered 1.5 cm distal to apex of patella on knee joint line, directed parallel to the tibial plateau orientation (typically requiring 5° cephalic angulation)	Angled 5° cephalad	Angled +30° from horizontal, directed at patella in the axis of the tibia / fibula
Collimation	Open to include distal 1/3rd of femur and proximal 1/3rd of tibia/ fibula. Open to include lateral skin margins	Open to include distal 1/3rd of femur and proximal 1/3rd of tibia/ fibula.	Collimate closely to patella
Markers	Placed in either bottom image corner, must not overlap subject. Applied in post preparation.		
Positioning	Subject standing in front of detector plate, long bone axis parallel to edges of plate	Subject rolled onto affected side. Knee placed in 5° flexion, radiolucent 'sand bags' or equivalent can be used to assist positioning	From the AP position, flex the knee 45°. Place the imaging detector plate perpendicular to the tibia and in plane to the beam direction at the mid tibial level.
Postprocessing	None	None	None

Results

For all imaging modalities, scanning protocols were correctly applied for the cadaveric specimen images and field of view coverage was adequate.

Magnetic Resonance Imaging

Metal interference

The appearance of a metal knee implant on MRI images is well known and resulted in the expected images. Considerable image distortions due to the CoCr implant were visible in all executed MRI sequences and obfuscated the structures that were possible to ascertain with a PEEK implant. The differences between both implants is demonstrated in Figure 3, where the image based on the T1 sequence is shown.

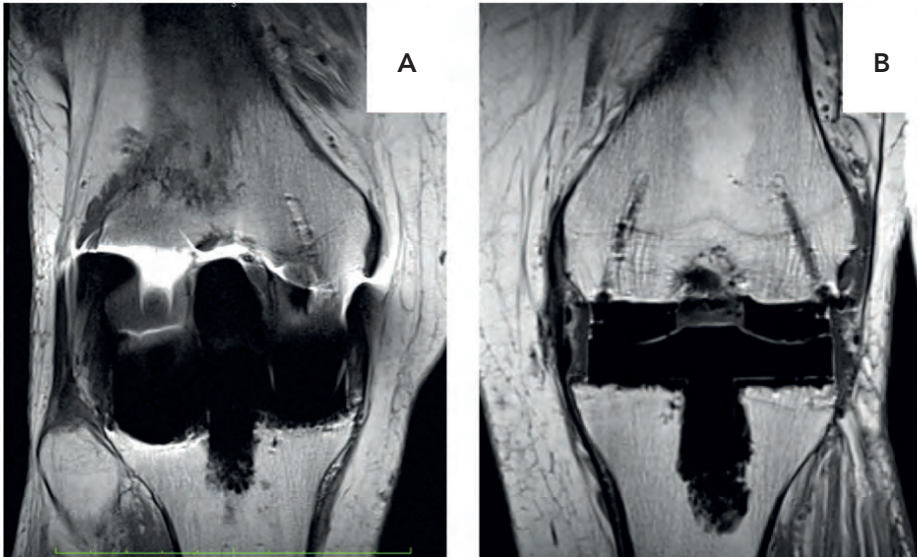


Figure 3. T1 weighted MRI images of the CoCr (a) and PEEK (b) implants. Image distortions are considerable in the CoCr periprosthetic area.

Proton Density (PD)

With the PEEK implant, excellent signal-to-noise ratio was achieved in all planes including immediately around the prosthesis. No significant noise artifact was appreciable throughout the images. Similarly, no image artifacts were attributable to the prosthesis. Interestingly, there was some metallic susceptibility artifact visible deep to the prosthesis at the cement-bone interface which is similar to that seen postoperatively after minimally invasive

orthopedic procedures involving bone cutting. This is most likely due to very small metal fragments deposited in the bone tissue, in this case from the oscillating saw. These artifacts are subtle and are not problematic in image interpretation on this sequence. They are not usually visible during prosthetic knee imaging due to the masking effect of a large metal prosthesis. The main features of this sequence are bright fat, bright fluid and total signal void for the PEEK prosthesis. These features resulted in excellent contrast resolution against the prosthesis. Finally, PD imaging (Figure 4) offered a reasonably high but not class leading spatial resolution.

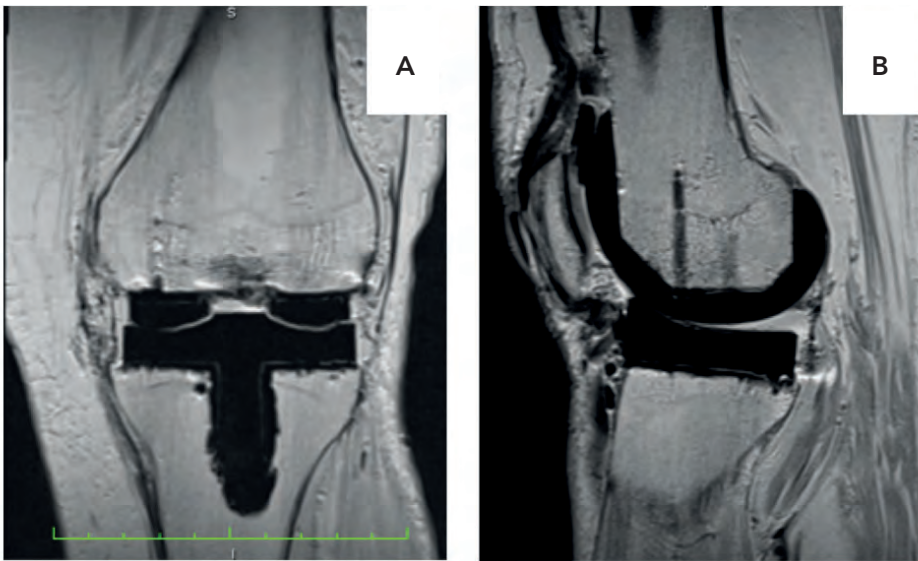


Figure 4. Proton Density (PD) MRI images of the PEEK knee. The implant contrasts well with its surroundings and does not produce image artifacts.

T1 weighted

A very high signal-to-noise ratio was achieved resulting in excellent detail even at a trabecular level immediately adjacent to the prosthesis. No artifacts were attributable to the prosthesis. A small amount of metallic (blooming) susceptibility artifact was present at the cement-bone interface due to metallic saw fragment remnants. The appearances of these were similar to PD sequences. Standard T1 imaging offers a very high contrast ratio due to the brightness of fat in normal bone marrow on this sequence. However, contrast immediately around the surface margins of the prosthesis is not as high as PD imaging since joint fluid is of intermediate signal. The PEEK prosthesis appeared as total signal void (black) in common with other sequences. The optimal spatial resolution was achieved using T1 sequences. Trabecular level detail was resolved throughout the 3 plane scans, including immediately adjacent to the cement-bone

interface. This is helped by the absence of prosthesis-induced artifact and should prove to be a very desirable feature for long term follow up and troubleshooting situations.

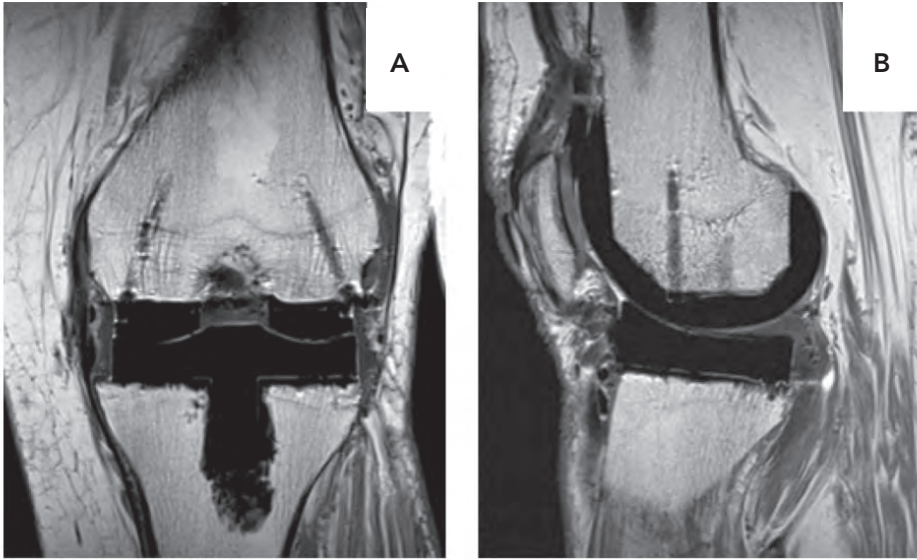


Figure 5. T1 weighted MRI images of the PEEK knee. Similar to PD, the implant contrasts well with its surroundings and does not produce image artifacts. Lower fluid signal compared to PD yielded slightly less clear implant surface delineation.

T2 weighted, fat saturated (T2FS)

A good signal-to-noise ratio was obtained from joint and soft tissue structures around the knee. Long TR times resulted in very high fluid signal. Noise levels were higher than non-fat saturated images, as expected. Metallic artifacts at the cement-bone interface are exaggerated on T2FS sequences due to the suppression of surrounding bone marrow. The prosthesis itself did not cause any discernible artifact. High contrast is rendered around the (totally black) prosthesis due to bright joint fluid and susceptibility artifact at the cement-bone interface. Whilst the joint fluid is a reliable contrast generating feature, metallic artifacts from sawing will be highly variable between patients. The use of weak fat saturation allowed some low signal to remain in the bone marrow and was sufficient to contrast against the cement and prosthesis. As with all fat saturated imaging, detail is reduced in the pursuit of superior water signal detection.

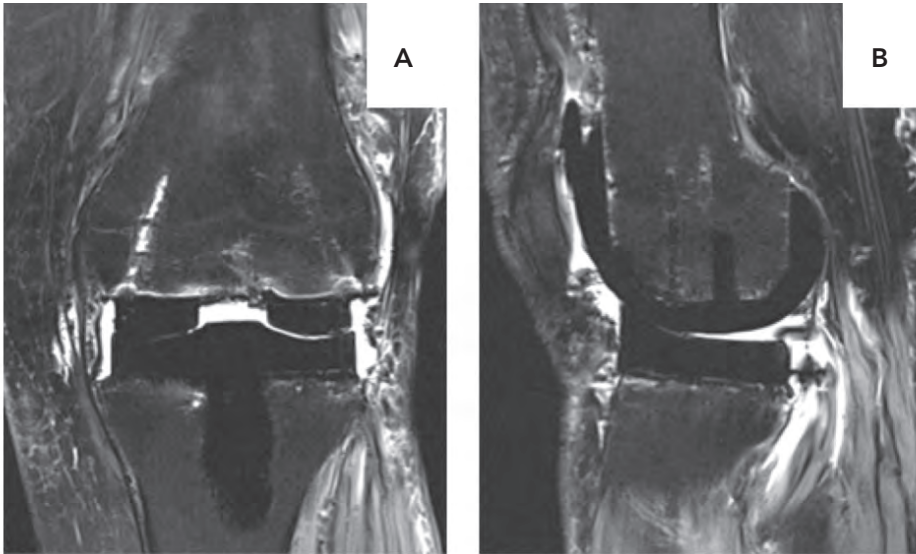


Figure 6. T2 weighted, Fat Saturated (T2FS) MRI images of the PEEK knee. Implant contrast against joint fluid is increased, at the expense of contrast against bone and soft tissue.

Short Tau Inversion Recovery (STIR)

A far lower signal-to-noise ratio was achieved using this sequence than any other fat-saturating technique such that meaningful detail was quite poor. In spite of the use of a reduced flip angle of 150° in an attempt to 'weaken' fat saturation, images were still extremely high contrast (bone/soft tissue black, fluid very white). Importantly, the delineation between bone, cement and PEEK was very poor since each substance generated very little signal on STIR imaging (i.e. looked black). Image noise levels were also uniformly higher across the field of view due to the lack of signal to mask their presence. The PEEK prosthesis did not cause any local or field wide artifact. Very high contrast resolution was achieved, possibly the only redeeming feature of the STIR sequence used in this context. It was difficult to truly assess spatial resolution of this sequence due to the poor signal generation achieved. STIR sequences generally trade detail for homogeneous fat saturation. In areas of better signal return (mostly soft tissues around the knee) there does appear to be reasonable detail, sufficient to differentiate structures of 2 mm diameter from adjacent objects. However, detail in important areas such as the bone-cement-prosthesis interface is virtually non-existent making this a poor sequence for anatomical analysis.



Figure 7. Short Tau Inversion Recovery (STIR) MRI images of the PEEK knee. Image quality is poor and produces inadequate contrast for prosthesis visualization purposes.

Computed Tomography

Image noise

With the chosen scan parameters, signal to noise ratio was excellent on images reconstructed to 1 mm. The PEEK prosthesis did not appear to contribute to image noise, since it was consistent and uniform throughout the FOV. The appearances seen were due to the sum of random background and added detector noise, no worse than is encountered on standard orthopedic CT scanning around the knee.

Artifacts due to prosthesis

The scanned volume contained no radiopaque foreign bodies other than the PEEK knee prosthesis and the polyethylene tibial component. There were also no external foreign body contaminants. Typical artifacts associated with metallic knees include streak artifacts, beam hardening artifacts halo/edge effects and apparent density shift effect on immediately surrounding structures. None of these were perceived in the PEEK knee (Figure 8a). Additional areas not usually amenable to CT assessment also became apparent with PEEK. These areas included the PEEK interface with the cement mantle, the bone-cement interface, the subarticular bone and the bone cuts. With the metallic prosthesis however, strong artifacts shielded these areas from meaningful analysis (Figure 8b). Metal Artifact Reduction Software (MARS) algorithms can improve matters to some extent.

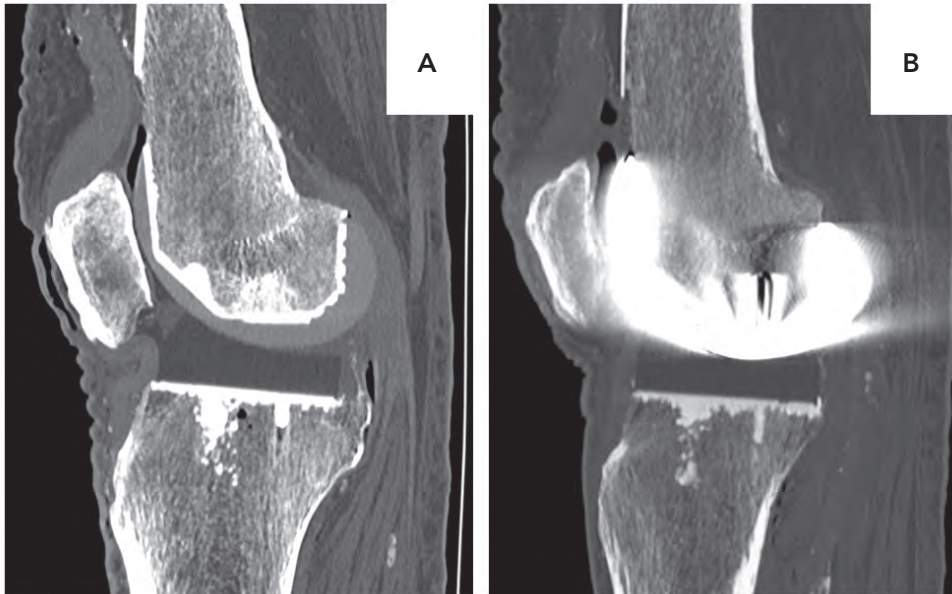


Figure 8. Representations of CT reconstructions of the PEEK (a) an CoCr (b) knee. CoCr-produced image artifacts are obvious and obfuscate the cement mantle entirely, contrary to the PEEK implant.

Contrast resolution

Interpretation was carried out using bone windows (window width: 1500, window level: 300). The PEEK prosthesis was clearly identifiable and rendered at an average Hounsfield Unit (HU) of ~180 (Figure 9). At this density level, PEEK was well separable from surrounding structures in the typical implanted joint setting, i.e. cement, bone, polyethylene tibial component, muscle and fat. It was less well separated from synovial fluid within the joint (typical HU 10-30). The contrast resolution achieved was also inadequate for subtraction imaging during post processing unless considerable manual segmentation is carried out.

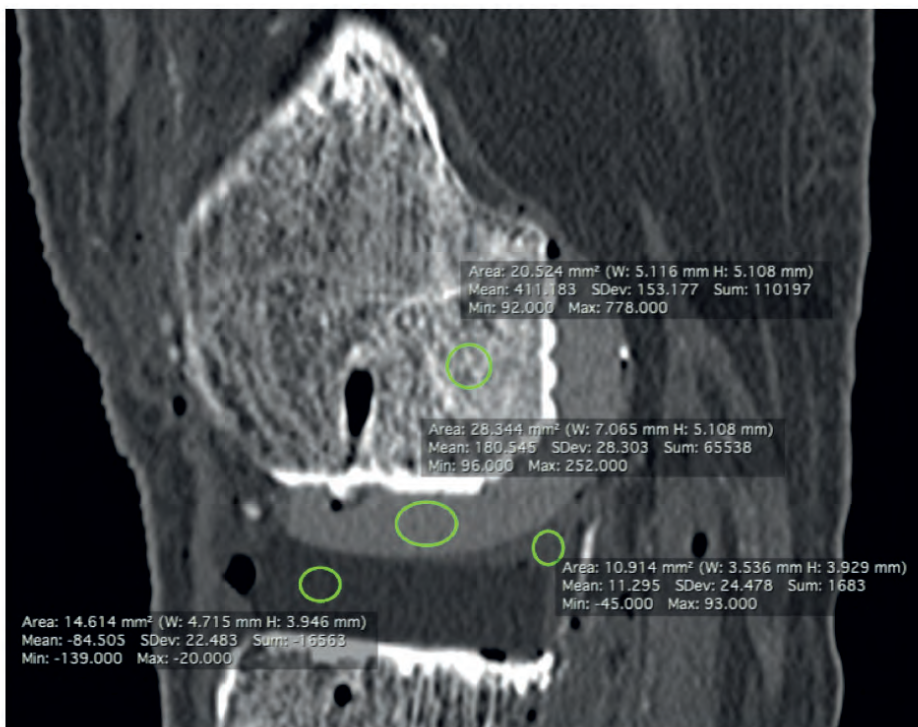


Figure 9. Contrast resolution in Hounsfield Units (HU) of several structures in the knee joint space. Trabecular bone, joint fluid, PEEK and UHMWPE were separable, but contrast between PEEK and joint fluid was limited.

Spatial resolution

Due to the lack of artifact created by the PEEK prosthesis, it was possible to scan with very fine slices and reconstruct to required slice thickness. This allowed for the resolution of very small structures in line with the maximum spatial resolution of the scanner used. The trial images (0.6 mm slice thickness) resolved structures <1 mm in size. The example in Figure 10 shows resolution of a very fine cement mantle and cement-bone interface in one of the prosthesis lug holes.

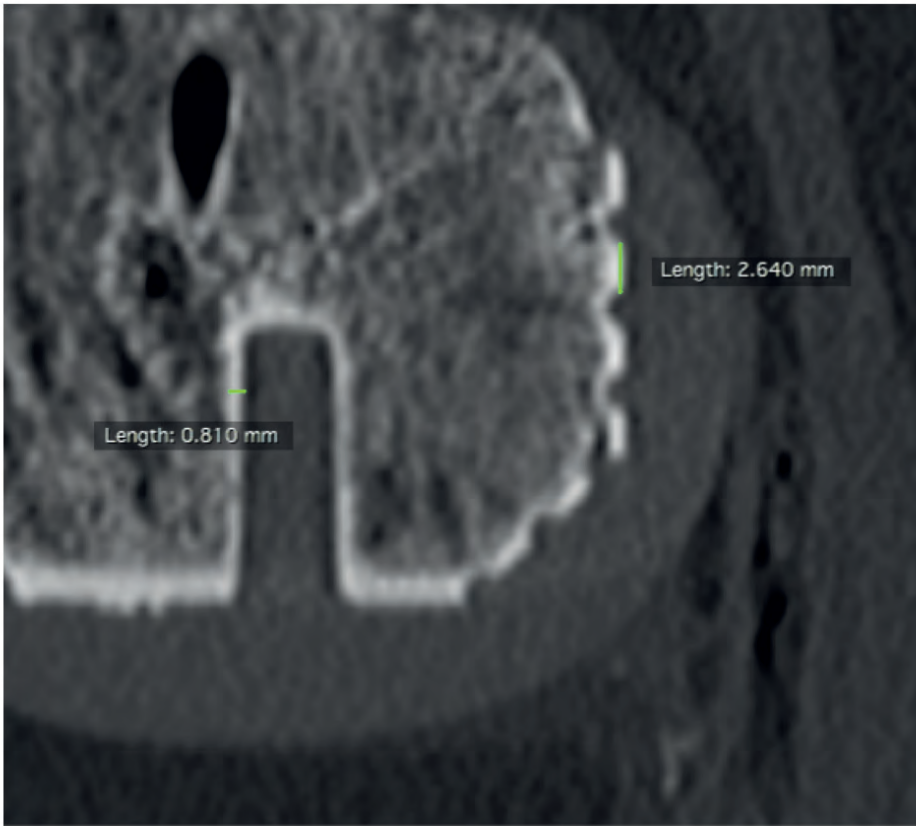


Figure 10. Spatial resolution of the sagittal reconstruction of the PEEK CT scan. This view contains the distal and posterior cross-section of the femoral component, showing the ability to assess the cement mantle (white band) in great detail. The width of the cement mantle could be measured and the cement pocket design of the PEEK implant could be observed in detail.

Ability to Multiplanar Reconstruct (MPR)

CT scans acquired with isotropic voxels allow 3D MPR of images in post-processing without reliance on the scanner to reprocess raw data. Trial images demonstrated that images acquired at 0.6 mm and reconstructed to 1 mm were still perfectly capable of client side MPR without visible interpolation artifacts at normal (100%) magnification. Minor interpolation artifacts became visible at 500% magnification, a situation not likely to be used in standard radiology practice.

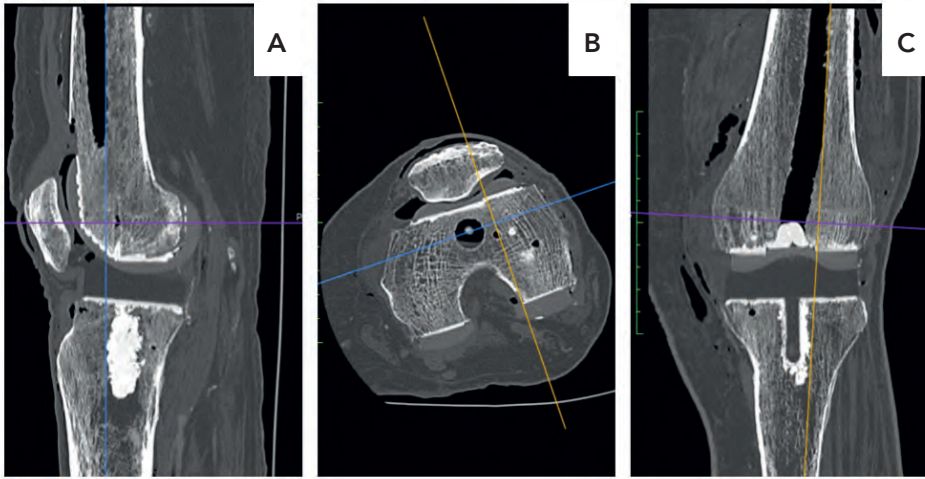


Figure 11. 3D Multiplanar sagittal (a), transverse (b) and coronal (c) reconstructions from 0.6mm isotropic source data. The images in all reconstructions are of high quality, with good contrast and without discernable (interpolation) artifacts.

X-ray

As anticipated secondary to the known radiolucent characteristics of PEEK in the usual diagnostic X-ray spectrum, the prosthesis in situ was barely visible against other surrounding structures due to limited achieved contrast resolution (Figure 12).

Compared to the CoCr implant, this renders quite different visual results. CoCr completely obscures the cement mantle and bone interfaces meaning that they are not assessable with plain X-ray, but the macroscopic position of the implant is clear. Whereas the PEEK prosthesis allows full X-ray penetration meaning that the macroscopic position of the implant is not assessable, but the bone-cement-implant interface microarchitecture is visible. This provides useful and completely novel information about the behavior of the immediate architecture around an implant which has never before been available using CoCr implants. It may potentially provide earlier warning signs of implant failure.

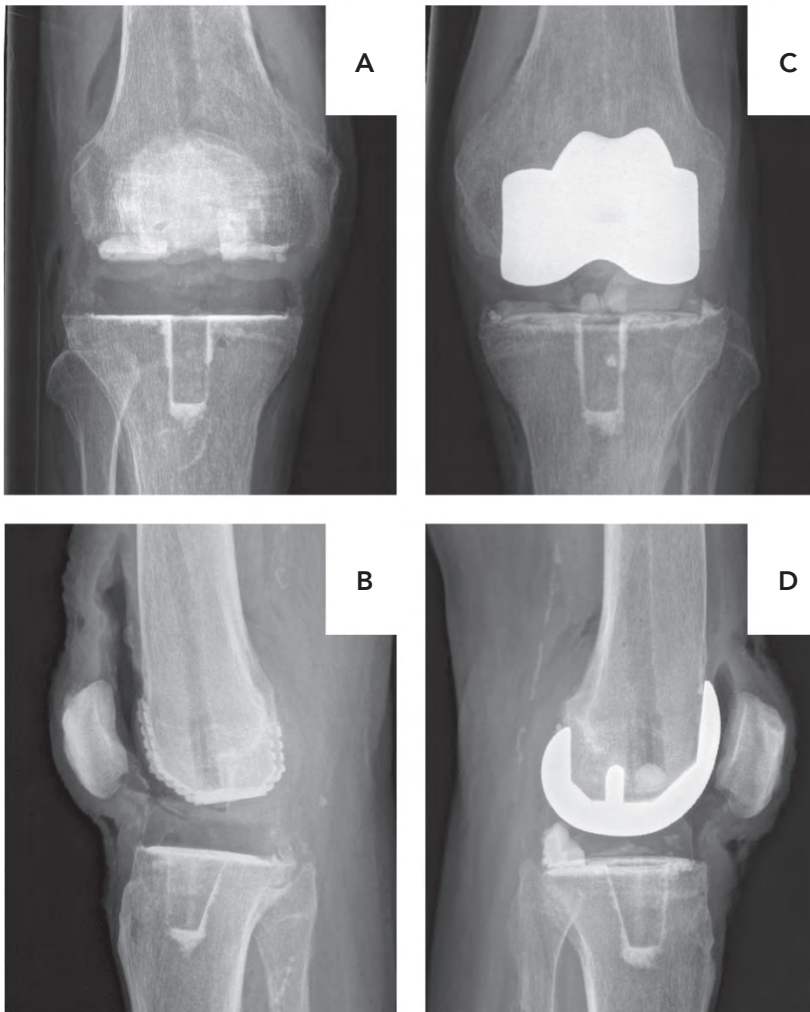


Figure 12. Coronal (a,c) and sagittal (b,d) X-ray radiographs of the PEEK (a,b) and CoCr (c,d) knee. The CoCr prosthesis is clearly visible, while the PEEK implant hardly produces a shade. An indirect assessment of the seating of the PEEK implant could be made via the cement mantle, which is visible with good detail.

Discussion

The aim of the study was to simulate as realistically as possible the expected appearance of the PEEK knee prosthesis in vivo under common or moderately adapted radiographic, MRI and CT imaging protocols. Where desirable, these appearances were compared to a CoCr implanted knee or otherwise assessed against current clinical experience. Cadaveric appearances of the PEEK knee represent no guarantee that the product shall perform in a similar manner in vivo. Attempts were made to simulate as accurately as possible an in vivo joint environment. However, a key difference with cadaver tissue will be hydration levels which is an important variable in medical imaging, and especially MRI which depends on the mobility of hydrogen ions.

Magnetic Resonance Imaging

The *PD sequence* in the presence of a prosthesis was an excellent choice of standard non-fat saturated sequence. The sequence will be most useful to those who already count PD as part of their standard knee protocol, meaning that little or no adaptation is needed due to an implanted PEEK knee. The bright joint fluid is particularly useful in highlighting the surface features of the prosthesis, and would also be expected to track deep to a poorly seated or loosened prosthesis. During the trial, fluid was artificially introduced into the joint in order to simulate the presence of synovial fluid with the assumption made that appearances should be similar in vivo. Caution must be exercised with this sequence in assessing bone marrow edema since fluid is bright. Fat saturation is required to distinguish between normal bright bone marrow and pathological marrow edema. In this regard, T1 imaging is superior. Other advantages already mentioned may make this compromise desirable for centers already using PD imaging intensively.

The *T1 weighted sequence* in the presence of a prosthesis is a good choice for baseline anatomical imaging around the PEEK prosthesis. It is a very common and well recognized sequence already in widespread use and worked well around the PEEK femoral component. T1 sequences offer good appreciation of bone marrow edema through darkening of the usually fatty marrow signal. Although this could not be tested on cadaveric specimens, it would be expected that this effect might be appreciable even at the immediate prosthetic interface with underlying bone due to the absence of prosthesis induced artifact. T1 sequences are expected to be inferior to PD sequences in the detection of early prosthetic loosening since sensitivity to the ingress of small amounts of fluid at the bone-prosthesis interface is inferior. This effect has been demonstrated incidentally during cadaveric trials through the use of an inappropriately sized PEEK femoral component. Use cases of this sequence would likely involve the detection of sub-prosthetic fractures, sub-prosthetic bone marrow edema and potential features of infection or loosening, but should be further studied in future (clinical) trials.

The *T2FS* sequence provided a good signal for joint and soft tissues. The higher signal noise is not problematic but highlights that anatomical sequences with lower noise should always be included in conjunction with fat-saturated sequences. Pertaining to the exaggerated metal artifacts of saw remnants, one might say that T2FS sequences show the artifact more clearly by removing the masking effect of bright bone marrow. This is an important observation because radiologists will be unfamiliar with being able to see bright metallic artifacts at this interface which is never visible with metallic prostheses. There is therefore the potential for misinterpretation of this finding as fluid ingress (implying prosthetic loosening) or bone marrow edema. Weak spectral fat saturation is already commonly used in musculoskeletal MRI and should not be a deviation from mainstream protocol for most centers. Detail is likely to be better preserved at higher field strengths, or by using proton density rather than true T2 weighted imaging. Fat saturated imaging is seldom carried out in isolation, so added spatial resolution can be obtained from other sequences.

The *STIR* sequence would not be recommended as part of the routine MR imaging protocol for the PEEK knee. STIR imaging is known to be useful in artifact reduction, particularly when a higher bandwidth is used. However, given the lack of artifact present using common spectral fat saturation around the PEEK material, it does not appear necessary to turn to STIR or other artifact reduction sequences (with their trade-offs). Given the generated contrast, a potential use could be in suspected infection cases for ultimate water (edema) detection, however the extreme bright signal generated from an effusion could prove quite distracting and difficult to window. STIR is a specialist sequence in the context of PEEK imaging. It should never be used in isolation due to poor signal-to-noise characteristics and an inability to deliver good anatomical detail. STIR may find use as part of the investigation of a complicated PEEK knee when functional data regarding bone marrow edema is an important question and field homogeneity is important.

Typically, MRI is not a very useful tool in the assessment of the postoperative metallic knee prosthesis due to metal artifacts severely distorting images. Although metal artifact reduction sequences have been developed to improve this situation, images around the PEEK knee without any MR adaptations are far superior. No specialized MR techniques are necessary to generate highly detailed and functionally useful (fat saturated) images around an implanted PEEK knee in cadaveric trials. PEEK generates no intrinsic signal during MRI scanning and appears as a signal void (total blackness). However, since this is an uncommon signal in human tissue, it contrasts well to the surrounding joint environment on most sequences. The PEEK knee prosthesis allows visualization of the bone-cement and cement-bone interface not previously achievable with metal prostheses. The prosthesis is almost totally artifact free but the implantation procedure leaves small metallic particles around the bone and cement interfaces which are visible as metallic bloom artifacts. These are readily visible due to the

lack of artifact generated by the PEEK material itself and will require familiarization by reading radiologists. Water signal is distinct from both the PEEK and cement materials, appearing as much higher signal. Combined with lack of artifact, the tracking of fluid around these interfaces has already been appreciated on cadaveric models and should prove clinically useful in the detection of loosening or complications of implantation and cementation. Additional MR technician and radiologist training will be required to interpret studies of a PEEK knee since it looks like no other current knee prosthesis in commonplace use.

Computed tomography

The cadaver used in this study would be considered a slim subject with low body fat. Hence, parameters may require either operator adjustment or machine automated dose modulation on a significantly larger subject³⁰. The already excellent signal to noise ratio may be further improved with post-processing algorithms or simply by working at thicker slice reconstructions, though the trade-off will be the ability to isotropically reconstruct images in 3-planes unless isotropic source data is preserved. To maintain the ability to generate the best quality multiplanar reconstructed images at a later date, the source axial volume should always be preserved even when thicker MPR images are presented for interpretation by the radiologist.

The PEEK knee prosthesis femoral component can be safely and accurately imaged with CT scanning. It allows superior observation of the cement-prosthesis and cement-bone interfaces when compared to metallic counterparts. It produces none of the metallic artifact usually inherent to CT scanning around knee arthroplasty and consequently requires no special metal artifact reduction nor other image enhancement algorithms. PEEK has a density (HU ~180) far closer to native medullary bone (HU ~700) than a metallic prosthesis (HU ~10,000) and even closer to osteoporotic bone (HU ~200). It may be hypothesized that it is therefore mitigating stress shielding compared to metallic prostheses when placed adjacent to bone, especially when osteoporotic. This hypothesis has been tested and published in previous simulation studies²⁻⁵. CT scanning is likely to prove an invaluable tool in the investigation of painful and complicated PEEK prostheses. Due to the proven problem of radiolucency on plain radiography, it is likely that CT scanning will form an important role of management of fracture around the prosthesis. Low contrast resolution is the main pitfall to contend with for both plain radiography and CT scanning of the PEEK prosthesis. CT is superior to plain film radiography but still produces lower contrast images than radiologists are used to in the imaging of prosthetic joints. The density shift created by edematous and inflamed tissue would also likely further reduce contrast resolution, as are other intra-articular substances of low-intermediate density such as synovial fluid or pus in an infected joint. Lack of familiarity amongst radiologists is also a potential risk to misinterpretation of findings.

X-ray

The radiolucent nature of the PEEK femoral component during standard X-ray assessment requires a rethink of the typical use case for this modality in the standard arthroplasty workflow with this novel material. It will also require a shift of thinking for both orthopedic surgeons and radiologists working with the new implants. Whilst the prosthesis is no longer clearly visible and amenable to macroscopic position assessment on X-ray, new opportunities arise to investigate microarchitecture at the bone-cement and cement-implant interface which could potentially opportunistically detect implant failure. Contrary to that, it may also be hypothesized that PEEK could lead to different or over-treatment of suspected failure as we can now detect thin or failed cement, while similar deficiencies remain undetected with a CoCr implant.

Further longitudinal studies would be required to explore these appearances once the implant gains wider in vivo use as our assumptions are currently based on small batch cadaveric models.

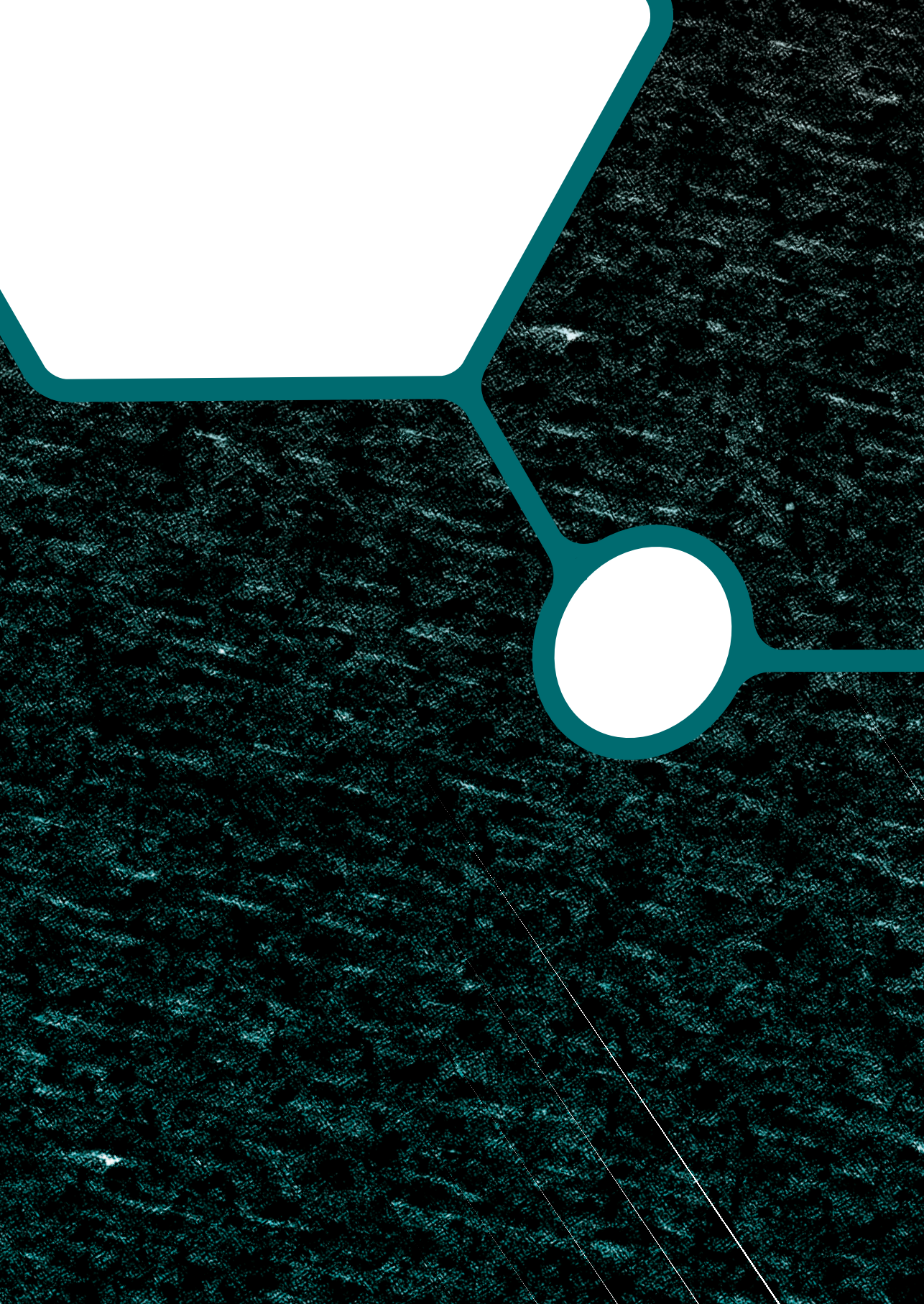
Conclusions

The introduction of a PEEK femoral component in TKA leads to an inevitable training need for radiologists and technicians. The appearances of the device in all tested imaging modalities differ substantially from common metallic knees and offer considerable advantages and a few new challenges. The ability to use MR and CT imaging in PEEK TKA unlocks great potential for radiological evaluation of the reconstructed knee joint and potentially allows more accurate surveillance of implant behavior and earlier detection of implant failure.

References

1. de Ruiter L, Janssen D, Briscoe A, et al. *Fixation strength of a polyetheretherketone femoral component in total knee arthroplasty*. Med Eng Phys 2017; 49: 157–162.
2. de Ruiter L, Janssen D, Briscoe A, et al. *The mechanical response of a polyetheretherketone femoral knee implant under a deep squatting loading condition*. Proc Inst Mech Eng H; 231.
3. de Ruiter L, Janssen D, Briscoe A, et al. *A preclinical numerical assessment of a polyetheretherketone femoral component in total knee arthroplasty during gait*. J Exp Orthop 2017; 4: 3.
4. Rankin KE. *Evaluation of Polyetheretherketone as a Candidate Material for Cemented Total Knee Replacement*. University of Southampton, Faculty of Engineering and the Environment, PhD Thesis.
5. Rankin KE, Dickinson AS, Briscoe A, et al. *Does a PEEK Femoral TKA Implant Preserve Intact Femoral Surface Strains Compared With CoCr? A Preliminary Laboratory Study*. Clin Orthop Relat Res 2016; 474: 2405–2413.
6. Cowie RM, Briscoe, Fisher, et al. *PEEK-OPTIMA™ as an alternative to cobalt chrome in the femoral component of total knee replacement: A preliminary study*. Proc Inst Mech Eng H 2016; 230: 1008–1015.
7. Cowie RM, Briscoe A, Fisher J, et al. *Wear and Friction of UHMWPE-on-PEEK OPTIMA™*. J Mech Behav Biomed Mater 2019; 89: 65–71.
8. East RH, Briscoe A, Unsworth A. *Wear of PEEK-OPTIMA® and PEEK-OPTIMA®-Wear Performance articulating against highly cross-linked polyethylene*. Proc Inst Mech Eng H 2015; 229: 187–93.
9. Baykal D, Siskey RS, Underwood RJ, et al. *The Biotribology of PEEK-on-HXLPE Bearings Is Comparable to Traditional Bearings on a Multidirectional Pin-on-disk Tester*. Clin Orthop Relat Res 2016; 474: 2384–2393.
10. Oikonomidis S, Ashqar G, Kaulhausen T, et al. *Clinical experiences with a PEEK-based dynamic instrumentation device in lumbar spinal surgery: 2 years and no more*. J Orthop Surg Res 2018; 13: 196.
11. Brandão RACS, Martins WC da S, Arantes SAAJ, et al. *Titanium versus polyetheretherketone implants for vertebral body replacement in the treatment of 77 thoracolumbar spinal fractures*. Surg Neurol Int 2017; 8: 1–7.
12. Adler D, Akbar M, Spicher A, et al. *Biomechanical Study of a Novel, Expandable, Non-Metallic and Radiolucent CF/PEEK Vertebral Body Replacement (VBR)*. Materials (Basel) 2019; 12: 1–11.
13. Junaid M, Rashid MU, Bukhari SS, et al. *Radiological and clinical outcomes in patients undergoing anterior cervical discectomy and fusion: Comparing titanium and PEEK (polyetheretherketone) cages*. Pakistan J Med Sci 2018; 34: 1412–1417.
14. Ewald F, C. *Roentgenographic Evaluation and Scoring System*. Clin Orthop Relat Res 1989; 2–5.
15. Goergen TG, Dalinka MK, Alazraki N, et al. *Evaluation of the patient with painful hip or knee arthroplasty*. American College of Radiology. ACR Appropriateness Criteria.. Radiology 2000; 215 Suppl: 295–298.

16. Kumar N, Yadav C, Raj R, et al. *How to Interpret Postoperative X-rays after Total Knee Arthroplasty*. *Orthop Surg* 2014; 6: 179–186.
17. Cyteval C. *Imaging of knee implants and related complications*. *Diagn Interv Imaging* 2016; 97: 809–821.
18. Solomon LB, Stamenkov RB, MacDonald AJ, et al. *Imaging periprosthetic osteolysis around total knee arthroplasties using a human cadaver model*. *J Arthroplasty* 2012; 27: 1069–1074.
19. Bellemans J, Vandenuecker H, Vanlauwe J. *Robot-assisted Total Knee Arthroplasty*. *Clin Orthop Relat Res* 2007; 111–116.
20. Berger A. *Magnetic resonance imaging*. *Br Med J* 2002; 324: 35.
21. Dean Deyle G. *The role of MRI in musculoskeletal practice: A clinical perspective*. *J Man Manip Ther* 2011; 19: 152–161.
22. Koch KM, Lorbiecki JE, Hinks RS, et al. *A multispectral three-dimensional acquisition technique for imaging near metal implants*. *Magn Reson Med* 2009; 61: 381–390.
23. Lu W, Pauly KB, Gold GE, et al. *SEMAC: Slice encoding for metal artifact correction in MRI*. *Magn Reson Med* 2009; 62: 66–76.
24. Vessely MB, Frick MA, Oakes D, et al. *Magnetic Resonance Imaging With Metal Suppression for Evaluation of Periprosthetic Osteolysis After Total Knee Arthroplasty*. *J Arthroplasty* 2006; 21: 826–831.
25. Sutter R, Hodek R, Fucentese SF, et al. *Total knee arthroplasty MRI featuring slice-encoding for metal artifact correction: Reduction of artifacts for STIR and proton density-weighted sequences*. *Am J Roentgenol* 2013; 201: 1315–1324.
26. Jawhar A, Reichert M, Kostrzewa M, et al. *Usefulness of slice encoding for metal artifact correction (SEMAC) technique for reducing metal artifacts after total knee arthroplasty*. *Eur J Orthop Surg Traumatol* 2019; 29: 659–666.
27. Schröder FF, Corine E, Post M, Wagenaar F-CBM, et al. *MRI as Diagnostic Modality for Analyzing the Problematic Knee Arthroplasty: A Systematic Review*. *J Magn Reson Imaging*.
28. Kasperek MF, Töpker M, Lazar M, et al. *Dual-energy CT and ceramic or titanium prostheses material reduce CT artifacts and provide superior image quality of total knee arthroplasty*. *Knee Surg, Sport Traumatol Arthrosc* 2019; 27: 1552–1561.
29. Fascia D. *Preparation of Cadavers for Multimodal PEEK Knee Imaging Trials*. Invibio white Pap.
30. Greffier J, Larbi A, Macri F, et al. *Effect of Patient Size, Anatomical Location and Modulation Strength on Dose Delivered and Image-Quality on CT Examination*. *Radiat Prot Dosimetry* 2017; 177: 373–381.



Chapter 8

Summary and general discussion

The research presented in this thesis investigated the potential of all-polymer total knee arthroplasty (TKA) with respect to the current standard in knee replacement surgery. Initial predictive mechanical experiments were conducted in-silico with finite element (FE) methodology, with models increasing in sophistication. Experimental cadaver studies were performed for additional validation of the computer models, which was necessary to accurately predict the effect of implant material on in-vivo stress shielding. When early simulations combined with experimental observations, raised concerns about the fixation and adhesion of the new polymer prosthesis, additional experimental studies were conducted to investigate the strength and quality of the cemented implant. In addition, research was performed on medical imaging of the all-polymer knee implants to explore the interpretation of imaging relative to implant stability and fixation in clinical practice.

The research was aimed at answering the research questions as stated in Chapter 1 of this thesis and will be addressed accordingly in this chapter.

How safe is PEEK-on-UHMWPE TKA compared to CoCr-on-UHMWPE?

During service, implant forces are estimated to reach up to three times the body weight during level walking, and about four times body weight during squatting or jogging^{1,2}. In case of trauma those loads can increase drastically to the point where the prosthesis may fracture and needs to be replaced^{3,4}. In this environment, it is understandable why metal has been the material of choice since the early days of the TKA procedure⁵, and obvious why a polymer component needs to be tested under similar circumstances.

In cemented total knee arthroplasty, fixation of the implant is achieved via mechanical interlock, created by impacting the implant onto the bone, with a doughy layer of polymethylmethacrylate (PMMA) cement in between. During impaction, the cement is forced into the exposed trabecular bone pores and the cement pockets in the implant. After cement curing, the component is locked into place on a cement-reinforced foundation of trabecular and cortical bone. The cement layer introduces two interfaces: the cement-bone interface and the cement-implant interface. The strength of the cement-bone interface has been investigated extensively through experimental research and post-mortem retrieval studies⁶⁻⁹. Those concluded that trabecular interdigitation of the bone cement is essential for good fixation. It provides excellent primary fixation, but the strength decreases over time since the trabeculae retreat from the cement due to stress shielding of the PMMA⁷⁻⁹. The importance of good interdigitation is further emphasized by studies that showed that bone preparation techniques play a key role in the cement-bone interface. Contact between cement and cortical bone should be avoided, or roughening should be applied⁶.

There are studies that investigated cement-implant debonding^{2,10,11}. Computational studies were capable of reproducing clinically observed debonding in the anterior flange of CoCr femoral implants^{2,11}. To understand what the influence of PEEK on the fixation of the prosthesis would be, the studies in Chapters 2,5 and 6 were conducted.

How does PEEK cope mechanically with activities of daily living?

In Chapters 2 and 3, we built computational models to determine the response of a TKA reconstruction with a PEEK or CoCr femoral component to the loads incurred during level gait (**Chapter 2**) and squatting (**Chapter 3**). As expected, the PEEK implant generally produced a more localized stress transfer, near joint contact sites. This led to an increase in compressive stresses, with maximum compressive stresses of up to 29% of yield strength; two to three times higher than in the CoCr component, occurring both during level walking and a deep squat. In the PEEK implant, during gait, tensile stresses reached 9% of yield strength, which is a 30% reduction from CoCr, where tensile stresses amounted to 13% of yield strength. During a deep squat this effect was even greater as relative tensile stresses in the PEEK implant were over 20 times lower than in the CoCr implant (0.4% vs. 9% of yield strength). Both implants functioned well within the yield limits. However, the dominant role of tensile stresses in documented implant fatigue failures did give reason to consider the possible increased resistance of a PEEK component to such failures. This suggests that PEEK offers more mechanical safety with respect to tensile stress within the material, relative to CoCr.

These computational studies have shown that a PEEK implant has a significant impact on the load transfer in the reconstructed knee joint. The compliant polymer deals with the imposed loads quite differently from the stiff Cobalt-Chromium alloy, leading to both potential advantages and disadvantages with regard to the mechanical integrity of the reconstruction. One of the predicted advantages is the increased resilience against implant fractures. Several studies have reported the occurrence of implant fractures, either due to trauma or to fatigue^{3,4,12-14}. The locations of these fractures were well-matched with the CoCr implant stress intensities that were calculated by the computational models in this thesis: the intercondylar notch and the corner of the posterior chamfer. These stress intensities were not seen in the PEEK prosthesis, due to its different transfer of stresses, thereby relieving these areas in this component from such stress intensities. Based on the model predictions, the mechanical integrity of the cement mantle may cause some concern. As the PMMA is relatively brittle, the localized, increased stress transfer that the PEEK component imposes may result in failure of the underlying cement mantle. This may especially concern osteopenic or osteoporotic patients, where the lack of support under the cement mantle could allow larger deformations, potentially leading to large cement cracks or sinking of the implant. Whether and how this presents clinically should be monitored in clinical trials.

What is the impact of altered mechanics on the underlying cement mantle?

The stress patterns in the cement mantles underneath the PEEK and CoCr implants in **Chapters 2 and 3** showed distinct differences and were similar for both activities. The 'PEEK' cement mantle displayed compressive stresses in the same areas as the femoral components. This was, again, to be expected due to the compliant nature of the PEEK implant. With the CoCr implant, compressive stress intensities were found in proximal areas, leaving the rest of the cement mantle largely unaffected. During level gait, the compressive cement stresses were reduced by 30% with a PEEK prosthesis but were twice that of the CoCr reconstruction during squat. Tensile stress intensities were mainly located in the proximal anterior flange area. The cement mantle in the CoCr reconstruction experienced higher tensile stresses in this region, during both exercises, corresponding to earlier studies that identified this area as a debonding initiation site in CoCr implants.

The effects of using a PEEK femoral component on the cement mantle are more difficult to interpret. Although the magnitude of the stresses did not raise concerns, the difference in location could. As the PEEK implant transfers loads more locally, the cement mantle directly underneath is loaded more heavily. With a CoCr component, the cement mantle is more shielded from stresses near contact sites, which could contribute to the success of the procedure to date. The effects that these changes with the PEEK implant have on the cement mantle are unknown and should thus be considered an increase in risk of complications, from a patient safety standpoint.

Does the PEEK implant provide adequate short- and long-term fixation?

In **Chapter 2** the cement-implant interface was studied for the influence of material change. More compliant PEEK was shown to distribute loads substantially different from metal, meaning that the cement-implant interface would have to be examined for its integrity. The only data available at this point were from the study by Zelle *et al.* (2010), where the authors experimented on coupon samples with different materials bonding with PMMA¹⁰. They then put these data in an FE model to determine the process of interface debonding. The same data for CoCr-on-PMMA were used in the study in Chapter 2. However, interface strength data was not yet available for PEEK-on-PMMA, with the exception of shear strength¹⁵. We hypothesized that compressive and tensile strength are weaker with PEEK, so using CoCr-on-PMMA parameters provided a best-case scenario for the failure index. Although the PEEK prosthesis and cement mantle showed markedly different stress patterns than the CoCr reconstruction, the failure index patterns were similar. The highest failure index for both reconstructions was found at the tip of the anterior flange. In contrast to expectations these were slightly lower for the PEEK implant.

An experimental study was then set up to investigate the actual force needed to dislocate the cemented implant from the bone and to see what role interface debonding plays in the process. In this study in **Chapter 5**, PEEK and CoCr implants were cemented onto bone-analogue foam blocks and extracted while monitoring the applied force and capturing debonding occurring during the pull-off exercise with a camera. The CoCr reconstruction failed at a pull-off force of 3,814 N. The PEEK reconstruction reached 2,525 N on average, which was significantly lower. In both groups cement-implant debonding was observed in the distal area prior to failure. However, at primary failure the cement mantle remained intact and instead the foam fractured underneath the cement. This supported the concept that localized debonding does not necessarily lead to loss of fixation. Secondary failure was different between both implants. While the CoCr reconstruction failed as a whole, the PEEK reconstruction failed in three stages. First one condyle failed and a little later also the second, with similar failure modes. However, the anterior chamfer and flange were usually still attached to the cement and foam. Increased extraction finally resulted in the PEEK implant debonding from the remainder of the cement mantle. The sequential failure of both PEEK condyles highlighted an uneven load distribution, which was further investigated with a FE simulation of the experiment. This led the authors to believe that similar stresses were present in the foam with initial failure of both PEEK and CoCr implants. When comparing the results with data from literature, the force needed to loosen the implants in this study seemed sufficient for clinical purposes¹⁶.

The observations of debonding that occurred during the previous experiments instigated an experimental study into the cement-implant interface of the PEEK prosthesis. In **Chapter 6** we set out to investigate the effects of long-term loading on the cement-implant interface bonding and the damage that may have accumulated in the cement mantle. Implants were cemented onto polyacetal blocks and exposed to 0 (unloaded control), 100,000 (gait control) or 10 million (long-term loading) load cycles, while submerged into a fluorescent dye penetrant to visualize debonded areas. Lateral condylar cross-sections were then made to reveal a complete sagittal internal plane of the implant and cement mantle and the cement-implant interface in between. Most notable was the amount of debonding already present in the unloaded soaked PEEK control, of which on average 80% of the cement-implant interface showed penetrated dye. This was further increased to 88% after 10 million load cycles. In contrast, the CoCr-PMMA interface was only 14% debonded after 100,000 load cycles but increased to 62% on average after 10 million cycles. Full-thickness cement mantle cracks were observed in both PEEK and CoCr reconstructions; most of them in the anterior area. They were hardly present after 100,000 load cycles (average 2 vs. 0.7), but substantially increased after 10 million cycles, with on average 24 and 19 full-thickness cracks underneath the PEEK and CoCr components, respectively. However, these differences were not statistically significant.

So, for the short- and long-term, the results indicate that the PEEK implant provides adequate fixation for clinical application. Throughout this thesis, cement-implant debonding has been shown to be present with the PEEK prosthesis, but pull-off experiments showed that this device matches forces reported in literature for good fixation¹⁶.

Regarding the mechanical safety, we can conclude that the PEEK femoral component would increase the factor of safety for the TKA reconstruction, based on the studies in Chapters 2 and 3 and the notion that tensile stresses generally play a larger role in (fatigue) failure of implants and bone cement. Fixation of the PEEK implant is expected to be adequate, but reduced when compared to CoCr, based on Chapters 5 and 6.

Can PEEK improve the mechanobiology of the periprosthetic bone tissue?

Mechanical loading of bone tissue plays an important part in the retention of the bone stock after TKA. It provides a mechanical stimulus to the biological process of bone remodeling, in which the balance of activity of osteoblasts and osteoclasts largely determine structural strength and rigidity¹⁷. This process of bone remodeling is constantly driving bone turnover. With aging, the balance tips increasingly to osteoclastic activity, effectively reducing bone density, contrary to the effects of physical activity¹⁸. In TKA, stiffness mismatch between prosthesis and underlying bone sorts a similar effect. A stiff (CoCr) femoral implant changes the load distribution such that the bone is shielded from the mechanical stimulus (stresses and strains) needed to maintain the preoperative blastic/clastic balance¹⁹⁻²⁴. As a result, bone tissue is lost and periprosthetic bone quality reduced, increasing the risk of periprosthetic fractures and complex revision surgery. In Chapters 2, 3 and 4 we investigated the effect of implant material on the stresses and strains in the periprosthetic femur. The hypothesis that a more compliant PEEK component would reduce stress shielding in the periprosthetic femur was first tested during the most common activity, being level gait (**Chapter 2**), followed by a more strenuous deep squat (**Chapter 3**). The latter delivered strain energy density information that was analyzed at 90°, 120° and 145° of flexion and could thus be representative of activities of daily living in which such kinematics are common. The effect of material change was explored in geometrically identical FE models with material properties of the intact femur, and in reconstructed femurs with either PEEK or CoCr implants. The strain energy density, as measure for the bone turnover stimulus^{23,25}, showed a strong correlation between the intact femur bone and the PEEK reconstruction, implying a good stiffness match between the resected bone and the PEEK material. The stiffness mismatch that was to be expected with the CoCr implant was clearly observed and present in both studies. These areas of stress shielding around the CoCr component matched areas of bone loss seen in other clinical and simulation studies^{20-23,26}.

In addition, an experimental validation study was performed to verify the model predictions (**Chapter 4**). Intact distal femur pairs were loaded while measuring the strains at the surface of the lateral femur. The femur pairs were then implanted with CoCr and PEEK implants and the test was repeated. The experiments were digitally reconstructed in matched FE models and experimental surface strain maps were compared to the FE results. The computational and experimental strain distributions and magnitudes were very similar, corroborating that the FE model was an accurate representation of the experiment and could thus be used for further analyses. The previous studies demonstrated that stress shielding occurred mainly in the areas underneath the load contact site. Hence, we were mainly interested in the strain energy density differences in the (antero)distal regions, as in this study the applied tibiofemoral loads were axial and slightly anterior of the condylar apex. Similar to the previous two studies, these simulations predicted stress shielding in the loaded regions in all CoCr reconstructions. It was notable that the amount of shielding was highly variable between specimens, confirming that parameters like bone quality, geometry and contact site play an important role in the distribution of strain energy. In the same regions but in the contralateral femur, the PEEK reconstruction always had a higher strain energy compared to CoCr. In the anterodistal area PEEK also showed stress shielding in two out of three specimens, but less than the CoCr implants. Elevated bone strains in the PEEK reconstruction obviously offset the stress shielding effect of the CoCr device, but they may also increase the risk of periprosthetic fractures. This trade-off between stress shielding and the potential risk of fractures should be monitored when the PEEK implant reaches clinical practice.

The conclusion from these three studies was that the PEEK implant is indeed able to reduce the amount of stress shielding by the femoral component, compared to CoCr. This might reduce bone loss after TKA, which is important to prevent complications such as implant loosening, implant and/or bone fractures and complex revision surgery.

What are the consequences of PEEK TKA on clinical imaging?

A good visualization of knee implants post-surgery is essential to determine the success of the procedure and for proper diagnosis of patients presenting with complaints. Since the conception of TKA in the late 1960's, in-situ assessment has relied on standard X-ray imaging, which is still the preferred method to date^{27,28}. Alignment of the implants in the coronal and sagittal plane is crucial to obtain usable images, because the metal blocks X-rays and can thus obfuscate other structures or interfaces. On the other hand, the implant will always be clearly distinguishable from its surroundings, which gives the application its robustness. A PEEK femoral prosthesis will have a large impact on this visualization. A radiolucent polymer will inevitably lead to challenges following the reduced capacity to distinguish the implant from its surrounding. However, increased radiolucency also provides new opportunities for

clinical assessment with other imaging modalities. In MRI and CT scanning the current metal implants induce considerable image artifacts, which make proper assessment difficult or in some cases impossible^{29,30}. Non-interfering polymers, such as PEEK, do not produce such artifacts and thus MRI and CT may have the potential to become valuable diagnostic tools. To determine this potential in **Chapter 7**, cadaver knees were implanted with PEEK and CoCr femoral components and polyethylene tibial components. Clinical imaging settings were used for MRI, CT and X-ray scans to study the appearance of the PEEK implant in these modalities.

Four **MRI** sequences were evaluated: proton density (PD), T1 weighted (T1w), T2 weighted fat saturated (T2FS) and short tau inversion recovery (STIR) sequences. Neither sequence showed artifacts caused by the PEEK component. The best contrast for the implant was achieved with the PD sequence, whereas T1w provided superior, trabecular level detail at the cement-bone interface. The latter may be a valuable feature for post-operative diagnostics. The T2FS sequence achieved superior water signal detection, which is useful in detection of fluid ingress between structures (implant loosening). The STIR sequence did not offer any obvious benefits for PEEK implant imaging.

The chosen **CT** parameters provided excellent signal to noise ratio, unaffected by the PEEK prosthesis and similar to the appearance of standard pre-operative orthopedic CT scanning around the knee. The PEEK prosthesis was clearly identifiable and well separable from surrounding structures, although limited with joint fluid. The lack of artifacts in the PEEK knee image array made it possible to distinguish very small structures in line with the maximum spatial resolution of the scanner used.

The PEEK implant was barely visible on **X-ray** radiography. Contours were observed, but the component only slightly contrasted with the surrounding structures. The metal prosthesis obscured any structure or feature surrounding it, making assessment of cement mantle and bone interfaces impossible. The macroscopic position of the implant is clear, contrary to the PEEK component. However, the radiolucent PEEK allowed for visualization of the bone-cement-implant interface microarchitecture.

It has become clear that the PEEK implant has a radically different appearance on all imaging modalities tested in this thesis. Firstly, standard radiography is challenged by the radiolucency of the PEEK polymer. As X-ray is the main assessment tool for postoperative evaluation, the PEEK implant complicates this assessment by being almost indistinguishable from its surroundings. The absence of ray-absorbing metal does create visibility of the cement mantle and the interfaces, which may be used to indirectly evaluate complaints related to the seating of the component, including (mal)alignment, fixation and migration. Either way, radiologists

and orthopedic specialists will require thorough training to become acquainted with the appearance of the PEEK device and to adequately interpret the images. With regard to the other imaging modalities – MRI and CT – PEEK has shown to be advantageous in visualizing the prosthesis amidst its surrounding tissues and components. With MRI it is in fact one of few implants that does not complicate the application of this modality. Metal components severely distort the entire image-array and are generally not evaluated with this method. PEEK has a distinct appearance that sets it apart from the other TKA components, the knee tissues and the synovial fluid. This may provide breakthrough possibilities in diagnosing postoperative complaints and introduces new avenues for postoperative TKA research. The latter relates to recent advancements in preoperative integration of MRI in understanding the (real-time) kinematics and functional anatomy of the knee for the purpose of surgical planning³¹. With the possibility of undistorted postoperative MRI, these techniques may be employed to evaluate the impact of the reconstruction on the functionality of knee tissues^{31,32}. This may too be a valuable addition to the ongoing debate regarding the gap-balancing and measured resection techniques for implant placement^{33–36}. Similarly, CT can be employed for PEEK knee assessment. Without any of the artefacts of metal, either CT or MRI (or both) can be chosen for whatever specific need.

Future perspectives

On methods used in this thesis

Throughout this thesis, we identified a number of important limitations to the methods, specifically regarding finite element modeling. As the models in Chapters 2 and 3 are based on single samples, the data are mainly usable as proof-of-concept, rather than providing claims for future patient populations. One way to solve that is to use population-based modelling. Population-based modelling in FE analysis is gaining more traction as it provides ways to account for variability in parameters related to the patient, surgery, or implant^{37–40}. Population-based modeling enables testing the mechanical integrity of the PEEK implant for an extensive range of cases, which improves the robustness of the analyses.

Calibration of FE models via experimental validation is another way to increase the reliability of the simulation outcomes, as done in Chapter 4. The studies in Chapters 2 and 3 relied on comparative data, where the same parameters were used for both PEEK and CoCr models, except for material properties. This did allow for the assessment of any relative changes in outcomes, but the results cannot be used as an absolute measure. Although this was not the aim of these studies, it would be useful in the future to perform experimental validation of such models to generate calibrated and quantitatively accurate results.

In Chapter 4 we were able to validate FE simulations with experimental data. We concluded that stress shielding is reduced and, with that, the stimulus for bone resorption is decreased. However, we know from literature that a certain threshold for the stimulus should be applied in order to simulate bone growth^{20,23}. It would be sensible to expand such models with bone adaptation algorithms to assess short- to mid-term effects of (reduced) stress shielding. Long-term adaptations are of interest, but also increasingly difficult to predict as the stimuli for the activities investigated in this thesis are not the only factors influencing the process of bone turnover^{17,18}.

On PEEK TKA development

The long-term testing of PEEK implants in the wear simulator, as investigated in Chapter 6, provided valuable insights into the impact of cyclic loading on the fixation of the device. As hypothesized in this Chapter, it may be worthwhile expanding these experiments to include (scanning electron) microscopic analysis of the implant and cement surfaces to assess the actual wear and damage that may have accumulated at the interface. Human and animal studies suggest that (carbon fiber reinforced) PEEK wear particles could potentially cause inflammatory responses in the knee joint or adjacent tissues⁴¹⁻⁴⁵. Results are inconclusive as to the extent and comparison with current materials, but it would be desirable to know if substantial PMMA or PEEK wear would take place at the implant-cement interface.

In three studies we investigated the potential for a PEEK femoral component to prevent periprosthetic bone loss. Clinical data to support this is desirable to verify these findings, and to compare the bone density changes to metal implants. A small-sample animal (goat) study was conducted by Du *et al.* (2018), demonstrating a light decrease in bone density at 12 weeks post-operative, which did not further increase until 24 weeks⁴⁶. Even though this concerns an animal model, in which kinematics are quite different from human applications, these results provide some confidence to the hypotheses and findings presented in this thesis. However, to further validate the findings of the computational analyses, studies should be executed on the first cohorts of patients receiving a PEEK knee implant to investigate periprosthetic bone changes in a clinical setting. If its benefit is substantiated in clinical studies, a PEEK knee would be a very interesting alternative for younger and active patients, as these would benefit most from a closer-to-natural bone turnover profile.

The current studies have focused exclusively on cemented TKA. Additional efforts could be made to investigate the fixation characteristics of non-cemented PEEK components. Reducing the number of interfaces can arguably increase safety from a wear perspective. Additionally, the periprosthetic bone might further benefit from the increased mechanical compatibility that PEEK offers over metal, when the cement mantle is removed as a buffering layer. As previously mentioned, the integrity of the cement-bone interface relies heavily

on local strain transfer through interdigitated trabeculae and artificial material⁷⁻⁹. If bone ingrowth in a non-cemented PEEK prosthesis would be possible, the quality of the implant-bone interface would be considered to increase substantially, compared to a stiff metal component. The possibility of such ingrowth in PEEK arthroplasty has been shown in animal studies and highlights this potential^{47,48}.

Another interesting application of PEEK in TKA would be for personalized implants. Increasingly often, 3D-printed implants or surgical tools are used and show promising applications⁴⁹⁻⁵². The advancements of patient-specific implants are closely related to the advancements of the 3D-printing technology. Special considerations go to articulating components, as tight tolerances on surface finish are of paramount importance to reduce wear rates. Currently, no printing technique for PEEK is available that can provide such small tolerances, making postprocessing necessary to stay within acceptable design parameters. Additional manufacturing steps are undesirable from a cost perspective and are to be overcome for personalized PEEK implants for TKA can be considered.

A major advantage of all-polymer TKA is the application for patients with metal hypersensitivity. About 10-15% of the population suffers from some form of metal hypersensitivity⁵³. Although this number is lower in the TKA population, metal allergy is considered a preoperative risk and a serious cause of TKA failure⁵³. Preoperative screening for metal allergy is therefore important, and patients with this condition would benefit from a metal free solution, such as with a PEEK femoral component combined with an all-polymer tibial component. Similarly, patients undergoing revision surgery following complications of metal allergy, would benefit from all-polymer implants.

Surgical technique in terms of cementing will likely affect the clinical result the cemented femoral PEEK component. The current PEEK component as investigated in this thesis was equipped with medial-to-lateral ridges in the cement pockets to improve mechanical interlock of the implant-cement interface. For proper implant fixation, achieving a good cement coverage is important. Following the changes to the design, a specific cementation technique may be required, as the ridges influence the distribution of cement when the component is impacted onto the prepared femur. The ridges may grip cement that is applied to the condyles and drag it forward, away from the implant flanges, leaving distal parts of the pockets uncemented. This may be prevented by additionally applying cement to (at least) the anterior and posterior flanges to fill up the spaces between the ridges before implantation, or by cementing both the femur and implant before implant insertion.

Aside from the parameters that were studied in this thesis, a number of additional properties are important to consider for their potential impact on clinical success. Wear-resistance is one

of the essential attributes of a bearing couple. The current PEEK-on-UHMWPE prosthesis has been studied for its wear performance in vitro. Relative to the identically shaped CoCr device, the PEEK-on-UHMWPE construct experienced a (non-statistically significant) slight increase in wear, but remained categorized as 'low' in terms of wear rate⁵⁴. Compared to current clinically used metal components, the PEEK implant performed better, likely due to the low conformity of the articulating components⁵⁵. An increase in friction coefficient and consequent frictional heating were also reported for the PEEK implant. Hypothesized complications of elevated joint temperature are protein deposition and denaturation, which may elevate friction and wear, and tissue necrosis⁵⁶. These wear and friction properties obviously require clinical data to assess their impact, but the comparison to successful metal devices does not raise major concerns.

The pre-clinical research in this thesis and the discussions following support further clinical exploration of the PEEK femoral component. The metal-free, stiffness-matched prosthesis arguably provide some much-desired benefits over current TKA devices and, as such, should be studied in a clinical setting. The ability to use multiple high-quality imaging modalities, creates many opportunities for clinical assessments and should be used to evaluate the potential drawbacks identified in this thesis. Important parameters to study would include the morphology of the periprosthetic bone stock. Any lesions or soft spots underneath the cement mantle should be identified to assess whether such inhomogeneities have an impact on clinical performance. At the same time, the integrity of the cement layer could be monitored to be able to retrospectively determine its relation to implant loosening, if any cases would loosen during the trial. The altered stiffness also warrants migration and creep measurements. With multiplanar reconstruction and segmentation of MRI and CT image-arrays these parameters could be accurately followed at different time intervals during service. This would be a welcome addition to the current standard in migration detection: roentgen stereophotogrammetry (RSA). This technique measures relative motion between sets of metal markers, but as it assumes rigid body motion – adequate for metal components – it can be hypothesized to be less accurate for compliant PEEK implants. Notwithstanding the accepted use of this technique, CT and MRI have the potential to be more accurate and informative in determining implant seating and, additionally, deformation and creep.

Conclusions

This thesis investigated the mechanical performance and primary fixation of a PEEK femoral TKA implant, evaluated the effect of such a low-stiffness femoral prosthesis on peri-prosthetic load transfer, and explored the implications for medical imaging of using a radiolucent polymer component. The findings of this thesis support further exploration of PEEK femoral TKA implants in a clinical trial and warrant further research on the use of PEEK in total joint replacement.

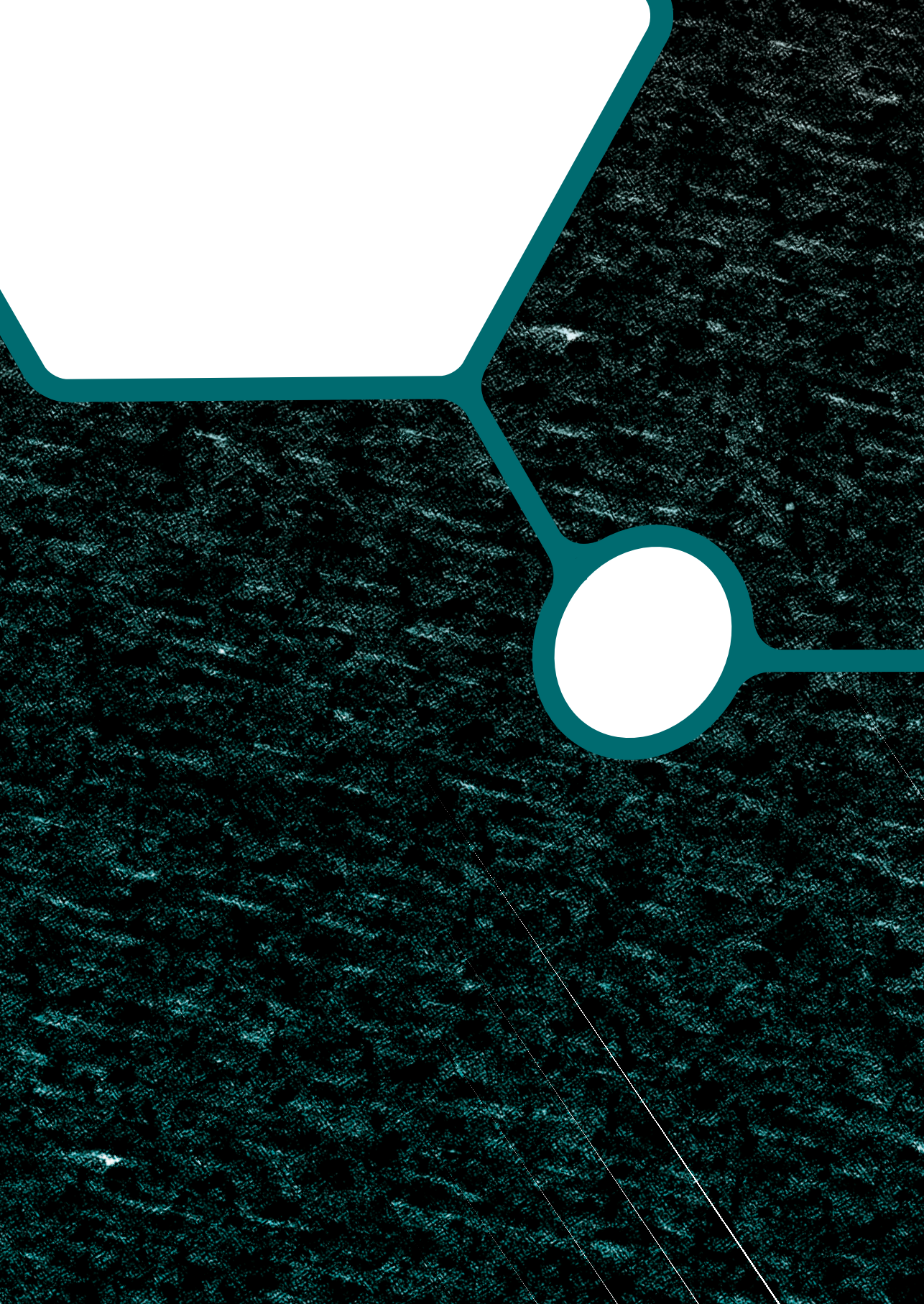
References

1. D'Lima D, Fregly BJ, Patil S, et al. *Knee joint forces: prediction, measurement, and significance*. Proc Inst Mech Eng H 2012; 226: 95–102.
2. Zelle J, Janssen D, Van Eijden J, et al. *Does high-flexion total knee arthroplasty promote early loosening of the femoral component?*. J Orthop Res 2011; 29: 976–983.
3. Krueger AP, Singh G, Beil FT, et al. *Ceramic femoral component fracture in total knee arthroplasty: an analysis using fractography, fourier-transform infrared microscopy, contact radiography and histology..* J Arthroplasty 2014; 29: 1001–4.
4. Gilg MM, Zeller CW, Leitner L, et al. *The incidence of implant fractures after knee arthroplasty*. Knee Surg, Sport Traumatol Arthrosc 2016; 24: 3272–3279.
5. Ranawat AS, Ranawat AS, Ranawat CS. *The history of total knee arthroplasty*. In: Bonnin M (ed) *The Knee Joint*. Springer-Verlag France, Paris, 2012.
6. van de Groes S, de Waal Malefijt M, Verdonschot N. *Influence of preparation techniques to the strength of the bone-cement interface behind the flange in total knee arthroplasty*. Knee 2012; 20: 186–190.
7. Goodheart JR, Miller MA, Mann KA. *In Vivo Loss of Cement-Bone Interlock Reduces Fixation Strength in Total Knee Arthroplasties*. J Orthop Res 2014; 32: 1052–1060.
8. Howard K, Miller M, Damron T, et al. *The distribution of implant fixation for femoral components of TKA: A postmortem retrieval study*. J Arthroplasty 2014; 29: 1863–1870.
9. Mann K, Miller M, Pray C, et al. *A new approach to quantify trabecular resorption adjacent to cemented knee arthroplasty*. J Biomech 2012; 45: 711–715.
10. Zelle J, Janssen D, Peeters S, et al. *Mixed-mode failure strength of implant-cement interface specimens with varying surface roughness*. J Biomech 2011; 44: 780–3.
11. Zelle J, van de Groes S, de Waal Malefijt M, et al. *Femoral loosening of high-flexion total knee arthroplasty: the effect of posterior cruciate ligament retention and bone quality reduction..* Med Eng Phys 2014; 36: 318–24.
12. Han CD, Han CW, Yang IH. *Femoral Component Fracture Due to Osteolysis After Cemented Mobile-Bearing Total Knee Arthroplasty*. J Arthroplasty 2009; 24: 323.e7-323.e12.
13. Huang C, Yang C, Cheng C. *Fracture of the femoral component associated with polyethylene wear and osteolysis after total knee arthroplasty*. J Arthroplasty 1999; 14: 375–379.
14. Duffy GP, Murray BE, Trousdale RR. *Hybrid Total Knee Arthroplasty. Analysis of Component Failures at an Average of 15 Years*. J Arthroplasty 2007; 22: 1112–1115.
15. Rankin KE. *Evaluation of Polyetheretherketone as a Candidate Material for Cemented Total Knee Replacement*. University of Southampton, Faculty of Engineering and the Environment, PhD Thesis.
16. Bergschmidt P, Dammer R, Zietz C, et al. *Adhesive strength of total knee endoprostheses to bone cement – analysis of metallic and ceramic femoral components under worst-case conditions*. Biomed Tech 2016; 61: 281–289.

17. Robling AG, Turner CH. *Mechanical Signaling for Bone Modeling and Remodeling*. Crit Rev Eukaryot Gene Expr 2009; 19: 319–338.
18. Boskey AL, Coleman R. *Aging and bone*. J Dent Res 2010; 89: 1333–1348.
19. Bobyn J, Mortimer E, Glassman A, et al. *Producing and avoiding stress shielding. Laboratory and clinical observations of noncemented total hip arthroplasty*. Clin Orthop Relat Res 1992; 79–96.
20. Lenthe G Van, de Waal Malefijt MC, Huiskes R. *Stress shielding after total knee replacement may cause bone resorption in the distal femur..* J Bone Joint Surg Br 1997; 79: 117–122.
21. Lavernia CJ, Rodriguez J a, Iacobelli D a, et al. *Bone mineral density of the femur in autopsy retrieved total knee arthroplasties..* J Arthroplasty 2014; 29: 1681–6.
22. Järvenpää J, Soininvaara T, Kettunen J, et al. *Changes in bone mineral density of the distal femur after total knee arthroplasty: a 7-year DEXA follow-up comparing results between obese and nonobese patients..* Knee 2014; 21: 232–5.
23. Huiskes R, Weinans H, Grootenboer HJ, et al. *Adaptive Bone-Remodeling Theory Applied to Prosthetic-Design Analysis*. J Biomech 1987; 20: 1135–1150.
24. Huiskes RR. *Failed innovation in total hip replacement. Diagnosis and proposals for a cure..* Acta Orthop Scand 1993; 64: 699–716.
25. Kummer B. *Biomechanics of bone: Mechanical properties, functional structure, and functional adaptation..* In: Fung Y, Perrone N, Anliker M (eds) *Biomechanics: Its Foundations and Objectives*. Englewood Cliffs, NJ: Prentice-Hall, 1972, p. 237:271.
26. Lenthe G Van, Willems M, Verdonchot N, et al. *Stemmed femoral knee prostheses: effects of prosthetic design and fixation on bone loss*. Acta Orthop Scand 2002; 73: 630–637.
27. Ewald F, C. *Roentgenographic Evaluation and Scoring System*. Clin Orthop Relat Res 1989; 2–5.
28. Goergen TG, Dalinka MK, Alazraki N, et al. *Evaluation of the patient with painful hip or knee arthroplasty. American College of Radiology. ACR Appropriateness Criteria..* Radiology 2000; 215 Suppl: 295–298.
29. Koch KM, Lorbiecki JE, Hinks RS, et al. *A multispectral three-dimensional acquisition technique for imaging near metal implants*. Magn Reson Med 2009; 61: 381–390.
30. Kasperek MF, Töpker M, Lazar M, et al. *Dual-energy CT and ceramic or titanium prostheses material reduce CT artifacts and provide superior image quality of total knee arthroplasty*. Knee Surg, Sport Traumatol Arthrosc 2019; 27: 1552–1561.
31. Naghibi H, Mazzoli V, Gijsbertse K, et al. *A noninvasive MRI based approach to estimate the mechanical properties of human knee ligaments*. J Mech Behav Biomed Mater 2019; 93: 43–51.
32. Leijendekkers RA, Marra MA, Ploegmakers MJM, et al. *Magnetic-resonance-imaging-based three-dimensional muscle reconstruction of hip abductor muscle volume in a person with a transfemoral bone-anchored prosthesis: A feasibility study*. Physiother Theory Pract 2019; 35: 495–504.

33. Daines BK, Dennis DA. *Gap Balancing vs. Measured Resection Technique in Total Knee Arthroplasty*. Clin Orthop Surg 2014; 6: 1–8.
34. Song DLJPD. *Accuracy of soft tissue balancing in TKA: comparison between navigation-assisted gap balancing and conventional measured resection*. Knee Surg, Sport Traumatol Arthrosc 2010; 18: 381–387.
35. Dennis DA, Komistek RD, Kim RH, et al. *Gap Balancing versus Measured Resection Technique for Total Knee Arthroplasty*. Clin Orthop Relat Res 2010; 468: 102–107.
36. Moon Y, Kim H, Ahn H, et al. *Comparison of soft tissue balancing, femoral component rotation, and joint line change between the gap balancing and measured resection techniques in primary total knee arthroplasty. A meta-analysis*. Medicine (Baltimore) 2016; 95: 1–7.
37. Laz PJ, Browne M. *A review of probabilistic analysis in orthopaedic biomechanics*. Proc Inst Mech Eng H 2010; 224: 927–943.
38. Easley SK, Pal S, Tomaszewski PR, et al. *Finite element-based probabilistic analysis tool for orthopaedic applications*. Comput Methods Programs Biomed 2007; 85: 32–40.
39. Sarkalkan N, Weinans H, Zadpoor AA. *Statistical shape and appearance models of bones*. Bone 2014; 60: 129–140.
40. Campbell JQ, Petrella AJ. *Automated finite element modeling of the lumbar spine: Using a statistical shape model to generate a virtual population of models*. J Biomech 2016; 49: 2593–2599.
41. Lorber V, Paulus AC, Buschmann A, et al. *Elevated cytokine expression of different PEEK wear particles compared to UHMWPE in vivo*. J Mater Sci Mater Med 2014; 25: 141–149.
42. Du Z, Zhu Z, Wang Y. *The degree of peri-implant osteolysis induced by PEEK, CoCrMo, and HXLPE wear particles: a study based on a porous Ti6Al4V implant in a rabbit model*. J Orthop Surg Res 2018; 13: 1–9.
43. Du Z, Wang S, Yue B, et al. *Effects of wear particles of polyether-ether-ketone and cobalt-chromium-molybdenum on CD4- and CD8-T-cell responses*. Oncotarget 2018; 9: 11197–11208.
44. Paulus AC, Haßelt S, Jansson V, et al. *Histopathological Analysis of PEEK Wear Particle Effects on the Synovial Tissue of Patients*. Biomed Res Int 2016; 2: 1–5.
45. Stratton-Powell AA, Pasko KM, Brockett CL, et al. *The Biologic Response to Polyetheretherketone (PEEK) Wear Particles in Total Joint Replacement: A Systematic Review*. Clin Orthop Relat Res 2016; 474: 2394–2404.
46. Du Z, Zhu Z, Yue B, et al. *Feasibility and Safety of a Cemented PEEK-on-PE Knee Replacement in a Goat Model: A Preliminary Study*. Artif Organs 2018; 42: E204–E214.
47. Nakahara I, Takao M, Bandoh S, et al. *In vivo implant fixation of carbon fiber-reinforced PEEK hip prostheses in an ovine model*. J Orthop Res 2012; 31: 485–92.
48. Choi D, Yoon YS, Hwang D. *Evaluation of sleeved implant fixation using a rat model*. Med Eng Phys 2011; 33: 310–314.
49. Liu D, Fu J, Fan H, et al. *Application of 3D-printed PEEK scapula prosthesis in the treatment of scapular benign fibrous histiocytoma: A case report*. J Bone Oncol 2018; 12: 78–82.
50. Wang L, Huang L, Li X, et al. *Three-Dimensional Printing PEEK Implant: A Novel Choice for the Reconstruction of Chest Wall Defect*. Ann Thorac Surg 2019; 107: 921–928.

51. Deng L, Deng Y, Xie K. AgNPs-decorated 3D printed PEEK implant for infection control and bone repair. *Colloids Surfaces B Biointerfaces* 2017; 160: 483–492.
52. Haleem A, Javaid M. Polyether ether ketone (PEEK) and its manufacturing of customised 3D printed dentistry parts using additive manufacturing. *Clin Epidemiol Glob Heal* 2019; 0–1.
53. Innocenti M, Vieri B, Melani T, et al. Metal hypersensitivity after knee arthroplasty: fact or fiction?. *Acta Biomed* 2017; 88: 78–83.
54. Cowie RM, Briscoe, Fisher, et al. PEEK-OPTIMA™ as an alternative to cobalt chrome in the femoral component of total knee replacement: A preliminary study.. *Proc Inst Mech Eng H* 2016; 230: 1008–1015.
55. Brockett CL, Carbone S, Fisher J, et al. Influence of conformity on the wear of total knee replacement: An experimental study. *Proc Inst Mech Eng H* 2018; 232: 127–134.
56. Bergmann G, Graichen F, Rohlmann A, et al. Frictional heating of total hip implants, Part 1: Measurements in patients. *J Biomech* 2001; 34: 421–428.



Chapter 9

Nederlandse samenvatting en discussie

De studies gepresenteerd in dit proefschrift onderzochten het potentieel van een volledig-kunststof totale knie vervanging (TKV) met betrekking tot de huidige standaard in knie vervangende chirurgie. De eerste voorspellende mechanische experimenten werden uitgevoerd *in-silico* met de eindige-elementenmethodologie (FE), met modellen die steeds verfijnder werden. Experimentele kadaverstudies werden uitgevoerd voor extra validatie van de computermodellen, wat nodig was om het effect van implantaatmateriaal op *in-vivo stress shielding* nauwkeurig te voorspellen. Toen vroege simulaties, gecombineerd met experimentele waarnemingen, aanleiding gaven tot bezorgdheid over de fixatie en hechting van de nieuwe kunststofprothese, werden aanvullende experimentele studies uitgevoerd om de sterkte en kwaliteit van het gecementeerde implantaat te onderzoeken. Daarnaast is onderzoek verricht naar medische beeldvorming van de kunststof knie-implantaten om de interpretatie daarvan te verkennen met betrekking tot implantaatstabiliteit en fixatie in de klinische praktijk.

Het onderzoek was gericht op het beantwoorden van de onderzoeksvragen zoals vermeld in Hoofdstuk 1 van dit proefschrift en zal overeenkomstig in dit hoofdstuk worden behandeld.

Hoe veilig is PEEK-op-UHMWPE TKV in vergelijking met CoCr-op-UHMWPE?

Tijdens gebruik wordt geschat dat de krachten op het implantaat tot driemaal het lichaamsgewicht bereiken tijdens lopen, en ongeveer viermaal het lichaamsgewicht tijdens een diepe kniebuiging of joggen^{1,2}. In het geval van een trauma kunnen die belastingen drastisch toenemen tot het punt waarop de prothese kan breken en moet worden vervangen^{3,4}. Onder die omstandigheden is het begrijpelijk waarom metaal het voorkeursmateriaal is geweest sinds de begindagen van de TKV-procedure⁵, en is duidelijk waarom een kunststofcomponent onder vergelijkbare omstandigheden moet worden getest.

Bij een gecementeerde totale knieprothese wordt fixatie van het implantaat gerealiseerd door een mechanische interlock, gecreëerd door het implantaat op het bot te slaan, met daartussen een deegachtige laag polymethylmethacrylaat (PMMA) cement. Tijdens impactie wordt het cement in het trabeculaire bot en in uitsparingen in het implantaat gedrukt. Na het uitharden van het cement is de component op zijn plaats vergrendeld op een cement-versterkte fundering van trabeculair en corticaal bot. De cementlaag introduceert twee interfaces: de cement-bot interface en de cement-implantaatinterface. De sterkte van de cement-bot interface is uitgebreid onderzocht door experimentele studies en post-mortem retrieval studies⁶⁻⁹. Die concludeerden dat trabeculaire interdigitering van het botcement essentieel is voor een goede fixatie. Het biedt uitstekende primaire fixatie, maar de sterkte neemt in de loop van de tijd af omdat de trabeculae zich terugtrekken uit het cement vanwege

de stress shielding door het PMMA⁷⁻⁹. Het belang van goede interdigitering wordt verder benadrukt door studies die aantoonen dat botvoorbereidingstechnieken een sleutelrol spelen op de cement-bot interface. Contact tussen cement en corticaal bot moet worden vermeden of opruiming moet worden toegepast⁶.

Er zijn onderzoeken gedaan naar loslating van cement en implantaat^{2,10,11}. Computersimulaties waren in staat om klinisch waargenomen loslating in de anterieure flens van CoCr femorale implantaten te reproduceren^{2,11}. Om te begrijpen wat de invloed van PEEK op de fixatie van de prothese zou zijn, werden de onderzoeken in de Hoofdstukken 2,5 en 6 uitgevoerd.

Hoe reageert PEEK mechanisch op dagelijkse activiteiten?

In de Hoofdstukken 2 en 3 hebben we computermodellen gebouwd om de respons te bepalen van een TKV-reconstructie met een PEEK of CoCr femorale component op de belastingen tijdens het lopen (**Hoofdstuk 2**) en een diepe kniebuiging (**Hoofdstuk 3**). Zoals verwacht, produceerde het PEEK-implantaat over het algemeen een meer lokale spanningsoverdracht, nabij de locatie van het gewrichtscontact. Dit leidde tot een toename van drukspanningen tot maximaal 29% van de vloeigrens; twee tot drie keer hoger dan in de CoCr-component, zowel tijdens lopen als een diepe kniebuiging. In het PEEK-implantaat bereikten de trekkrachten tijdens het lopen 9% van de vloeigrens, wat een vermindering van 30% is ten opzichte van CoCr, waarbij de trekspanningen 13% van de vloeigrens bedroegen. Tijdens een diepe kniebuiging was dit effect nog groter omdat de relatieve trekspanningen in het PEEK-implantaat meer dan 20 keer lager waren dan in het CoCr-implantaat (0,4% versus 9% van de vloeigrens). Beide implantaten functioneerden goed binnen de vloeigrenzen. De dominante rol van trekspanningen bij gedocumenteerde faalgevallen van implantaten door materiaalmoedheid gaf echter aanleiding om te veronderstellen dat een PEEK-component mogelijk een verhoogde weerstand tegen dergelijk falen biedt. Dit suggereert dat PEEK meer mechanische veiligheid biedt dan CoCr, met betrekking tot trekspanning in het materiaal.

Deze computersimulaties hebben aangetoond dat een PEEK-implantaat een significante invloed heeft op de belastingoverdracht in het gereconstrueerde kniegewricht. Het meer flexibele kunststof hanteert de opgelegde belastingen heel anders dan de stijve kobalt-chroomlegering, wat leidt tot zowel potentiële voordelen als nadelen met betrekking tot de mechanische integriteit van de reconstructie. Eén van de voorspelde voordelen is de verhoogde weerbaarheid tegen implantaatfracturen. Verschillende onderzoeken hebben het vóórkomen van implantaatfracturen gemeld, hetzij door trauma, hetzij door materiaalmoedheid^{3,4,12-14}. De locatie van deze fracturen kwam goed overeen met de spanningsintensiteiten in de CoCr-component die door de computermodellen in dit proefschrift werden geïdentificeerd: de intercondylaire *notch* en de hoek van de posterieure afschuiving. In de PEEK-prothese werden de spanningsintensiteiten in deze gebieden niet

waargenomen, doordat ze werden ontzien als gevolg van de veranderde overdracht van spanningen in dit component. Op basis van de modelvoorspellingen kan de mechanische integriteit van de cementmantel enige bezorgdheid oproepen. Omdat het PMMA relatief bros is, kan de lokaal verhoogde spanningsoverdracht die de PEEK-component veroorzaakt, leiden tot falen van de onderliggende cementmantel. Dit kan met name betrekking hebben op patiënten met osteopenie of osteoporose, waar het gebrek aan ondersteuning onder de cementmantel grotere vervormingen kan veroorzaken, wat mogelijk kan leiden tot grote cementscheuren of migratie van het implantaat. Of en hoe dit zich klinisch presenteert, moet in klinische onderzoeken worden gemonitord.

Wat is de impact van veranderde mechanica op de onderliggende cementmantel?

De spanningspatronen in de cementmantels onder de PEEK- en CoCr-implantaten in **Hoofdstukken 2 en 3** vertoonden duidelijke verschillen tussen de implantaten en waren vergelijkbaar voor beide activiteiten. De 'PEEK' cementmantel vertoonde drukspanningen in dezelfde gebieden als de femorale componenten. Dit was wederom te verwachten vanwege de flexibiliteit van het PEEK-implantaat. Met het CoCr-implantaat werden drukspanningsintensiteiten gevonden in proximale gebieden, waardoor de rest van de cementmantel grotendeels onaangetast bleef. Tijdens lopen werden de drukspanningen in het cement met 30% verlaagd door een PEEK-prothese, maar waren ze tweemaal zo groot als die in de CoCr-reconstructie tijdens een diepe kniebuiging. Trekspanningsintensiteiten bevonden zich voornamelijk proximaal in het anterieure flensgebied. De cementmantel in de CoCr-reconstructie ondervond tijdens beide oefeningen hogere trekspanningen in ditzelfde gebied, overeenkomstig met eerdere studies die deze locatie identificeerden als een initiatieplaats voor loslating in CoCr-implantaten.

De effecten van het gebruik van een PEEK femorale component op de cementmantel zijn moeilijker te interpreteren. Hoewel de grootte van de spanningen geen zorgen baarde, zou het verschil in locatie dat wel kunnen. Naarmate het PEEK-implantaat belastingen meer lokaal overbrengt, wordt de cementmantel direct eronder zwaarder belast. Met een CoCr-component is de cementmantel meer afgeschermd voor spanningen rondom contactlocaties, wat zou kunnen bijdragen aan het succes van de procedure tot nu toe. De effecten die deze veranderingen met het PEEK-implantaat op de cementmantel hebben, zijn onbekend en moeten daarom vanuit het oogpunt van de patiënt als een toename van het risico op complicaties worden beschouwd.

Biedt het PEEK-implantaat voldoende fixatie op korte en lange termijn?

In **Hoofdstuk 2** werd de cement-implantaatinterface onderzocht op de invloed van de verandering van materiaal. Het minder stijve PEEK bleek belastingen aanzienlijk anders te

verdelen dan metaal, wat betekent dat de cement-implantaatinterface zou moeten worden onderzocht op zijn integriteit. De enige gegevens die op dat moment beschikbaar waren, kwamen uit de studie van Zelle *et al.* (2010), waar de auteurs experimenteerden met coupon samples waarbij verschillende materialen werden gebonden aan PMMA¹⁰. Vervolgens zetten zij deze gegevens in een FE-model om het proces van interface-loslating te bepalen. Dezelfde gegevens voor CoCr-op-PMMA werden gebruikt in de studie in Hoofdstuk 2. Echter, voor PEEK-op-PMMA waren deze gegevens over de interfacesterkte nog niet beschikbaar, met uitzondering van de afschuifsterkte¹⁵. Onze hypothese was dat druk- en treksterkte zwakker zijn bij PEEK, dus het gebruik van CoCr-op-PMMA parameters bood een best-case scenario voor de faalindex. Hoewel de PEEK-prothese en de cementmantel aanzienlijk verschillende spanningspatronen vertoonden dan de CoCr-reconstructie, waren de patronen voor de faalindex vergelijkbaar. De hoogste faalindex voor beide reconstructies werd gevonden aan het uiteinde van de anterieure flens. In tegenstelling tot de verwachtingen waren deze iets lager voor het PEEK-implantaat.

Een experimenteel onderzoek werd vervolgens opgezet om de werkelijke kracht te bepalen die nodig is om het gecementeerde implantaat van het bot te tillen en om te zien welke rol interface-loslating in het proces speelt. In deze studie in **Hoofdstuk 5** werden PEEK- en CoCr-implantaten op bot-analoge schuimblokken gecementeerd en losgetrokken onder gecontroleerde kracht. Ondertussen werd de loslating tijdens de pull-off procedure vastgelegd met een camera. De CoCr-reconstructie faalde bij een trekkracht van 3.814 N. De PEEK-reconstructie bereikte gemiddeld 2.525 N, wat aanzienlijk lager was. In beide groepen werd, voorafgaand aan falen, cement-implantaat-loslating waargenomen in het distale gebied. Bij primair falen bleef de cementmantel echter intact en in plaats daarvan brak het schuim onder het cement. Dit ondersteunde het concept dat gelokaliseerde loslating niet noodzakelijk leidt tot verlies van fixatie. Secundair falen was verschillend tussen beide implantaten. Terwijl de CoCr-reconstructie in zijn geheel faalde, faalde de PEEK-reconstructie in drie fasen. Eerst faalde de ene condyle en iets later ook de andere, met vergelijkbare faalmechanismen. De anterieure afschuining en flens waren meestal echter nog steeds bevestigd aan het cement en het schuim. Verdere extractie resulteerde er uiteindelijk in dat het PEEK-implantaat losliet van de rest van de cementmantel. Het opeenvolgende falen van beide PEEK-condyles wees op een ongelijke belastingsverdeling, wat verder werd onderzocht met een FE-simulatie van het experiment. Dit wees erop dat vergelijkbare spanningen aanwezig waren in het schuim tijdens het primaire falen van zowel PEEK- als CoCr-implantaten. Bij het vergelijken van de resultaten met gegevens uit de literatuur leek de kracht die nodig was om de implantaten in dit onderzoek los te maken voldoende voor klinische doeleinden¹⁶.

De waarnemingen van loslating tijdens de vorige experimenten waren aanleiding voor een experimenteel onderzoek naar de cement-implantaatinterface van de PEEK-prothese. In

Hoofdstuk 6 wilden we de effecten van langdurige belasting op de hechting van de cement-implantaatinterface en de mogelijke opbouw van schade in de cementmantel onderzoeken. Implantaten werden gecementeerd op polyacetaalblokken en blootgesteld aan 0 (onbelaste controle), 100.000 (belaste controle) of 10 miljoen (langdurige belasting) belastingscycli, terwijl ze ondergedompeld werden in een fluorescerende kleurstof om losgelaten gebieden zichtbaar te maken. Vervolgens werden dwarsdoorsneden gemaakt van de laterale condylen om een volledig sagittaal inwendig vlak van het implantaat, de cementmantel en het tussenliggende cement-implantaatoppervlak zichtbaar te maken. Het meest opvallend was de hoeveelheid loslating die al aanwezig was in de onbelaste PEEK-controle, waarvan gemiddeld 80% van de cement-implantaatinterface penetratie van de kleurstof vertoonde. Dit nam toe tot 88% na 10 miljoen belastingscycli. De CoCr-PMMA-interface daarentegen was slechts 14% losgelaten na 100.000 belastingscycli, maar dit percentage nam na 10 miljoen cycli toe tot 62%. Cementmantelscheuren door de volledige dikte werden waargenomen in zowel PEEK- als CoCr-reconstructies; de meeste in het anterieure gebied. Ze waren nauwelijks aanwezig na 100.000 belastingscycli (gemiddeld 2 versus 0,7), maar namen aanzienlijk toe na 10 miljoen cycli, met gemiddeld 24 en 19 volledige scheuren onder respectievelijk de PEEK- en CoCr-componenten. Deze verschillen waren echter niet statistisch significant.

Deze resultaten geven aan dat het PEEK-implantaat voldoende korte en lange termijnfixatie biedt voor klinische toepassing. In dit proefschrift is aangetoond dat cement-implantaatloslating aanwezig is bij de PEEK-prothese, maar pull-off experimenten toonden aan dat deze prothese voldoet aan krachten die in de literatuur zijn vermeld voor een goede fixatie¹⁶.

Met betrekking tot de mechanische veiligheid kunnen we concluderen dat de PEEK femorale component de veiligheidsfactor voor de TKV-reconstructie zou verhogen, gebaseerd op de studies in Hoofdstukken 2 en 3 en het besef dat trekspanningen in het algemeen een grotere rol spelen bij falen (door vermoeidheid) van implantaten en botcement. De fixatie van het PEEK-implantaat is naar verwachting voldoende, maar verminderd in vergelijking met CoCr, op basis van de Hoofdstukken 5 en 6.

Kan PEEK de mechanobiologie van het periprothetisch weefsel verbeteren?

Mechanische belasting van botweefsel speelt een belangrijke rol bij het behouden van de botmassa na TKV. Het biedt een mechanische stimulans voor het biologische proces van botremodellering, waarbij de balans in activiteit van osteoblasten en osteoclasten grotendeels de sterkte en stijfheid van de structuur bepalen¹⁷. Dit proces van botremodellering zorgt voor een constante botomzet. Met het ouder worden verschuift de balans steeds meer naar osteoclastische activiteit, waardoor de botdichtheid effectief vermindert, in tegenstelling tot

de effecten van fysieke activiteit¹⁸. Bij TKV veroorzaakt de mismatch in stijfheid tussen prothese en onderliggend bot een soortgelijk effect. Een stijf (CoCr) femoraal implantaat verandert de belastingsverdeling zodanig dat het bot wordt afgeschermd van de mechanische stimulus (spanningen en vervormingen) die nodig zijn om de preoperatieve blastische/clastische balans te handhaven¹⁹⁻²⁴. Als gevolg hiervan gaat botweefsel verloren en vermindert de botkwaliteit rondom het implantaat, waardoor het risico op periprothetische fracturen en complexe revisiechirurgie toeneemt. In de Hoofdstukken 2, 3 en 4 onderzochten we het effect van implantaatmateriaal op de spanningen en vervormingen in het periprothetische femur. De hypothese dat een minder stijf PEEK-component stress shielding in het periprothetische femur zou verminderen, werd eerst getest tijdens de meest voorkomende activiteit, zijnde het vlak lopen (**Hoofdstuk 2**), gevolgd door een meer inspannende diepe kniebuiging (**Hoofdstuk 3**). De laatste leverde informatie over de *strain energy density* die werd geanalyseerd bij 90°, 120° en 145° flexie en zou dus representatief kunnen zijn voor activiteiten in het dagelijks leven waarin dergelijke kinematica gebruikelijk zijn. Het effect van materiaalverandering werd onderzocht in geometrisch identieke FE-modellen met materiaaleigenschappen van het intacte femur, en in gereconstrueerde femurs met PEEK- of CoCr-implantaten. De *strain energy density*, als maat voor de botomzetstimulus^{23,25}, vertoonde een sterke correlatie tussen het intacte femur en de PEEK-reconstructie, hetgeen een goede match in stijfheid tussen het verwijderde botweefsel en het PEEK-materiaal impliceert. De mismatch in stijfheid die te verwachten was met het CoCr-implantaat werd duidelijk waargenomen en was aanwezig in beide studies. Deze gebieden van stress shielding rond de CoCr-component kwamen overeen met locaties van botverlies die werden gezien in andere klinische en simulatiestudies^{20-23,26}.

Daarnaast is een experimentele validatiestudie uitgevoerd om de modelvoorspellingen te verifiëren (**Hoofdstuk 4**). Gepaarde intacte distale femurs werden belast terwijl de vervormingen aan het oppervlak van het laterale femur werden gemeten. De femurparen werden vervolgens geïmplanteerd met CoCr- en PEEK-implantaten en de test werd herhaald. De experimenten werden digitaal gereconstrueerd in FE-modellen en experimentele oppervlaktevervormingen werden vergeleken met de FE-resultaten. De gesimuleerde en experimentele verdelingen en groottes van de vervormingen waren zeer vergelijkbaar, wat bevestigt dat het FE-model een nauwkeurige weergave van het experiment was en dus voor verdere analyses kon worden gebruikt. De voorgaande studies toonden aan dat stress shielding voornamelijk plaatsvond in de gebieden onder de plek waar het contact van de belasting plaatsvond. Daarom waren we vooral geïnteresseerd in de verschillen in *strain energy density* in de (antero)distale gebieden, omdat in dit onderzoek de toegepaste tibiofemorale belastingen axiaal waren en enigszins anterieur van de condylaire apex. Net als de vorige twee studies voorspelden deze simulaties stress shielding in de belaste regio's in alle CoCr-reconstructies. Het was opmerkelijk hoe variabel de hoeveelheid stress shielding was tussen de femurs, wat bevestigt dat parameters zoals botkwaliteit, geometrie en contactlocatie een

belangrijke rol spelen bij de verdeling van strain energy density. In diezelfde regio's in het contralaterale femur vertoonde de PEEK reconstructie altijd grotere vervormingen dan CoCr. In het anterodistale gebied vertoonde PEEK ook stress shielding in twee van de drie samples, maar minder dan de CoCr-implantaten. Grotere botvervormingen in de PEEK-reconstructie compenseren duidelijk het stress shielding effect van de CoCr-prothese, maar ze kunnen ook het risico op periprothetische fracturen vergroten. Deze wisselwerking tussen stress shielding en het potentiële risico op fracturen moet worden gemonitord wanneer het PEEK-implantaat de klinische praktijk bereikt.

De conclusie van deze drie studies was dat het PEEK-implantaat inderdaad in staat is om de hoeveelheid stress shielding door de femorale component te verminderen in vergelijking met CoCr. Dit kan botverlies verminderen na TKV, wat belangrijk is om complicaties te voorkomen zoals het losraken van implantaten, implantaat- en/of botfracturen en complexe revisiechirurgie.

Wat zijn de gevolgen van PEEK TKV op klinische beeldvorming?

Een goede visualisatie van knie-implantaten na de operatie is essentieel om het succes van de procedure te bepalen en voor een juiste diagnose van patiënten met klachten. Sinds de ontwikkeling van TKV in de late zestiger jaren, is in-situ beoordeling gebaseerd op standaard röntgenfoto's, wat tot op heden de voorkeursmethode is^{27,28}. Uitlijning van de implantaten in het coronale en sagittale vlak is cruciaal om bruikbare beelden te verkrijgen, omdat het metaal röntgenstralen blokkeert en dus andere structuren of interfaces kan verhullen. Aan de andere kant zal het implantaat altijd duidelijk te onderscheiden zijn van zijn omgeving, wat de toepassing zijn robuustheid geeft. Een femorale PEEK-prothese zal een grote impact hebben op deze visualisatie. Een radiolucent kunststof zal onvermijdelijk leiden tot uitdagingen als gevolg van de verminderde capaciteit om het implantaat van zijn omgeving te onderscheiden. Verhoogde radioluentie biedt echter ook nieuwe mogelijkheden voor klinische beoordeling met andere beeldvormingsmodaliteiten. Bij MRI- en CT-scans veroorzaken de huidige metalen implantaten aanzienlijke beeldartefacten, die een goede beoordeling moeilijk of in sommige gevallen onmogelijk maken^{29,30}. Niet-interfererende kunststoffen, zoals PEEK, produceren dergelijke artefacten niet en dus kunnen MRI en CT mogelijk waardevolle diagnostische hulpmiddelen worden. Om dit potentieel in **Hoofdstuk 7** te bepalen, werden kadaverknieën geïmplantéerd met PEEK en CoCr femorale componenten en polyethyleen tibiale componenten. Klinische beeldvormingsinstellingen werden gebruikt voor MRI-, CT- en röntgenscans om het voorkomen van het PEEK-implantaat in deze modaliteiten te bestuderen.

Vier **MRI**-sequenties werden geëvalueerd: protondichtheid (PD), T1-gewogen (T1w), T2-gewogen vetverzadigd (T2FS) en short tau inversion recovery (STIR) -sequenties. Geen van de sequenties vertoonde artefacten veroorzaakt door de PEEK-component. Het beste contrast voor het implantaat werd bereikt met de PD-sequentie, terwijl T1w superieure, details op trabeculair niveau op het grensvlak van cement en bot opleverde. Dit laatste kan een waardevolle functie zijn voor postoperatieve diagnostiek. De T2FS-reeks bereikte superieure signaaldetectie voor water, wat nuttig is bij het detecteren van vloeistofingressie tussen structuren (losraken van implantaten). De STIR-sequentie bood geen duidelijke voordelen voor beeldvorming van PEEK-implantaten.

De gekozen **CT**-parameters zorgden voor een uitstekende signaal-ruisverhouding, niet beïnvloed door de PEEK-prothese en vergelijkbaar met het uiterlijk van standaard preoperatieve orthopedische CT-scans rond de knie. De PEEK-prothese was duidelijk identificeerbaar en goed scheidbaar van omliggende structuren, hoewel beperkt naast gewrichtsvloeistof. Het gebrek aan artefacten in de PEEK-knie beeldarray maakte het mogelijk om zeer kleine structuren te onderscheiden in overeenstemming met de maximale spatiële resolutie van de gebruikte scanner.

Het PEEK-implantaat was nauwelijks zichtbaar op een **röntgenfoto**. Contouren werden waargenomen, maar de component contrasteerde slechts matig met de omliggende structuren. De metalen prothese verborg elke structuur of kenmerk eromheen, waardoor beoordeling van de cementmantel en botinterfaces onmogelijk was. De macroscopische positie van het implantaat is duidelijk, in tegenstelling tot de PEEK-component. Het radiolucente PEEK maakte echter visualisatie mogelijk van de micro-architectuur van de interfaces tussen bot, cement en implantaat.

Het is duidelijk geworden dat het PEEK-implantaat er radicaal anders uitziet op alle in dit proefschrift geteste beeldvormingsmodaliteiten. Ten eerste wordt standaard radiografie bemoeilijkt door de radioluentie van het PEEK-polymeer. Aangezien de röntgenfoto het belangrijkste beoordelingsinstrument is voor postoperatieve evaluatie, bemoeilijkt het PEEK-implantaat deze beoordeling doordat het bijna niet te onderscheiden is van zijn omgeving. De afwezigheid van radiopaak metaal zorgt wel voor zichtbaarheid van de cementmantel en de interfaces, die kunnen worden gebruikt om klachten indirect te beoordelen met betrekking tot de plaatsing van de prothese, waaronder (slechte) uitlijning, fixatie en migratie. In elk geval hebben radiologen en orthopedisch specialisten een grondige training nodig om vertrouwd te raken met de weergave van het PEEK-implantaat en om de beelden adequaat te interpreteren. Met betrekking tot de andere beeldvormingsmodaliteiten – MRI en CT – heeft PEEK aangetoond dat het gunstig is bij het visualiseren van de prothese te midden van de omliggende weefsels en componenten. Met MRI is het in feite een van de weinige

implantaten die de toepassing van deze modaliteit niet bemoeilijken. Metalen componenten vervormen de gehele beeldarray ernstig en worden over het algemeen niet geëvalueerd met deze methode. PEEK onderscheidt zich op MRI van de andere TKV-componenten, de knieweefsels en de synoviale vloeistof. Dit kan baanbrekende mogelijkheden bieden bij het diagnosticeren van postoperatieve klachten en het introduceert nieuwe kansen voor postoperatief TKV-onderzoek. Het laatste heeft betrekking op recente vorderingen in preoperatieve integratie van MRI voor het begrijpen van de (real-time) kinematica en functionele anatomie van de knie ten behoeve van chirurgische planning³¹. Met de mogelijkheid van onvervormde postoperatieve MRI kunnen deze technieken worden gebruikt om de impact van de reconstructie op de functionaliteit van knieweefsels te evalueren^{31,32}. Dit kan ook een waardevolle aanvulling zijn op het lopende debat over de *gap-balancing* en *measured resection* technieken voor protheseplaatsing³³⁻³⁶. Evenzo kan CT worden gebruikt voor de beoordeling van de PEEK-knie. Zonder de artefacten van metaal, kan CT of MRI (of beide) worden gekozen voor eender welke specifieke behoefte.

Toekomstperspectieven

Over de methoden die in dit proefschrift werden gebruikt

In dit proefschrift hebben we een aantal belangrijke beperkingen met betrekking tot de methoden geïdentificeerd, met name aangaande de eindige-elementenmodellering. Aangezien de modellen in de **Hoofdstukken 2 en 3** zijn gebaseerd op slechts één sample, zijn de gegevens vooral bruikbaar als proof-of-concept, en zijn daarom minder geschikt om uitspraken te doen over toekomstige patiëntenpopulaties. Een manier om dat op te lossen is door modellen te gebruiken die op een populatie zijn gebaseerd. Populatie-brede modellering in FE-analyse wordt steeds vaker gebruikt en biedt manieren om rekening te houden met variabiliteit in parameters met betrekking tot de patiënt, chirurgie of implantaat³⁷⁻⁴⁰. Op populatie gebaseerde modellering maakt het testen van de mechanische integriteit van het PEEK-implantaat voor een uitgebreid aantal gevallen mogelijk, wat de robuustheid van de analyses verbetert.

Kalibratie van FE-modellen via experimentele validatie is een andere manier om de betrouwbaarheid van de simulatie-resultaten te vergroten, zoals gedaan in **Hoofdstuk 4**. De studies in de Hoofdstukken 2 en 3 waren gebaseerd op vergelijkende gegevens, waar dezelfde parameters werden gebruikt voor zowel PEEK- als CoCr-modellen, behalve voor materiaaleigenschappen. Dit maakte het mogelijk om relatieve veranderingen in uitkomsten te beoordelen, maar de resultaten kunnen niet als absolute maatstaf worden gebruikt. Hoewel dit niet het doel van deze studies was, zou het in de toekomst nuttig zijn om experimentele validatie van dergelijke modellen uit te voeren om gekalibreerde en kwantitatief nauwkeurige resultaten te genereren.

In **Hoofdstuk 4** waren we in staat FE-simulaties met experimentele gegevens te valideren. We concludeerden dat stress shielding is verminderd en daarmee de prikkel voor botresorptie is verminderd. We weten echter uit de literatuur dat een bepaalde drempel voor de stimulus moet worden toegepast om botgroei te simuleren^{20,23}. Het zou redelijk zijn om dergelijke modellen uit te breiden met botadaptatie-algoritmen om de effecten op de korte tot middellange termijn van (verminderde) stress shielding te beoordelen. Adaptaties op lange termijn zijn van belang, maar ook steeds moeilijker te voorspellen, omdat de stimuli voor de in dit proefschrift onderzochte activiteiten niet de enige factoren zijn die het proces van botomzet beïnvloeden^{17,18}.

Over de ontwikkeling van PEEK TKV

De lange-termijn testen van PEEK-implantaten in de slijtagesimulator, zoals onderzocht in **Hoofdstuk 6**, hebben waardevolle inzichten opgeleverd over de impact van cyclische belasting op de fixatie van de prothese. Zoals in dit Hoofdstuk wordt verondersteld, kan het de moeite waard zijn om deze experimenten uit te breiden met (elektronen) microscopische analyse van het implantaat en cementoppervlakken om de daadwerkelijke slijtage en schade die zich op de interface heeft verzameld te beoordelen. Studies bij mensen en dieren suggereren dat slijtagedeeltes van (met koolstofvezels versterkte) PEEK mogelijk ontstekingsreacties in het kniegewricht of aangrenzende weefsels kunnen veroorzaken⁴¹⁻⁴⁵. Resultaten zijn niet eenduidig wat betreft de omvang en vergelijking met huidige materialen, maar het zou wenselijk zijn om te weten of substantiële PMMA- of PEEK-slijtage zou plaatsvinden op cement-implantaatinterface.

In drie studies onderzochten we het potentieel voor een PEEK femorale component om periprothetisch botverlies te voorkomen. Klinische gegevens om dit te ondersteunen zijn wenselijk om deze bevindingen te verifiëren en om de veranderingen in de botdichtheid te vergelijken met metalen implantaten. Een kleine dierstudie (geit) werd uitgevoerd door Du *et al.* (2018), wat 12 weken postoperatief een lichte afname van de botdichtheid aantoont, die niet verder steeg na 24 weken⁴⁶. Hoewel dit een diermodel betreft, waarin de kinematica behoorlijk verschilt van menselijke toepassingen, geven deze resultaten enig vertrouwen aan de hypothesen en bevindingen in dit proefschrift. Om de bevindingen van de computeranalyses verder te valideren, moeten echter studies worden uitgevoerd bij de eerste patiëntcohorten die een PEEK-knieprothese krijgen, om periprothetische botveranderingen in een klinische setting te onderzoeken. Als het voordeel ervan wordt onderbouwd in klinische studies, zou een PEEK-knie een zeer interessant alternatief zijn voor jongere en actieve patiënten, omdat deze het meest zouden profiteren van een meer natuurlijke botomzet.

De huidige studies hebben zich uitsluitend gericht op gecementeerde TKV. Extra inspanningen kunnen worden verricht om de fixatiekenmerken van niet-gecementeerde

PEEK-componenten te onderzoeken. Het is aannemelijk dat het verminderen van het aantal interfaces de veiligheid kan verhogen op het gebied van slijtage. Bovendien kan het periprothetische bot verder profiteren van de verhoogde mechanische compatibiliteit die PEEK biedt ten opzichte van metaal, wanneer de cementmantel wordt verwijderd als bufferlaag. Zoals eerder vermeld, is de integriteit van het cement-botinterface sterk afhankelijk van lokale spanningsoverdracht door geïnterdigiteerde trabeculae en kunstmatig materiaal¹⁷⁻⁹. Als botingroei in een niet-gecementeerde PEEK-prothese zou plaatsvinden, zou de kwaliteit van de implantaat-botinterface substantieel toenemen, vergeleken met een stijf metalen component. De mogelijkheid van dergelijke ingroei in PEEK-gewrichtsvervangings is aangetoond in dierstudies wat dit potentieel onderstreept^{47,48}.

Een andere interessante toepassing van PEEK in TKV zou zijn voor gepersonaliseerde implantaten. Steeds vaker worden 3D-geprinte implantaten en chirurgische hulpmiddelen gebruikt en die vertonen veelbelovende toepassingen. Momenteel wordt PEEK gebruikt in patiëntspecifieke 3D-geprinte implantaten voor reconstructieve tandheelkundige chirurgie⁴⁹⁻⁵². De vooruitgang van patiëntspecifieke implantaten hangt nauw samen met de vooruitgang van de 3D-printtechnologie. Speciale overwegingen gaan naar articulerende componenten, omdat nauwe toleranties op de oppervlakteafwerking van cruciaal belang zijn om slijtage te verminderen. Momenteel is er geen printtechniek voor PEEK beschikbaar die dergelijk nauwe toleranties kan bieden, waardoor nabewerking noodzakelijk is om binnen aanvaardbare ontwerpparameters te blijven. Aanvullende productiestappen zijn vanuit kostenperspectief ongewenst en moeten worden overwonnen voordat gepersonaliseerde PEEK-implantaten voor TKV kunnen worden overwogen.

Een groot voordeel van volledig-kunststof TKV is de toepassing voor patiënten met overgevoeligheid voor metalen. Ongeveer 10-15% van de patiëntenpopulatie lijdt aan enige vorm van metaalovergevoeligheid⁵³. Hoewel dit aantal lager is in de TKV-populatie, wordt metaalallergie beschouwd als een preoperatief risico en een onmiskenbare oorzaak van TKV-falen⁵³. Preoperatieve screening op metaalallergie is daarom belangrijk en patiënten met deze aandoening zouden baat hebben bij een metaalvrije oplossing, zoals met een PEEK femorale component gecombineerd met een volledig-kunststof tibiale component. Evenzo zouden patiënten die revisie-operaties ondergaan na complicaties van metaalallergie, baat hebben bij volledig-kunststof implantaten.

De chirurgische techniek en met name het cementeren zal waarschijnlijk het klinische resultaat van de gecementeerde femorale PEEK-component beïnvloeden. De huidige PEEK-component, zoals onderzocht in dit proefschrift, was uitgerust met mediaal-naar-laterale ribbels in de cementuitsparingen om de mechanische interlock van de interface tussen implantaat en cement te verbeteren. Voor een goede implantaatfixatie is het belangrijk om

een goede cementdekking te bereiken. Na de wijzigingen in het ontwerp kan een specifieke cementeringstechniek vereist zijn, omdat de ribbels de verdeling van cement beïnvloeden wanneer de component op het geprepareerde femur wordt geplaatst. De ribbels kunnen cement vasthouden dat op de condyles is aangebracht en het met zich meeslepen, weg van de implantaatflenzen, waardoor distale delen van de uitsparingen ongecementeerd blijven. Dit kan worden voorkomen door extra cement aan te brengen op (tenminste) de voorste en achterste flenzen om de ruimtes tussen de ribbels op te vullen vóór implantatie, of door zowel het femur als het implantaat te cementeren vóór het aanbrengen van het implantaat.

Afgezien van de parameters die in dit proefschrift bestudeerd zijn, is een aantal extra eigenschappen belangrijk om te overwegen voor hun potentiële impact op klinisch succes. Slijtvastheid is een van de essentiële kenmerken van articulerende onderdelen. De huidige PEEK-op-UHMWPE prothese is in vitro onderzocht op zijn slijtageprestaties. Ten opzichte van de identiek gevormde CoCr-prothese vertoonde het PEEK-op-UHMWPE construct een (niet-statistisch significante) lichte toename van slijtage, maar bleef gecategoriseerd als 'lage' slijtagesnelheid⁵⁴. In vergelijking met de huidige klinisch gebruikte metalen componenten, presteerde het PEEK-implantaat beter, waarschijnlijk vanwege de lage conformiteit van de articulerende onderdelen⁵⁵. Een toename van de wrijvingscoëfficiënt en de daaruit voortvloeiende verwarming door frictie werden ook gerapporteerd voor het PEEK-implantaat. Hypothetische complicaties van verhoogde gewrichtstemperatuur zijn eiwitdepositie en denaturatie, die wrijving en slijtage kunnen vergroten, en weefselnecrose⁵⁶. Deze slijtage- en wrijvingseigenschappen vereisen uiteraard klinische gegevens om hun impact te beoordelen, maar de vergelijking met succesvolle metalen protheses geeft geen grote zorgen.

Het preklinische onderzoek in dit proefschrift en de daaropvolgende discussies ondersteunen verdere klinische verkenning van de PEEK femorale component. Een metaalvrije prothese met een gunstige stijfheid biedt naar verwachting een aantal zeer gewenste voordelen ten opzichte van huidige TKV-apparaten en moeten als zodanig in een klinische setting worden bestudeerd. De mogelijkheid om meerdere hoogwaardige beeldvormingsmodaliteiten te gebruiken, biedt veel mogelijkheden voor klinische beoordelingen en moet worden gebruikt om de mogelijke nadelen die in dit proefschrift zijn geïdentificeerd te evalueren. Belangrijke parameters om te bestuderen zijn de morfologie van de periprothetische botmassa. Eventuele laesies of zachte plekken onder de cementmantel moeten worden geïdentificeerd om te beoordelen of dergelijke inhomogeniteiten een impact hebben op de klinische prestaties. Tegelijkertijd zou de integriteit van de cementlaag kunnen worden gecontroleerd om achteraf de relatie met het losraken van het implantaat te kunnen bepalen, mochten er tijdens de studie gevallen van loslating optreden. Door de gewijzigde stijfheid zijn migratie- en kruipmetingen van de prothese ook relevant. Met multiplanare reconstructie en segmentatie van MRI- en CT-beeldarrays konden deze parameters nauwkeurig worden

gevolgd op verschillende tijdsintervallen tijdens gebruik. Dit zou een welkome aanvulling zijn op de huidige standaard in migratiedetectie: röntgen stereofotogrammetrie (RSA). Deze techniek meet de relatieve beweging tussen sets van metalen markers, maar omdat het uitgaat van beweging tussen stijve lichamen – voldoende voor metalen componenten – kan worden aangenomen dat het minder nauwkeurig is voor minder stijve PEEK-implantaten. Ondanks het geaccepteerde gebruik van deze techniek, kunnen CT en MRI mogelijk meer nauwkeurig en informatief zijn bij het bepalen van de plaatsing van de prothese en daarnaast ook vervorming en kruip.

Conclusies

Dit proefschrift onderzocht de mechanische prestaties en primaire fixatie van een PEEK femoraal TKV-implantaat, evalueerde het effect van een dergelijke femorale prothese met lage stijfheid op periprothetische belastingoverdracht en verkende de implicaties voor medische beeldvorming bij het gebruik van een radiolucent kunststof component. De bevindingen van dit proefschrift ondersteunen verdere verkenning van PEEK femorale TKV-implantaten in een klinische studie en rechtvaardigen verder onderzoek naar het gebruik van PEEK bij totale gewrichtsvervangning.

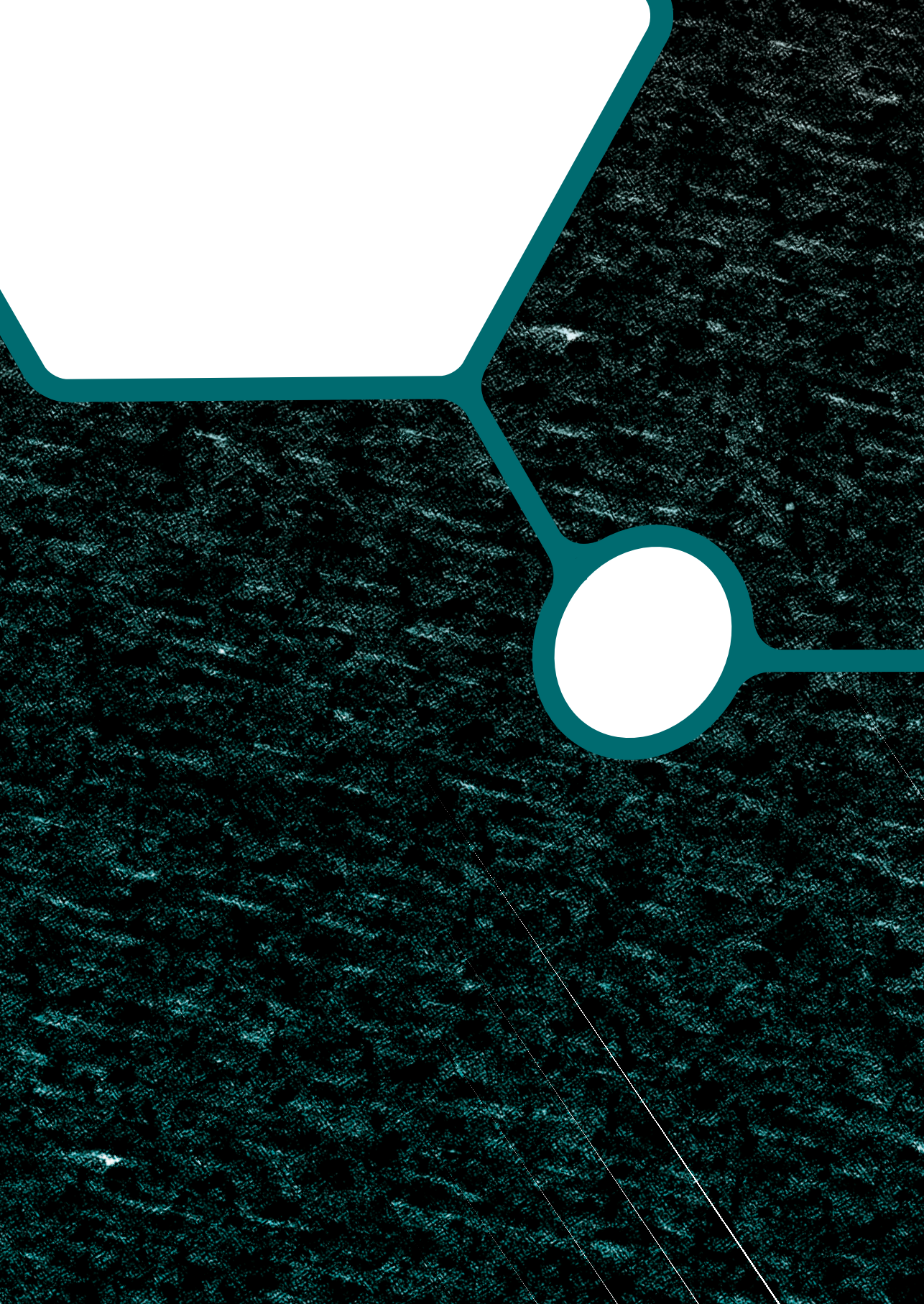
Referenties

1. D'Lima D, Fregly BJ, Patil S, et al. *Knee joint forces: prediction, measurement, and significance*. Proc Inst Mech Eng H 2012; 226: 95–102.
2. Zelle J, Janssen D, Van Eijden J, et al. *Does high-flexion total knee arthroplasty promote early loosening of the femoral component?*. J Orthop Res 2011; 29: 976–983.
3. Krueger AP, Singh G, Beil FT, et al. *Ceramic femoral component fracture in total knee arthroplasty: an analysis using fractography, fourier-transform infrared microscopy, contact radiography and histology..* J Arthroplasty 2014; 29: 1001–4.
4. Gilg MM, Zeller CW, Leitner L, et al. *The incidence of implant fractures after knee arthroplasty*. Knee Surg, Sport Traumatol Arthrosc 2016; 24: 3272–3279.
5. Ranawat AS, Ranawat AS, Ranawat CS. *The history of total knee arthroplasty*. In: Bonnin M (ed) *The Knee Joint*. Springer-Verlag France, Paris, 2012.
6. van de Groes S, de Waal Malefijt M, Verdonschot N. *Influence of preparation techniques to the strength of the bone-cement interface behind the flange in total knee arthroplasty..* Knee 2012; 20: 186–190.
7. Goodheart JR, Miller MA, Mann KA. *In Vivo Loss of Cement-Bone Interlock Reduces Fixation Strength in Total Knee Arthroplasties*. J Orthop Res 2014; 32: 1052–1060.
8. Howard K, Miller M, Damron T, et al. *The distribution of implant fixation for femoral components of TKA: A postmortem retrieval study*. J Arthroplasty 2014; 29: 1863–1870.
9. Mann K, Miller M, Pray C, et al. *A new approach to quantify trabecular resorption adjacent to cemented knee arthroplasty*. J Biomech 2012; 45: 711–715.
10. Zelle J, Janssen D, Peeters S, et al. *Mixed-mode failure strength of implant-cement interface specimens with varying surface roughness*. J Biomech 2011; 44: 780–3.
11. Zelle J, van de Groes S, de Waal Malefijt M, et al. *Femoral loosening of high-flexion total knee arthroplasty: the effect of posterior cruciate ligament retention and bone quality reduction..* Med Eng Phys 2014; 36: 318–24.
12. Han CD, Han CW, Yang IH. *Femoral Component Fracture Due to Osteolysis After Cemented Mobile-Bearing Total Knee Arthroplasty*. J Arthroplasty 2009; 24: 323.e7-323.e12.
13. Huang C, Yang C, Cheng C. *Fracture of the femoral component associated with polyethylene wear and osteolysis after total knee arthroplasty*. J Arthroplasty 1999; 14: 375–379.
14. Duffy GP, Murray BE, Trousdale RR. *Hybrid Total Knee Arthroplasty. Analysis of Component Failures at an Average of 15 Years*. J Arthroplasty 2007; 22: 1112–1115.
15. Rankin KE. *Evaluation of Polyetheretherketone as a Candidate Material for Cemented Total Knee Replacement*. University of Southampton, Faculty of Engineering and the Environment, PhD Thesis.
16. Bergschmidt P, Dammer R, Zietz C, et al. *Adhesive strength of total knee endoprostheses to bone cement – analysis of metallic and ceramic femoral components under worst-case conditions*. Biomed Tech 2016; 61: 281–289.

17. Robling AG, Turner CH. *Mechanical Signaling for Bone Modeling and Remodeling*. Crit Rev Eukaryot Gene Expr 2009; 19: 319–338.
18. Boskey AL, Coleman R. *Aging and bone*. J Dent Res 2010; 89: 1333–1348.
19. Boby J, Mortimer E, Glassman A, et al. *Producing and avoiding stress shielding. Laboratory and clinical observations of noncemented total hip arthroplasty*. Clin Orthop Relat Res 1992; 79–96.
20. Lenthe G Van, de Waal Malefijt MC, Huiskes R. *Stress shielding after total knee replacement may cause bone resorption in the distal femur..* J Bone Joint Surg Br 1997; 79: 117–122.
21. Lavernia CJ, Rodriguez J a, Iacobelli D a, et al. *Bone mineral density of the femur in autopsy retrieved total knee arthroplasties..* J Arthroplasty 2014; 29: 1681–6.
22. Järvenpää J, Soininvaara T, Kettunen J, et al. *Changes in bone mineral density of the distal femur after total knee arthroplasty: a 7-year DEXA follow-up comparing results between obese and nonobese patients..* Knee 2014; 21: 232–5.
23. Huiskes R, Weinans H, Grootenboer HJ, et al. *Adaptive Bone-Remodeling Theory Applied to Prosthetic-Design Analysis*. J Biomech 1987; 20: 1135–1150.
24. Huiskes RR. *Failed innovation in total hip replacement. Diagnosis and proposals for a cure..* Acta Orthop Scand 1993; 64: 699–716.
25. Kummer B. *Biomechanics of bone: Mechanical properties, functional structure, and functional adaptation..* In: Fung Y, Perrone N, Anliker M (eds) *Biomechanics: Its Foundations and Objectives*. Englewood Cliffs, NJ: Prentice-Hall, 1972, p. 237:271.
26. Lenthe G Van, Willems M, Verdonchot N, et al. *Stemmed femoral knee prostheses: effects of prosthetic design and fixation on bone loss*. Acta Orthop Scand 2002; 73: 630–637.
27. Ewald F, C. *Roentgenographic Evaluation and Scoring System*. Clin Orthop Relat Res 1989; 2–5.
28. Goergen TG, Dalinka MK, Alazraki N, et al. *Evaluation of the patient with painful hip or knee arthroplasty. American College of Radiology. ACR Appropriateness Criteria..* Radiology 2000; 215 Suppl: 295–298.
29. Koch KM, Lorbiecki JE, Hinks RS, et al. *A multispectral three-dimensional acquisition technique for imaging near metal implants*. Magn Reson Med 2009; 61: 381–390.
30. Kasperek MF, Töpker M, Lazar M, et al. *Dual-energy CT and ceramic or titanium prostheses material reduce CT artifacts and provide superior image quality of total knee arthroplasty*. Knee Surg, Sport Traumatol Arthrosc 2019; 27: 1552–1561.
31. Naghibi H, Mazzoli V, Gijsbertse K, et al. *A noninvasive MRI based approach to estimate the mechanical properties of human knee ligaments*. J Mech Behav Biomed Mater 2019; 93: 43–51.
32. Leijendekkers RA, Marra MA, Ploegmakers MJM, et al. *Magnetic-resonance-imaging-based three-dimensional muscle reconstruction of hip abductor muscle volume in a person with a transfemoral bone-anchored prosthesis: A feasibility study*. Physiother Theory Pract 2019; 35: 495–504.

33. Daines BK, Dennis DA. *Gap Balancing vs. Measured Resection Technique in Total Knee Arthroplasty*. Clin Orthop Surg 2014; 6: 1–8.
34. Song DLJPD. *Accuracy of soft tissue balancing in TKA: comparison between navigation-assisted gap balancing and conventional measured resection*. Knee Surg, Sport Traumatol Arthrosc 2010; 18: 381–387.
35. Dennis DA, Komistek RD, Kim RH, et al. *Gap Balancing versus Measured Resection Technique for Total Knee Arthroplasty*. Clin Orthop Relat Res 2010; 468: 102–107.
36. Moon Y, Kim H, Ahn H, et al. *Comparison of soft tissue balancing, femoral component rotation, and joint line change between the gap balancing and measured resection techniques in primary total knee arthroplasty. A meta-analysis*. Medicine (Baltimore) 2016; 95: 1–7.
37. Laz PJ, Browne M. *A review of probabilistic analysis in orthopaedic biomechanics*. Proc Inst Mech Eng H 2010; 224: 927–943.
38. Easley SK, Pal S, Tomaszewski PR, et al. *Finite element-based probabilistic analysis tool for orthopaedic applications*. Comput Methods Programs Biomed 2007; 85: 32–40.
39. Sarkalkan N, Weinans H, Zadpoor AA. *Statistical shape and appearance models of bones*. Bone 2014; 60: 129–140.
40. Campbell JQ, Petrella AJ. *Automated finite element modeling of the lumbar spine: Using a statistical shape model to generate a virtual population of models*. J Biomech 2016; 49: 2593–2599.
41. Lorber V, Paulus AC, Buschmann A, et al. *Elevated cytokine expression of different PEEK wear particles compared to UHMWPE in vivo*. J Mater Sci Mater Med 2014; 25: 141–149.
42. Du Z, Zhu Z, Wang Y. *The degree of peri-implant osteolysis induced by PEEK, CoCrMo, and HXLPE wear particles: a study based on a porous Ti6Al4V implant in a rabbit model*. J Orthop Surg Res 2018; 13: 1–9.
43. Du Z, Wang S, Yue B, et al. *Effects of wear particles of polyether-ether-ketone and cobalt-chromium-molybdenum on CD4- and CD8-T-cell responses*. Oncotarget 2018; 9: 11197–11208.
44. Paulus AC, Haßelt S, Jansson V, et al. *Histopathological Analysis of PEEK Wear Particle Effects on the Synovial Tissue of Patients*. Biomed Res Int 2016; 2: 1–5.
45. Stratton-Powell AA, Pasko KM, Brockett CL, et al. *The Biologic Response to Polyetheretherketone (PEEK) Wear Particles in Total Joint Replacement: A Systematic Review*. Clin Orthop Relat Res 2016; 474: 2394–2404.
46. Du Z, Zhu Z, Yue B, et al. *Feasibility and Safety of a Cemented PEEK-on-PE Knee Replacement in a Goat Model: A Preliminary Study*. Artif Organs 2018; 42: E204–E214.
47. Nakahara I, Takao M, Bandoh S, et al. *In vivo implant fixation of carbon fiber-reinforced PEEK hip prostheses in an ovine model*. J Orthop Res 2012; 31: 485–92.
48. Choi D, Yoon YS, Hwang D. *Evaluation of sleeved implant fixation using a rat model*. Med Eng Phys 2011; 33: 310–314.
49. Liu D, Fu J, Fan H, et al. *Application of 3D-printed PEEK scapula prosthesis in the treatment of scapular benign fibrous histiocytoma: A case report*. J Bone Oncol 2018; 12: 78–82.
50. Wang L, Huang L, Li X, et al. *Three-Dimensional Printing PEEK Implant: A Novel Choice for the Reconstruction of Chest Wall Defect*. Ann Thorac Surg 2019; 107: 921–928.

51. Deng L, Deng Y, Xie K. AgNPs-decorated 3D printed PEEK implant for infection control and bone repair. *Colloids Surfaces B Biointerfaces* 2017; 160: 483–492.
52. Haleem A, Javaid M. Polyether ether ketone (PEEK) and its manufacturing of customised 3D printed dentistry parts using additive manufacturing. *Clin Epidemiol Glob Heal* 2019; 0–1.
53. Innocenti M, Vieri B, Melani T, et al. Metal hypersensitivity after knee arthroplasty: fact or fiction?. *Acta Biomed* 2017; 88: 78–83.
54. Cowie R M, Briscoe A, Fisher J, et al. PEEK-OPTIMA™ as an alternative to cobalt chrome in the femoral component of total knee replacement: A preliminary study.. *Proc Inst Mech Eng H* 2016; 230: 1008–1015.
55. Brockett CL, Carbone S, Fisher J, et al. Influence of conformity on the wear of total knee replacement: An experimental study. *Proc Inst Mech Eng H* 2018; 232: 127–134.
56. Bergmann G, Graichen F, Rohlmann A, et al. Frictional heating of total hip implants, Part 1: Measurements in patients. *J Biomech* 2001; 34: 421–428.



Appendix

**List of publications
Data management
PhD portfolio
Curriculum Vitae
Dankwoord**

List of publications

Journal papers

de Ruiter L, Janssen D, Briscoe A, Verdonschot N. A preclinical numerical assessment of a polyetheretherketone femoral component in total knee arthroplasty during gait. *Journal of Experimental Orthopaedics* 2017; 4(1): 3

de Ruiter L, Janssen D, Briscoe A, Verdonschot N. The mechanical response of a polyetheretherketone femoral knee implant under a deep squatting loading condition. *Proceedings of the Institution of Mechanical Engineers, Part H: Journal of Engineering in Medicine* 2017; 231(12): 1204-1212

de Ruiter L, Janssen D, Briscoe A, Verdonschot N. Fixation strength of a polyetheretherketone femoral component in total knee arthroplasty. *Medical Engineering and Physics* 2017; 49: 157–162

de Ruiter L, Rankin K, Browne M, Janssen D, Verdonschot N. Decreased stress shielding with a PEEK femoral total knee prosthesis measured in validated computational models. *Submitted*

de Ruiter L, Cowie R, Jennings L, Janssen D, Verdonschot N. The effects of cyclic loading and motion on the implant-cement interface and cement mantle of PEEK and cobalt-chromium femoral total knee arthroplasty implants: a preliminary study. *Materials* 2020; 13(15): E3323

de Ruiter L, Fascia D, Tomaszewski P, Janssen D, Verdonschot N. Clinical imaging protocols for in-vivo assessment of an all-polymer PEEK-on-UHMWPE total knee replacement with magnetic resonance imaging, computed tomography and X-ray radiography. *Manuscript in preparation*

Conference abstracts

de Ruiter L, Janssen D, Briscoe A, Verdonschot N. Interface Stresses of a Polyetheretherketone Femoral Component in Cemented Total Knee Arthroplasty. *26th Annual Congress of the International Society for Technology in Arthroplasty, 2013, Palm Beach, USA.*

de Ruiter L, Janssen D, Briscoe A, Verdonschot N. A Biomechanical Analysis of a PEEK-Optima[®] Femoral Component on Implant Fixation, Construct Integrity and Bone Remodeling Opportunities in Total Knee Arthroplasty. *Annual Meeting of the Orthopaedic Research Society, 2014, New Orleans, USA.*

de Ruiter L, Janssen D, Briscoe A, Verdonschot N. Biomechanical Compatibility of a PEEK-Optima Femoral Total Knee Arthroplasty Implant Design During Gait. *27th Annual Congress of the International Society for Technology in Arthroplasty, 2014, Kyoto, Japan.*

de Ruiter L, Janssen D, Briscoe A, Verdonschot N. Durability of a polyetheretherketone (PEEK) femoral total knee arthroplasty implant design during gait. *12th International Symposium on Computer Methods in Biomechanics and Biomedical Engineering, 2014, Amsterdam, The Netherlands.*

de Ruiter L, Janssen D, Briscoe A, Verdonschot N. Peek femoral component in TKA: bone remodelling and device performance during gait and squatting. *5th Dutch Bio-Medical Engineering Conference, 2015, Egmond aan Zee, The Netherlands.*

de Ruiter L, Janssen D, Briscoe A, Verdonschot N. PEEK Femoral Component in TKA: Bone Remodeling and Device Performance during Gait and Squatting. *2nd International PEEK meeting, 2015, Washington DC, USA.*

de Ruiter L, Janssen D, Briscoe A, Verdonschot N. High-Demand Implant Loading and the Benefits of a PEEK Femoral Component on the Periprosthetic Bone Remodeling Stimulus. *28th Annual Congress of the International Society for Technology in Arthroplasty, 2015, Vienna, Austria.*

Janssen D, **de Ruiter L**, Rankin K, Briscoe A, Verdonschot N. Pre-clinical biomechanical evaluation of fixation of a cemented PEEK Femoral Component in TKA. *3rd International PEEK meeting, 2017, Washington DC, USA.*

Sadhvani S, Picache D, Janssen D, **de Ruiter L**, Rankin K, Briscoe A, Verdonschot N, Shah A. Pre-Clinical Biomechanical Evaluation of Fixation of a Cemented PEEK Femoral Component in TKA. *32nd Annual Congress of the International Society for Technology in Arthroplasty, 2019, Toronto, Canada.*

Sadhvani S, Picache D, Janssen D, **de Ruiter L**, Rankin K, Briscoe A, Verdonschot N, Shah A. Assessment of Fixation Strength and Stress Shielding of an All-Polymer Poly-ether-ether-ketone (PEEK) Femoral Component in Total Knee Arthroplasty. *Annual Congress of Orthopaedic Research Society, 2020, Phoenix, AZ, USA.*

Data management

The primary and secondary data obtained during this PhD project at the Radboud university medical center (Radboudumc) have been archived and backed-up on the secured department-specific drive on the Radboudumc network and are accessible by the associated senior staff members of the Orthopaedic Research Laboratory. Published data generated or analyzed in this thesis are part of published articles and its additional files are available from the associated corresponding authors on request. To ensure interpretability of the data, associated program code and scripts used to provide the final results are stored along with the data. Physical documents and materials are stored in a fireproof safe at the department archive (Radboudumc, room M379.-1.219). Cadaveric samples are stored in freezers under appropriate conditions at the department laboratory (Radboudumc, room M379.-1.215).

RIHS PhD portfolio



Name PhD candidate: L. de Ruiter, MSc

PhD period: 15-09-2012 – 15-12-2016

Department: Orthopaedic Research Laboratory

Promotor: Prof. dr. Ir. N.J.J. Verdonschot

Graduate School: Radboud Institute for Health Sciences


Co-promotor: Dr. Ir. D.J. Janssen

TRAINING ACTIVITIES

	Years(s)	ECTS
Courses and workshops		
- NCEBP Introduction Course for PhD students	2012	1,75
- Workshop "Poster design and presentation"	2014	0,1
- Workshop "How to write a medical scientific abstract"	2016	0,1
Symposia & congresses		
- 26th Annual Congress of the International Society for Technology in Arthroplasty, Palm Beach, USA. (PP)	2013	1,25
- NCEBP PhD Retreat, Wageningen, NL. (PP)	2013	0,75
- RIHS Science Day, Nijmegen, NL. (Laptop presentation)	2014	0,5
- 12th International Symposium on Computer Methods in Biomechanics and Biomedical Engineering, Amsterdam, NL. (OP)	2014	1,25
- 27th Annual Congress of the International Society for Technology in Arthroplasty, Kyoto, JP. (PP)	2014	1,25
- RIHS PhD Retreat, Wageningen, NL. Organizing committee.	2014	0,5+2
- 5th Dutch Bio-Medical Engineering Conference, Egmond aan Zee, NL. (OP)	2015	0,75
- 2nd International PEEK Meeting, Washington D.C., USA. (OP)	2015	1
- 28th Annual Congress of the International Society for Technology in Arthroplasty, Vienna, AT. (OP)	2015	1,25
- RIHS PhD Retreat, Wageningen, NL. Organizing committee.	2015	0,5+2
Other		
- Journal club Orthopaedic Research Lab	2012-2016	4
- Lab lunch Orthopaedic Research Lab	2012-2016	4
- Research meetings dept. Orthopaedics	2013-2014	1
- Chairman PhD Council for NCEBP/RIHS	2013-2015	2
TEACHING ACTIVITIES		
Lecturing		
- BSc course 5DT03 – Determinanten 3: Fysische factoren	2013-2016	1,6
- MSc course – Advanced Matlab	2012-2014	1
- MSc course 5HM02 – Tissue: Biomechanics and engineering	2013-2015	4,1
Supervision of internships / other		
- BSc internships		
R. Doodkorte	2013	1
S. Zuidema	2014	1
M. Belt	2015	1
TOTAL		31,65

Curriculum vitae

Lennert de Rooter was born in Geldrop on December 27th, in 1987. In 2006 he obtained his VWO-diploma, after which he studied Biomedical Sciences at the Radboud University in Nijmegen. During his studies he obtained his Bachelor's degree by completion of his internship and thesis at the Orthopaedic Research Laboratory on a method validation study. In 2012, this was followed by a Master's degree, with a major in Clinical Human Movement Sciences. Lennert completed his Master's thesis at the department of Clinical Neurophysiology on real-time detection of muscle fiber recruitment. In September 2012, he started his PhD at the Orthopaedic Research Laboratory, in collaboration with an international team, led by Invibio Ltd (UK), for the development of an all-polymer knee prosthesis. During this project, he published the previously mentioned journal articles and conference abstracts. Furthermore, he was involved in teaching students and supervising interns of Clinical Human Movement Sciences at the Radboud University Nijmegen. In addition to his research activities, Lennert has been the chairman of the PhD Council of the Nijmegen Center for Evidence-Based Practice and Radboud Institute for Health Sciences.

The background of the page is a dark, textured surface, possibly a microscopic view of a material, with a teal-colored graphic overlay. The graphic consists of a large, irregular shape in the upper left corner, a vertical line extending downwards from its bottom edge, and a circular shape at the bottom right, resembling a magnifying glass or a stylized 'G'.

Substantial alterations to conventional implant design requires thorough preclinical screening to mitigate clinical risks. This dissertation investigates the potential benefits of all-polymer total knee replacement through introduction of a PEEK femoral component. To do so, it tests the device's mechanical response to relevant loading scenarios against a clinically tested metal component and studies the quality and durability of postoperative fixation.

In addition, it explores indications for biological adaptation of the bone stock and describes the polymer implant's appearance on common medical imaging modalities.